



A Systematic Methodology for Estimation of Safe Distances for Hydrogen Storage Containers

Angus MacMillan - 201732968

Jacob Currie - 201718558

James Hinshelwood - 201732900

Supervisor: Eero Immonen

eero.immonen@turkuamk.fi

*A thesis submitted in partial fulfilment of
the requirements of the Degree, MEng
Mechanical Engineering at the University
of Strathclyde.*

2022

Word count: 25,987

Abstract

Traditional calculation methods and modern machine learning methods are utilised to predict safety distances from hydrogen gas storage containers. These safety distances are evaluated by considering a plausible worst-case scenario where hydrogen gas leaks from a storage vessel, forming a hydrogen vapour cloud which - when ignited – results in a shockwave realised by overpressure. Heat flux radiation is simultaneously released as a result of this explosion. ANSYS Fluent software was used to simulate and investigate the scenario central to this investigation and was also used to provide input values required for the various calculation methods.

An extensive literature review and background research into the topic - which incorporates; hydrogen behaviours, related industry standards and potential reasons for hydrogen leakage - contributed to the creation of the methodology described in this study.

The developed methodology is presented in this report as a ‘users guide’ which can be used to establish safety distances for other potential hydrogen leakage scenarios. This will prove useful as society transitions towards a future of clean, renewable energy where hydrogen powered technology continues to develop and grow in demand. As this demand increases so too will the demand for hydrogen storage. This investigation will prove useful in the creation of such storage facilities as well as hydrogen production plants and hydrogen fuelling stations.

This hydrogen leakage safety analysis is a Masters group project carried out in co-operation with engineering and consultancy company, Elomatic. The Finland based firm serve the needs of clients across the globe, specialising in several industries such as energy, pharmaceuticals, oil & gas, marine and offshore, process industries, machinery and manufacturing. Project management, software development, engineering and technical consulting are just some of the services Elomatic provide to their clients. In recent years the company has been heavily involved in projects related to hydrogen fuel applications such as the development of a hydrogen powered ferry and green hydrogen production. Elomatic not only have significant experience and made substantial contributions in developing this technology but have displayed much enthusiasm in the future of hydrogen and its place in society as a clean energy source.

Acknowledgements

The group have thoroughly enjoyed the process of completing this project over the course of the first semester of our final year. We are thankful for being given the opportunity to complete this Masters project abroad in Turku, Finland as well as working in co-operation with a professional engineering consultancy, Elomatic. Thank you to the team at Elomatic for sharing your knowledge and expertise and for welcoming us to Turku. It was a pleasure working with you.

The group also wish to thank Turku University of Applied Sciences for being such an inviting and accommodating place to study and complete our group work on this Erasmus exchange. A special thank you to TUAS' International Relations Coordinator, Reetta Partala who helped organise this exchange and our group supervisor, Eero Immonen whose advice and guidance was essential to the success of this project.

The group would also like to thank the University of Strathclyde - and in particular the department of Mechanical and Aerospace Engineering - for giving our group the opportunity to study abroad and for the many ways this experience has benefited us. In addition, thank you to Kate Kenyon and the Strathclyde exchange team for organising this exchange opportunity.

We wish to thank our friends and families who have encouraged and motivated us through this experience. We would not be where we are today without their love and support.

While our group started this process as student colleagues, we have returned safely to Scotland as friends, having produced a piece of work which we hope will go on to prove most useful in the field of hydrogen storage.

Contents

1	Introduction	18
2	Literature Review & Background.....	19
2.1	Hydrogen Characteristics.....	19
2.1.1	Ignition.....	19
2.1.2	Dispersion	19
2.1.3	Expansion	20
2.1.4	Explosion Characteristics	22
2.1.5	The Joule-Thompson Effect	23
2.1.6	Investigations of Hydrogen Characteristics	25
2.2	Safety Considerations and Standards	25
2.2.1	Hydrogen Storage Safety	25
2.2.2	Studies of Standards & Governing Bodies	26
2.2.3	Safe Distance Standards.....	28
2.2.4	Hydrogen Storage and Leakage Risks.....	30
2.2.5	Hydrogen Leakage Detection.....	31
2.2.6	Hydrogen Safety Mitigation & Prevention Technology	31
2.2.7	Storage tank types and material properties.....	32
2.3	Safety Analyses and Prior investigations	33
2.3.1	Fuel Cell Vehicles and Fuelling Stations	33
2.3.2	Confined/Unconfined Scenario.....	33
2.3.3	Fuel Cell Ships Investigations	34
2.4	Potential Leakage Sources	34
2.5	Shockwaves & Overpressure.....	35
2.5.1	Characteristics.....	35
2.5.2	Overpressure Investigations.....	36
2.5.3	Scaling Law	37
2.5.4	Mach Stems	38
2.5.5	Measurement	39
2.5.6	Modelling.....	39
2.5.7	TNT Equivalency Method	39
2.5.8	TNO Multi-Energy Method.....	41
2.5.9	Baker-Strehlow-Tang (BST) Method	42
2.5.10	Experimental Data Curve Fitting Model	43
2.5.11	Ideal Waves with the Friedlander Equation.....	43
2.5.12	Damaging effects	44

2.6	Thermal Heat Flux Models.....	45
2.6.1	Solid Flame Model.....	45
2.6.2	BLEVE Model.....	45
2.7	Machine Learning Regression Models.....	45
2.7.1	Relevance	45
2.7.2	Previous Research	46
2.7.3	Considerations of Model Design	47
2.7.4	Training Data Considerations.....	47
2.8	“Decision Tree” Machine Learning Algorithms	48
2.8.1	Decision Tree Learning	48
2.8.2	Random Forest Model.....	48
2.8.3	Extremely Randomised Trees Model	48
2.8.4	Gradient Boosting Models	49
2.9	Alternative Machine Learning Algorithms.....	49
2.9.1	K-Nearest Neighbours.....	49
2.9.2	Support Vector Regression	50
2.9.3	Multi-Layer Perceptron	50
2.9.4	Model Performance Metrics	51
2.9.5	Model Validation Techniques	53
2.10	CFD Governing Equations.....	54
2.10.1	Conservation of mass	55
2.10.2	Conservation of momentum	55
2.10.3	Conservation of energy.....	55
2.10.4	Species Transport Modelling.....	56
2.10.5	Turbulence Modelling.....	56
2.11	Hydrogen Leakage Safety Analysis Software.....	57
2.11.1	PHAST	58
2.11.2	Gexcon Software Including FLACS – CFD	58
3	Applications.....	60
3.1	Better than Batteries	60
3.2	Shipping Industry	60
3.3	Fuel Cell Vehicles	62
3.4	Space Industry.....	62
4	Methodology	63
4.1	Method Aim.....	63
4.2	Safety Limits	63

4.2.1	Safety Limits for Overpressure	63
4.2.2	Safety Limits for Thermal Radiation	65
4.3	Hydrogen Leakage: Possible Worst-Case Scenario	66
4.3.1	Layout of hydrogen storage facilities	67
4.3.2	Pressure vessel data.....	68
4.3.3	Surroundings and Environmental factors	69
4.4	Traditional Methods for Overpressure Calculation.....	69
4.4.1	Curve Fitting Estimation Method	69
4.4.2	TNT Equivalency Method	70
4.4.3	TNO Multi-Energy Method.....	71
4.4.4	Baker-Strehlow-Tang (BST) Method	72
4.5	Traditional Methods for Heat Flux Calculation	72
4.5.1	Solid Flame Model.....	73
4.5.2	Radiation due to BLEVE's Model	74
4.6	Machine Learning for Overpressure Calculation.....	75
4.6.1	Experimental Method Goals	75
4.6.2	Experimental Data.....	75
4.6.3	Machine Learning Model Selection	75
4.6.4	Model Hyperparameter Tuning.....	76
4.6.5	Model Validation.....	77
4.7	Implementation	77
4.7.1	Implementation Of Estimation Methods.....	77
4.7.2	Considerations	77
5	CFD.....	78
5.1	CFD Model.....	78
5.2	Geometry Design	78
5.3	Mesh Design.....	80
5.4	Setup	82
5.5	CFD Post	83
6	Sensitivity Analysis.....	84
6.1	Traditional Method Analysis.....	84
6.2	Machine Learning Method Analysis	84
7	Results	85
7.1	Machine Learning Model Performance Scores	85
7.2	Traditional Methods Sensitivity Analysis	87
7.3	Machine Learning Methods Sensitivity Analysis	90

7.5	CFD Results	91
7.6	Final Prediction Results	94
7.6.1	Overpressure Results.....	95
7.6.2	Heat Flux Results	98
7.6.3	Overpressure Method Performance Scores	99
8	Discussion.....	101
8.1	Machine Learning Performance Comparison.....	101
8.2	Pressure Methods Performance Comparison	101
8.3	Sensitivity Analysis	102
8.4	CFD Results Analysis	102
8.5	Pressure Methods Results Analysis	103
8.6	Heat Flux Methods Results Analysis	104
8.7	Limitations.....	104
8.7.1	Data Sparsity.....	104
8.7.2	Time Scale	105
9	Guided example	106
10	Further Work	109
11	Conclusion	111
12	References.....	112
13	Appendices	124
13.1	Appendix 1 – Hydrogen VCE Experimental Dataset.....	124
	Appendix 2: Group Work and Project Management Reflection	126

Nomenclature

Symbol	Description	Units
AEGL	Acute Exposure Guideline Levels	
AI	Artificial intelligence	
ATEX	Explosive atmospheres	
BLEVE	Boiling Liquid Expanding Vapour Explosions	
BST	Baker-Strehlow-Tang	
CE	Construction Equipment	
CFD	Computational Fluid Dynamics	
CO ₂	Carbon Dioxide	
DDT	Deflagration to Detonation Transition	
DNV	Det Norske Veritas	
EU	European Union	
FCV	Fuel Cell Vehicles	
FLACS	Flame Acceleration Simulator	
H ₂	Hydrogen	
HAZ	Heat Affected Zones	
HHV	Higher Heating Value	
HIAD	Hydrogen incident and Accident Database	
HIRD	Hydrogen Incident Reporting Database	
IHA	Ignition Hazard Assessment	
LAPs	Legal and Administrative Processes	
LHV	Lower Heating Value	
MAE	Mean Absolute Error	
ML	Machine Learning	
MSE	Mean Square Error	
N ₂	Nitrogen	
NASA	National Aeronautics and Space Administration	
O ₂	Oxygen	
PHAST	Process Hazard Development Software	
RMSE	Root Mean Square Error	
SMAPE	Symmetric Mean Absolute Percentage Error	
SVM	Support Vector Machine	
SVR	Support Vector Regressor	
TDU	Thermal Does Unit	
TNO-ME	TNO Multi-Energy	
TNT	Trinitrotoluene	
UAC	Umoe Advanced Composites	
UN	United Nations	
VCE	Vapour Cloud Explosion	

∂P	Rate of change of pressure	Bar/s
∂T	Rate of change of temperature	K/s
ΔH	Lower heat of combustion of hydrogen	kJ/kg
ΔH_{TNT}	Lower heat of combustion of TNT	kJ/kg
μ_{JT}	Joule-Thompson Coefficient	K/bar
A	Curve fitting coefficient 1	
B	Curve fitting coefficient 2	
C	Hydrogen volume fraction in the vapour cloud	K/Pa

C_p	Heat capacity of the gas	J/K
D	Distance	m
D_f	Fireball diameter	m
$D_{i,m}$	Species' mass diffusion coefficient	
$D_{T,i}$	Thermal diffusion coefficient	
e	Emissivity factor	
E	Energy	J
F	Body force	N
G_b	Turbulence kinetic energy generated (as a result of buoyancy)	J
g_i	Gravitational component in the direction i	m/s^2
G_k	Generation of turbulence kinetic energy due to the mean velocity gradient	
H_c	Heat of combustion	J/m^3
J_i	Diffusion flux for a species, i	$mol m^{-2} s^{-1}$
m	Mass of gas molecules present	kg
M_{cloud}	Mass of hydrogen cloud	kg
M_{TNT}	Mass of equivalent TNT	kg
n	Number of moles of gas molecules present	moles
P	Pressure	Pa
P'	Scaled pressure	
P_a	Ambient pressure	Pa
Pr_t	Turbulent Prandtl number for energy	
P_w	Partial vapour water pressure at atmospheric conditions	Pa
q	Thermal radiation from the cloud	kW/m^2
R	Universal gas constant	8.31434 Nm/molK
R^2	Coefficient of determination	
R_H	Specific gas constant for hydrogen	4124.18 Nm/kg K
R_i	Net rate of production by chemical reaction for a species, i	
Z	Scaled distance	
S_i	Rate of creation by addition from the dispersed phase plus any user-defined source	
S_m	Source Term	
SS_{res}	Sum of squares of residuals	
SS_{total}	Total sum of squares	
T	Temperature	K
t^+	Duration of positive pressure phase	s
T_f	Fireball flame temperature	K
t_n	Time of arrival of shockwave	s
V	Volume	m^3
V_c	Volume of hydrogen in the cloud	m^3
W_n	Mass of explosive substance	kg
X	Distance from origin for the given overpressure	m
Y_a	Actual values from the test dataset	
Y_M	Fluctuating dilatation contribution overall dissipation rate for compressible turbulence	

y_p	Predicted values from the model	
Z	Compressibility factors	
Z_p	Flame height	m
α or β	Coefficient of thermal expansion	1/K
ΔH	Lower heat of combustion of hydrogen	MJ/kg
ΔH_{TNT}	Lower heat of combustion of TNT	MJ/kg
ΔP	Pressure change	Pa
ϵ	Dissipation rate	
η	Explosion efficiency	%
θ	View factor angle (in degrees)	°
μ	Molecular viscosity	
ρ_c	Density of hydrogen at atmospheric conditions	kg/m ³
ρg	Body force	N
τ	Atmospheric transmissivity	

Table of Figures

Figure 1: Ideal and Real Gas Relationships for Pressure vs. Density [9].....	21
Figure 2: HHV and LHV Values for Hydrogen Compared to Various Fuels [9].	23
Figure 3: Energy Densities for Hydrogen Compared to Various Fuels [9]....	23
Figure 4: Joule-Thompson Coefficient Curve.....	24
Figure 5: Threat levels Associated with Hydrogen [15].....	25
Figure 6: Propagation of Shockwaves.	39
Figure 7: Overpressure vs. Scaled Distance Curves for TNO Multi-Energy Method.....	41
Figure 8: Mach Number Overpressure-Distance Curves.	42
Figure 9: Pressure-Time Graph of a Blast Wave measured from inside a Vehicle [73]	43
Figure 10: Decaying Profile of a Pressure Curve.	44
Figure 11: Illustration of Perceptron (left) and Multi-Layer Perceptron (right) Neurons and Layers[101].....	51
Figure 12: Visual Representation of 10-fold Cross Validation Dataset Train/Test Splitting [104].	54
Figure 13: Example Images of Hydrogen Release and Explosion CFD Modelling Using FLACS Software [109].....	59
Figure 14: Overpressure Values for Expected Damages to Buildings and Structures [125].....	63
Figure 15: Effects Observed at Various Overpressure Values [126].....	63
Figure 16: Damage Observed at Various Overpressure Values [126].	63
Figure 17: Pressure Wave Effects at Various Overpressure levels (kPa) [24].	64
Figure 18: Map of Health, Radiation and Pressure Effects [24].	65
Figure 19: Varying Thermal Radiation Effects Diagram [24].	66
Figure 20: Potential Outcomes of an Accidental Hydrogen Release [109]... <td>66</td>	66
Figure 21: Pressure Vessel Data Relevant to the Selected Hydrogen Storage (highlighted in the red box) [42].....	68
Figure 22: Aerial View of the Storage Facility CFD Model. 3 Hydrogen Gas Cylinders and 2 Buildings can be Observed.	79
Figure 23: Enlarged Isometric View of the 3 Cylindrical Hydrogen Gas Storage Vessels. The Leak Orifice is Located at the Origin.....	79
Figure 24: Isometric View of the 3 Hydrogen Gas Cylinders and 2 Buildings.	80
Figure 25: Close-up view of Pressure Vessel Leakage hole in CFD Mesh..	81
Figure 26: Vertical Cross Section view of CFD Mesh, Showing Spheres of Element Size Influence.	81
Figure 27: View of CFD Mesh around Pressure Vessel Geometry.	82
Figure 28: Graph of Best Performing Estimators R2 Scores.....	86
Figure 29: Graph of Best Performing Estimators Mean Square Errors.	86
Figure 30: Traditional Methods Sensitivity Analysis - All Results.....	88
Figure 31: Traditional Methods Sensitivity Analysis - Mean, Maximum and Minimum Results.	89
Figure 32: ExtraTrees Model Sensitivity Analysis - All Results.	90

Figure 33: ExtraTrees Model Sensitivity Analysis - Mean, Maximum and Minimum Results.....	90
Figure 34: Cloud Volume vs. Time Plot from CFD Results.....	91
Figure 35: Mass of Hydrogen in Cloud vs. Time Plot from CFD Results.....	91
Figure 36: Average Hydrogen Volume Fraction vs. Time Plot from CFD Results.....	92
Figure 37: 3D Visualisation of CFD Hydrogen Dispersion at Various Timesteps (Growth of Cloud).	94
Figure 38: Overpressure vs. Distance Predictions for 0.2s CFD Hydrogen Cloud Data.....	95
Figure 39: Overpressure vs. Distance Predictions for 1.0s CFD Hydrogen Cloud Data.....	96
Figure 40: Overpressure vs. Distance Predictions for 5.0s CFD Hydrogen Cloud Data.....	96
Figure 41: Overpressure vs. Distance Predictions for 10.0s CFD Hydrogen Cloud Data.....	97
Figure 42: Heat Flux vs. Distance Predictions for Solid Flame Model.....	98
Figure 43: Heat Flux vs. Distance Predictions for BLEVE Heat Flux Model.	99
Figure 44: Comparison of Mean Square Error of Pressure Methods with 10-Fold Cross Validation.....	100
Figure 45: Comparison of R2 Score of Pressure Methods with 10-Fold Cross Validation.....	100
Figure 46: Overpressure vs. Distance Results Highlighting Machine Learning Behaviour.....	103

Executive Summary

While batteries are an effective solution to combat the effects of climate change and the impact of fossil fuels on the environment, humankind cannot solely rely on this technology to support our everyday lives in the 21st century. Alternative solutions which provide clean energy are crucial to the future of society. Hydrogen is one such alternative which is produced as a gas through the emission-free process of electrolysis where it can be easily transported and stored for future use. This form of green energy is already used in emission-free hydrogen fuel cell vehicles and breakthrough changes in the shipping industry. This is an area which shows huge potential, with significant developments made in recent years. As with any new technology, potential dangers and safety implications must be considered to ensure a safe rollout for various applications. Investigations and studies into this topical area are highly anticipated and the safety analysis presented in this work aims to better prepare society for the future applications of hydrogen gas. As demand for these applications increases, so too will the need for hydrogen and hydrogen storage which is the specific area this study is concerned with. This research presents a systematic methodology for calculating safety distances from hydrogen gas containers, should leakage followed by an explosion occur. These safe distances are determined corresponding to maximum levels of overpressure and heat flux from the explosion.

Hydrogen is renowned as a highly flammable and potentially dangerous chemical which should be used with caution, particularly in large quantities and industrial applications. Substantial research was carried out to investigate these behaviours as well as the dispersion, ignition and explosion characteristics of hydrogen gas. A number of studies concerned with these concepts were consulted and found to be most insightful in gaining a background understanding of the topic. Other safety investigations related to existing hydrogen applications were analysed to appreciate current knowledge and findings associated with this topic, and any recommendations which should be considered for future safety analyses. Standards and regulations play an important role in preparing society for new innovative technologies as well as highly explosive and dangerous substances which can result in fatalities. Therefore, European and international safety standards related to the handling of hydrogen and hydrogen storage were explored in detail. As this investigation is primarily concerned with hydrogen gas storage in Finland, Finnish chemical agency (Tukes) standards were useful in establishing safety distances for the hydrogen gas leakage scenario at the heart of this project. Reasons for hydrogen leakage and the ways this is measured are also explored. For example, material defects and hydrogen embrittlement of the storage vessel are potential explanations for leakage which can be detected using specialist thermal imaging cameras. These areas all played a crucial role in understanding the background of the topic and were discussed as part of an extensive literature review which may be a useful reference for similar studied in future.

While this project is a hydrogen safety analysis where the principal aim is establishing safe distances from hydrogen gas containers, it is worthwhile acknowledging the real-world applications which may benefit from the creation of new hydrogen gas storage facilities and the developed methodology which can be used to establish safe distances at such places. In 2021 one of the first hydrogen powered ferries in the world – with completely zero emissions - underwent operational testing in the San Francisco Bay area of California. The launch of Cellcentric – a hydrogen fuel cell manufacturer - was announced in April 2021 further demonstrating the increasing demand for hydrogen powered technology. The potential use of hydrogen to power haulage trucks, construction equipment and even rockets for future space missions are also investigated.

The initial research stage of this study also involved investigating various methods which were later utilised to evaluate the overpressure at a range of distances resulting from a hydrogen vapour cloud explosion as well as heat flux values at various distances. In total, 4 methods were employed in this research to investigate overpressure – the pressure over and above atmospheric pressure, resulting from the shockwave of the explosion. These 4 methods are the Curve Fitting Estimation Method, TNT Equivalence Method, TNO-ME Method and BST Method. During this research, overpressure methods were found to be well documented across the literature. This became the primary area of focus as heat flux methods associated with hydrogen vapour cloud explosions were seldom documented. As a result, only 2 methods for calculating heat flux from hydrogen vapour cloud explosions could be utilised. Furthermore, these methods required various assumptions to be made and were therefore not as reliable as the methods related to overpressure. Nonetheless, 6 traditional methods were implemented allowing for the production of notable results.

As well as traditional methods, a new, data-driven method was successfully developed, implemented, and tested using an experimental dataset of results from controlled unconfined, open-air hydrogen cloud explosion tests. This new method is implemented using a machine learning model that is based around an ensemble of decision trees, known as the Extremely Randomised Trees model. During development, the Random Forest, Gradient Boosted Trees k-Nearest Neighbours, Support Vector Machine, and Multi-Layer Perceptron algorithms were also tested in an attempt to find the best suited for this problem. The models were also extensively validated with 10-fold randomly shuffled cross validation used to ensure confidence in the results. The models were also extensively tuned to find the best performing parameters that produce the most accurate results. During testing this new method showed good performance when compared using statistical accuracy and error metrics.

CFD can enhance safety in industry with the capability of accurately modelling a number of different leakage accidents which can then lead to improvements in mitigation measures. The main purpose of CFD in this project is to provide the input variables which are utilised within traditional

calculation methods and machine learning methods. ANSYS Fluent software was selected to model the hydrogen gas leakage scenario under investigation and provide values of the flammable hydrogen cloud volume (m^3) and hydrogen volume fraction. The hydrogen leakage scenario which forms a potentially explosive cloud is simulated with species transport modelling which uses a convective-diffusion equation. The realisable k- ϵ model was selected to model turbulence where the distinctive buoyancy properties of hydrogen are considered.

The specific hydrogen storage leakage scenario under investigation is a difficult challenge to model successfully for various reasons such as complex flows resulting from high storage pressures and a high number of required elements to capture the simulation making the simulation computationally intensive. A 3D transient simulation of a potential worst-case leakage scenario was successfully created using CFD, forming the basis of what is required to calculate safety distances, should ignition and explosion occur. The CFD simulation conducted in this report is purely concerned with modelling the hydrogen cloud formation and dispersion, while avoiding any simulation of an explosion.

The stakeholder's recommendations on the general layout of the storage site and also Type IV pressure vessel data were used to create the geometry of the model. An iso-volume representing the flammability limits of hydrogen and an inserted formula to calculate hydrogen mole fraction were used to produce final CFD results. The final results were then used as inputs for the following calculation methods to produce safe distance estimations.

A sensitivity analysis was undertaken to observe how small changes in the input values for the various pressure methods affected the produced results. A Monte-Carlo simulation was executed for the sensitivity analysis of both traditional pressure calculation methods and machine learning methods. The simulations found results corresponding to 1000 random samples of cloud volume for each method (and hydrogen concentration where applicable), assuming a uniform distribution of values for each variable, with a maximum variation of 20%. Ultimately this analysis established confidence in the various pressure methods, ensuring they can be used for real-world hydrogen safety distance predictions.

Several important results are produced in this report in order to determine final estimations of safe distances and also test the performance and sensitivity of both the traditional calculation methods and machine learning methods used. The final average R^2 (coefficient of determination) scores and mean square error results of the 10-fold cross validation scheme, as well as the tuned hyperparameter values were all parameters investigated for machine learning model performance scores (for the best performing estimators). Extremely randomised trees showed to have the highest general performance out of the best machine learning estimators. A Monte Carlo sensitivity analysis was performed for the various traditional pressure estimation methods, using CFD outputs for the analysis. Important CFD results such as cloud volume and hydrogen volume fraction are described

through various figures and in an extensive dataset. Hydrogen leakage results up to a time of 15s after initial release, with an increment of 0.2s are displayed in results which show the cloud volume increasing with time as expected and the average volume fraction of the flammable cloud decreasing with time. Safety distances are provided for a wide range of ignition time scenarios. Various overpressure vs distance and heat flux vs distance curves were produced which represent each calculation method investigated. The most important overpressure and thermal radiation values used to produce safe distances for the purposes of the project were 10kPa of overpressure and 8kW/m² for thermal radiation as agreed with the stakeholders. This is in line with recommended values described by the Finnish Safety and Chemicals Agency, Tukes. The safe distances were calculated by inputting an overpressure or heat flux guideline value into the calculation methods which returned a distance output.

The results of the Monte Carlo sensitivity analysis, accuracy metric results for the traditional and machine learning pressure estimation methods, CFD simulation results, as well as the overall estimation results of both the pressure and heat flux estimation methods were analysed and discussed, in order to establish the behaviours and trends of each method, as well as to investigate the optimal choice for estimation. This allowed for meaningful conclusions to be drawn from the results of the project. This also proved useful in establishing the results from comparison of different estimation methods.

A full guided example is included in the report with the intention of making this project fully repeatable for other researchers/students or otherwise. With this in mind, people may use this project as a starting point for further studies and adapt the methods used here in a way that may be more relevant to their research. The guided example is useful to anyone who wishes to analyse safe distances for hydrogen storage. This project focussed on safe distances for an industrial environment, but the same methodology could be applied - with some adjustments - to simulate safe distances for other environments such as a hydrogen refuelling station for example. The guided example outlines 5 main requirements that are needed in order for the numerical code to successfully predict safety distances. Once the code has the required inputs, graphs of Overpressure vs Distance and Heat Flux vs Distance are produced by the various traditional methods and machine learning methods. It is up to the user's discretion which regulation or standards they wish to follow for maximum overpressure and maximum heat flux (this may be a regional based decision). Once the maximum values have been decided, the corresponding minimum safety distances can be prescribed.

Given the limited time allocated to complete this research, there are a number of areas which could have been further investigated or given greater consideration. While a sensitivity analysis was performed to validate the machine learning methods and code which ultimately provide the results of this study, a CFD mesh sensitivity analysis was not considered in this investigation due to the project schedule and the high computational

demands of the CFD model. However, this would be a very useful analysis and area of future work which would give greater confidence in the suitability of the mesh. The effect of weather conditions such as wind speed and direction on the final results could also be investigated. Other important parameters which could be explored in future work are; the size of the leakage orifice, the level of congestion such as surrounding buildings, vessel pressure and flammable cloud shape. Future work is highly anticipated in this area, as with more investigations and research comes greater knowledge of safety considerations related to the storage and use of hydrogen.

The advancements made in hydrogen powered innovations are a viable solution to reducing the effects of climate change and show great potential in transforming society towards a state of carbon neutrality. The dangerous nature of hydrogen calls to the need for safety analyses such as this research, which aims to be of great benefit in the creation of hydrogen storage locations (and other hydrogen-related facilities) where safe distances must be evaluated. This study investigated a potential worst-case scenario where hydrogen gas leaks from a storage cylinder, forming a vapour cloud which - when ignited - results in an explosion. The explosion leads to the creation of a shockwave (overpressure) and releases significant heat flux radiation. The methodology developed as part of this study evaluates the minimum safety distances from the storage vessel which should be put in place to prevent major accidents and fatalities. This safe distance is found corresponding to the location of maximum overpressure and maximum heat flux. A user guide was developed as part of this methodology, for use in future analyses like this. This user guide, methodology and extensive background research aim to better prepare the world for hydrogen powered applications which will improve the future of society.

1 Introduction

As climate change and global warming tightens its grip on our planet, mankind is increasingly looking for alternative sources of clean energy generation and storage in an effort to lower our carbon footprint or “decarbonise”. Many solutions have been brought to life as a result of this effort. The last few decades have seen a global shift from fossil fuels as a means of energy generation, to clean alternatives such as solar and wind power. While the solution of clean renewable energy is clear, energy storage remains an unresolved problem in terms of storage efficiency, storage medium, and the harmful emissions of constructing energy storage solutions. Traditional batteries - while an effective energy storage solution - cannot scale to meet the needs of mankind as a sole solution without considerable advancement in energy density and charging technology, as well as requiring large amounts of rare earth minerals to build, leading to a large carbon footprint during production. It is clear that batteries cannot solve every carbon dioxide (CO_2) related problem.

Hydrogen is a viable alternative as an energy storage solution. The clean power generated from renewable sources can be used to generate and store the gas for later consumption, and the process of production from water is emission-free. Hydrogen can be used as a replacement for traditional battery technology in applications such as hydrogen fuel cell powered vehicles and can also be used as an alternative fuel in existing internal combustion engines with little modification. Hydrogen fuel cells are currently in use to power many forms of vehicle, including cars, buses, and fork lifts. Hydrogen is also used as a fuel for rockets.

Hydrogen's use as a clean fuel presents many challenges in terms of safety and has proven to be very dangerous in the case of accidents. Hydrogen is most often stored at very high pressure in static tanks and is naturally highly flammable. This could lead to catastrophic consequences in the event of a pressure vessel rupture and/or ignition. This paper aims to provide a systematic methodology for estimating the safe distances of hydrogen storage containers in an industrial processing environment. This methodology uses CFD (Computational Fluid Dynamics) simulations to model a hydrogen leakage scenario in order to generate input variables for both traditional calculation methods and machine learning calculation methods.

As hydrogen demand increases with developing technologies over the coming years, safety analyses will play a crucial role in minimising the likelihood of catastrophic hydrogen leakage accidents. The methodology will take into consideration both a safe pressure limit and thermal radiation limit when estimating the safe distance from a hydrogen vessel.

2 Literature Review & Background

To better understand the topic and gain insight into the area of hydrogen and hydrogen storage, substantial research was carried out and numerous investigations were consulted as part of the extensive literature review and background introduction, presented in this section.

2.1 Hydrogen Characteristics

2.1.1 Ignition

Hydrogen has been extensively documented as a highly flammable and dangerous substance when ignited, combusting with incredible speed and energy. In addition, hydrogen gas possesses some interesting characteristics concerning its combustibility limits and behaviour relating to its environment.

The flammability envelope of a hydrogen-air mixture is between 4% and 75% [1]. Mixtures outside of this range do not pose a risk of ignition or explosion, however the nature of a high-pressure hydrogen leakage - alongside the buoyancy force of the gas - poses a significant chance of efficient turbulent mixing, leading to a flammable cloud. Atmospheric conditions also play a significant role in the creation and dispersion of a flammable hydrogen-air mixture, with a noticeable atmospheric current leading to an overall reduction in hydrogen mixture concentration and faster dispersion of the gas [2]. Hydrogen has a very low density and is lighter than air by a factor of approximately 14 [3]. Its low density and buoyancy also tend to result in a faster decay and dispersion of the gas, leading to a mixture of lower concentration within a shorter time [4].

The stoichiometric mixture of hydrogen in air is 29.53%, and at this ideal mixture the ignition energy needed to start combustion is only 0.02mJ [5]. This allows for the possibility for trivial sources of ignition such as weak sparks of static electricity. The ignition energy at or near the flammability limits is much greater at around 1mJ [6], greatly reducing the chance of combustion, as a stoichiometric ratio cloud would quickly disperse to the lower flammability limit [6].

Fire damage is a non-trivial threat from ignition of hydrogen-air clouds, as the air mixture has a burn temperature of 2045°C [6], much higher than more conventional hydrocarbon mixtures.

Hydrogen has an auto-ignition temperature of 585°C [7]. The auto-ignition temperature refers to the minimum temperature that hydrogen will spontaneously ignite without the presence of an external ignition source such as a spark or flame when the gas is at standard atmospheric conditions.

2.1.2 Dispersion

The hydrogen concentration of a cloud caused by a leakage has been found to be highest when the atmospheric conditions are slight winds (around 1m/s) [6]. This behaviour is due to the light winds causing efficient turbulent mixing of the cloud, assisting in its dispersion without spreading the cloud over a very large area.

Initially after a pressure vessel rupture occurs, the hydrogen escape velocity is at its highest, before decaying with time as the pressure inside the vessel is released to the atmosphere. During the later stages of the rupture when the escape velocity is low, the hydrogen mixture concentration is generally below the lower flammability limit during low wind conditions [6]. However, the rupture escape velocity required to create a flammable mixture increases with wind velocity.

Pasquil stability classes are a way of categorising meteorological stability for a certain situation. This categorisation ranges from very unstable weather conditions (denoted by 'A') to stable (denoted by 'F') and depends on factors such as windspeed, solar radiation and cloud cover [8]. It is expected that wind will disperse the cloud, making it less well formed.

2.1.3 Expansion

It has been found that the state of hydrogen can be very closely approximated using the ideal gas law. Due to the nature of hydrogen's atomic structure, it has a very low amount intermolecular interaction, allowing it to behave very similarly to a perfect gas with zero interaction. Hydrogen's acceptable range of accuracy when idealised includes a very wide range of temperature and pressure.

Hydrogen is an exception to most gases because it heats up rather than cools upon expansion via throttling as would be expected by the Joule-Thompson effect. There are only two other gases which heat upon expansion like hydrogen due to the Joule-Thompson effect at normal temperatures [7].

The equation of the ideal gas law is as follows:

Equation 1:

$$PV = nRT$$

This gas law combines Charles' and Boyle's laws where [9]:

P = Pressure (Pa)

V = Volume of gas (m^3)

n = Number of moles of gas molecules present

T = Temperature (K)

R = Universal gas constant (8.31434 Nm/ mol K)

The previous relationship can then produce the following equation in terms of mass for a specific gas:

Equation 2:

$$PV = mR_H T$$

Where:

m = Mass of gas molecules present

R_H = Specific gas constant for hydrogen (4124.18 Nm/kg K)

In reality, hydrogen does not accurately follow this ideal gas relationship past certain pressure values. This is because it is often stored as a high-pressure gas at pressures around 250 to 350 bar and the ideal gas relationship is only accurate up to pressures of approximately 100 bar at ambient temperature [9].

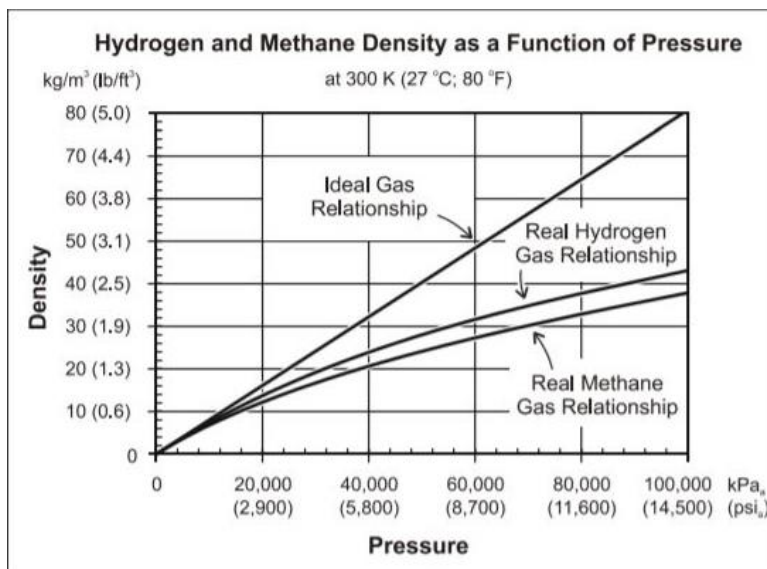


Figure 1: Ideal and Real Gas Relationships for Pressure vs. Density [9].

This graph shows how the ideal gas relationship becomes less and less accurate compared to the real gas relationship as pressure increases. There are important safety implications for which gas relationship is used to describe the gas. When considering hydrogen stored at a pressure of around 300 bar, if the ideal gas relationship was used, this would overestimate the mass flow rate of gas from a leak and therefore the amount of gas discharged [10].

Compressibility (or 'Z') factors formed from experimental data can be used to change the ideal gas relationship to fit the real gas relationship. This is given in the following relationship:

Equation 3:

$$P = z\rho RT$$

Where:

z = Compressibility factor

ρ = Density (kg/m^3)

There are benefits to storing certain fuels as liquids compared to gases. For example, they generally require less storage space in liquid form and can be handled and transported easier. However, hydrogen is naturally a gas at atmospheric conditions so must be stored cryogenically as a liquid or as a pressurised gas.

Hydrogen's expansion ratio is 1:848 meaning that at atmospheric conditions, gaseous hydrogen occupies 848 times as much volume compared to liquid hydrogen. This expansion ratio changes to 1:240 when hydrogen is stored at high pressures such as 250 bar (gauge) and atmospheric temperature [9].

Gas pressure is equal in all directions within a container according to Pascal's Law. This is the force exerted by molecules of a gas on the walls of the container it is held in.

2.1.4 Explosion Characteristics

Combustion explosions can be separated into detonations and deflagrations with the key difference between the two terms being the velocity of the wavefront. In the unburnt gas mixture, the combustion wave front propagates below the speed of sound for deflagration whereas the wave front propagates above the speed of sound for detonations [11].

Explosions from hydrogen storage can be generated by an event as trivial as a static electrical spark caused by friction. After a gas cloud of hydrogen between flammability limits is ignited, the gas molecules react forcefully, resulting in a fire or an explosion in some cases. The reaction produces water as a product which often cannot be seen as it is a superheated vapour until it cools and then appears as a cloud spreading from the leakage. This type of explosion has occurred at a number of hydrogen refuelling stations in recent years, leading to several investigations which are further discussed in section 2.3.1.

Fuels have a Higher Heating Value (HHV) and Lower Heating Value (LHV) associated with them. This is an amount of energy liberated in a complete reaction of the fuel with oxygen which forms water as the product. The key difference between HHV and LHV is an amount of energy for a fuel known as the 'heat of vaporisation'. For HHV, the combustion products are returned to

pre-combustion temperatures whereas LHV is calculated by the difference between HHV and heat of vaporisation.

Fuel	Higher Heating Value (at 25 °C and 1 atm)	Lower Heating Value (at 25 °C and 1 atm)
Hydrogen	61,000 Btu/lb (141.86 kJ/g)	51,500 Btu/lb (119.93 kJ/g)
Methane	24,000 Btu/lb (55.53 kJ/g)	21,500 Btu/lb (50.02 kJ/g)
Propane	21,650 Btu/lb (50.36 kJ/g)	19,600 Btu/lb (45.6 kJ/g)
Gasoline	20,360 Btu/lb (47.5 kJ/g)	19,000 Btu/lb (44.5 kJ/g)
Diesel	19,240 Btu/lb (44.8 kJ/g)	18,250 Btu/lb (42.5 kJ/g)
Methanol	8,580 Btu/lb (19.96 kJ/g)	7,760 Btu/lb (18.05 kJ/g)

Figure 2: HHV and LHV Values for Hydrogen Compared to Various Fuels [9].

The amount of energy liberated per mass of hydrogen fuel in a reaction is approximately 2.5 times greater than other traditional fuels given in the table above. This is a certain advantage as a smaller mass of hydrogen can be used to match the same energy produced by comparative hydrocarbon fuels for a particular function.

Fuel	Energy Density (LHV)
Hydrogen	270 Btu/ft ³ (10,050 kJ/m ³); gas at 1 atm and 60 °F (15 °C) 48,900 Btu/ft ³ (1,825,000 kJ/m ³); gas at 3,000 psig (200 barg) and 60 °F (15 °C) 121,000 Btu/ft ³ (4,500,000 kJ/m ³); gas at 10,000 psig (690 barg) and 60 °F (15 °C) 227,850 Btu/ft ³ (8,491,000 kJ/m ³); liquid
Methane	875 Btu/ft ³ (32,560 kJ/m ³); gas at 1 atm and 60 °F (15 °C) 184,100 Btu/ft ³ (6,860,300 kJ/m ³); gas at 3,000 psig (200 barg) and 60 °F (15 °C) 561,500 Btu/ft ³ (20,920,400 kJ/m ³); liquid
Propane	2,325 Btu/ft ³ (86,670 kJ/m ³); gas at 1 atm and 60 °F (15 °C) 630,400 Btu/ft ³ (23,488,800 kJ/m ³); liquid
Gasoline	836,000 Btu/ft ³ (31,150,000 kJ/m ³); liquid
Diesel	843,700 Btu/ft ³ (31,435,800 kJ/m ³) minimum; liquid
Methanol	424,100 Btu/ft ³ (15,800,100 kJ/m ³); liquid

Figure 3: Energy Densities for Hydrogen Compared to Various Fuels [9].

A key point to note is that hydrogen burns more intensely compared to other fuels such as gasoline but this lasts for a shorter duration in comparison. Combustive energy tends to be inversely proportional to the time period of conflagration. Conflagration is a large, destructive fire.

2.1.5 The Joule-Thompson Effect

There is a nuanced behaviour of hydrogen exhibited during the process of "throttling" (the forcing of a fluid or gas through a small orifice at considerable pressure). The Joule-Thompson effect describes the change in temperature of an imperfect gas during the throttling process and can be calculated using the Joule-Thompson coefficient - a unique quantity that varies with the temperature of the gas. This quantity can be negative or positive, depending

on the temperature of the gas in relation to its “inversion temperature”. If the gas is below the inversion temperature, the coefficient is positive and the gas cools upon expansion from throttling, while the opposite is true if the gas is above the inversion temperature. Most gases tend to cool upon expansion at standard atmospheric conditions. This is due to work which is done to overcome the long-range attraction between gas molecules as they separate from each other. However, in the case of hydrogen these long-range attraction forces are exceptionally weak. Therefore, hydrogen heats up upon expansion at temperatures above the inverse Joule-Thomson temperature. [10]. Helium also possesses a negative Joule-Thompson coefficient at regular working temperatures, with an inversion temperature of 40K.

The inversion temperature of hydrogen is 220K. Any throttling of hydrogen above this temperature will result in the gas warming. A graph of the Joule-Thompson coefficient curve against temperature is shown below [12].

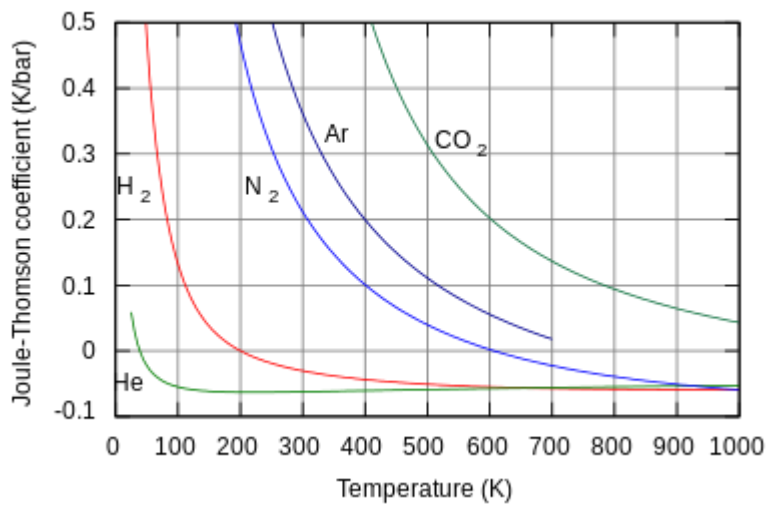


Figure 4: Joule-Thompson Coefficient Curve.

The Joule-Thompson coefficient is calculated as the rate of change of temperature of the gas with respect to the rate of change of its pressure (at constant enthalpy) and can also be expressed with respect to its properties as shown below.

Equation 4:

$$\mu_{JT} = \left(\frac{\partial T}{\partial P} \right) = \frac{V}{C_p} (\alpha T - 1)$$

Where:

μ_{JT} = Joule-Thompson Coefficient

∂T = Rate of change of temperature

∂P = Rate of change of pressure

V = Volume of the gas

C_p = Heat capacity of the gas

α = Coefficient of thermal expansion

T = Temperature of the gas

2.1.6 Investigations of Hydrogen Characteristics

A study of explosion characteristics related to hydrogen-air and hydrogen-oxygen mixtures by Schroeder et al was consulted during research into this topic for it is necessary to understand more about the behaviour of hydrogen gas and how it reacts in atmospheric conditions before understanding its involvement in industrial processes [13]. Furthermore, the study brings to the attention of the reader important industry standards related to explosion limits and the associated testing methods for such explosions. Akin to the present study, Schroeder et al investigated pressure effects on explosion limits.

Similar studies regarding hydrogen characteristics such as flammability, safety distances and deflagration were explored. These topics are discussed in depth by multiple studies and more importantly, controlled and regulated by various standards committees and bodies [14]. Given the present study is a safety analysis, these standards which have been created will play a fundamental role in the calculation of safety distances and therefore were given great consideration. More information regarding standards is provided in the following section.

2.2 Safety Considerations and Standards

2.2.1 Hydrogen Storage Safety

The ignition and explosive characteristics of hydrogen coupled with its physical properties related to its density at room temperature, as well as its colourless, odourless, and tasteless nature, present it as extremely dangerous. This is a potential hazard when stored in high pressure containers in large volumes, with the possibility of leakage, rupture and ignition. Hydrogen was assigned a level 4 (highest) status for flammability by the U.S. based National Fire Protection Association, in the NFPA-704 "Identification of Hazards of Materials" safety standard [15].

NFPA 704			
Diamond	Hazard	Value	Description
	Health	0	No hazard beyond that of ordinary combustible material.
	Flammability	4	Burns readily. Rapidly or completely vaporizes at atmospheric pressure and normal ambient temperature.
	Instability	0	Normally stable, even under fire conditions.
	Special		

(NFPA, 2010)

Figure 5: Threat levels Associated with Hydrogen [15].

Numerous safety and regulatory standards concerning the general safety guidelines of hydrogen storage and related systems, hydrogen storage vessel requirements, hydrogen processing safety guidelines, and many other hydrogen related operations and situations, have been developed and implemented by many regulatory committees. These have been adopted by countries and governing bodies around the world.

2.2.2 Studies of Standards & Governing Bodies

'Flammability of gases in focus of European and US standards' also written by Schroeder et al [16] was useful as an initial means of understanding various specific European and American standards – although only European standards will be consulted in this research. In their study, different standard test methods were carried out and the results compare. This was interesting to understand how different standards in different countries are created. The standards are so profoundly relied upon, to ensure the safety and protection of human lives, yet different international committees follow separate criteria to distinguish and create these standards. It was concluded that the varying test methods affected explosion limits and gas concentrations. As the study points out, it is important to follow the discussion on both sets of standards in the hope that one day global standards may be determined primarily through calculation methods, CFD modelling and any relevant incident data.

Other country-specific standards related to hydrogen safety regulations were also researched. The German hydrogen regulation, codes and standards road map from Wuster and Hof [17] sets out a projected year-by-year timeline of the creation of hydrogen legislation and the corresponding hierarchy of UN (United Nations) regulations, EU (European Union) law, German law and standards. Like other studies, the paper agrees that German standards and regulation are highly necessary for the future success and growing demand of hydrogen and that the development of international and European standards will continue to aid in this task. This notion is further evident across the associated literature.

On the point of European standards, HyLAW - a relatively new public access database coordinated by Hydrogen Europe - was created with the express purpose of documenting legal requirements and other regulations concerning innovative hydrogen technologies across 18 countries within Europe [18]. A user may define specific inputs such as an origin country, hydrogen application, legal and administrative processes (LAPs) and the tool will return specific requirements concerning the user defined hydrogen application and related legislation particular to that region. It is efforts such as HyLAW which aim to break down the barriers and accelerate society towards a hydrogen economy.

The advent of a hydrogen economy has been further derived from many nations' commitment to achieving net-zero carbon status, as well bringing the agreements specified in the Paris agreement to fruition. This is highlighted in reports such as the European Commissions "a Hydrogen strategy for a climate neutral Europe", which promotes a future of hydrogen-based technology [19]. With regards to improving safety standards in this area, the report emphasises that research such as this is highly necessary.

While this research considers European standards, there is a clear worldwide desire for emerging hydrogen energy, related hydrogen technologies and global standards. This is evident in countless articles and reports from several nations across the globe – more so in recent years [20][21]. With

efforts such as this research, the world may be better prepared for these innovative and sustainable hydrogen technologies.

The International Conference on Hydrogen Safety was held in Edinburgh, Scotland between 21-24th September 2021 which is fitting for Scotland, who the Scottish Government claim to have a “favourable reputation as an early adopter and innovation leader in hydrogen initiatives, hosting some of Europe’s major demonstration fleets” [22]. This is evident in Scotland’s Hydrogen assessment project which was initiated after the Scottish government declared their aim to be net zero by 2045 [23].

The Finnish Safety and Chemicals Agency, Tukes produced a document concerning production facilities’ placement. This will henceforth be referred to as the ‘Tukes document’ or ‘Tukes report’, including important safety information and recommendations regarding chemical leakages and explosions for a number of different industrial scenarios. In conjunction with Elomatic, this report would focus on an outdoor, semi-unobstructed hydrogen leakage scenario. Furthermore, this project would focus more heavily on hydrogen storage scenarios in an industrial environment (which the Tukes document provides insightful descriptions of) with process equipment as opposed to fuelling stations for hydrogen powered vehicles.

However, the developed methodology may be applied to any site where hydrogen leaks are possible. The Tukes report gives insight into potential accidents that may arise from the storage of hazardous chemicals, and advice on where the chemical storage should be located on the industrial site in terms of the surroundings. Potential accidents from chemical storage include leaks and explosions and these can have a large variation in impact and severity depending on the situation. The consequences of different accident scenarios are discussed in Tukes guidelines as well as safety distance recommendations. Although quite useful, Tukes’ report does not include calculation models for predicting the consequences of an accident [24].

Acute Exposure Guideline Levels (AEGL) describes the human health effects when an individual is exposed to a hazardous concentration of airborne chemicals. Leakage from a gas storage vessel is an example of when hazardous airborne chemicals can be produced. AEGL standards can be consulted when investigating the worst-case scenario of a gas leakage to better understand how these chemicals affect people (general public including susceptible individuals) in the vicinity of the leakage site for a given exposure time. AEGL standards should be used for a rare, unlikely chemical event which does not exceed 8 hours. Workplace exposure limits should be used instead for workers routinely exposed to certain chemicals. AEGLs can be separated into 3 tiers for a given exposure duration, each one differing in severity of health consequences. AEGL-3 is the airborne concentration of a chemical that can cause life-threatening effects or death. AEGL-2 is for serious long-term or irreversible effects and AEGL-1 describes concentration levels that can cause irritation and discomfort, however for AEGL-1 these effects are reversible after the affected person is no longer subjected to the

chemical for a period of time. There are 5 standard exposure periods for each AEGL standard ranging from 10 minutes to 8 hours [25].

For a health risk assessment, the Finnish Safety and Chemicals Agency, Tukes suggests that AEGL-3 for 30 minutes should be used as a starting point if the value is not specified. If those at risk from the chemical leakage are well protected, in a building which is easy to exit and the leakage is small then AEGL-3 for 10 minutes can be used [24].

AEGL values can be useful in gas leakage scenarios as they can be used in the safety layout of storage sites when planning where to place hazardous chemicals and also for emergency and disaster control planning [26].

2.2.3 Safe Distance Standards

“Safe distances” can be defined in several ways. Important safety considerations when selecting the location of hydrogen storage are the number of people and type of person in neighbouring buildings. Groups such as children and elderly are more at risk than the other members of the general public and so the distance of sites with a risk of explosion from buildings such as schools should be carefully considered. Other important considerations for the location of hydrogen storage are; if it is nearby an industrial site which may have reactive/explosive chemicals, the landscape of the surroundings, the surrounding environment and wildlife, and escape routes for people in the vicinity [24].

Standards SFS 3350 and SFS 3353 are described in section 5 of the Tukes report and are important for the location of chemical storage in an industrial site. These are both useful in helping to determine safe distances from storage of flammable liquids to surrounding places such as bordering neighbours. The following table, given in the Tukes report gives information regarding safe distances for storage tanks of varying volumes to external sites. Distance 1 describes a safe distance from the storage tank to non-operational buildings and Distance 2 is for places of higher risk such as schools and residential buildings [24].

Table 1: Safe Distances for Storage Vessel Sizes Defined by TUKES [24].

Storage capacity or tank size (m^3)	Distance 1 (m)	Distance 2 (m)
$1 \leq V < 10$	5	10
$10 \leq V < 50$	10	20
$50 \leq V < 200$	15	25

As a rough guide, the Tukes report reports that impact distances of toxic cloud can spread several kilometres depending on the situation. For a pipeline fire scenario, Tukes suggests that the pipe diameter could be

dimensioned as 25cm if this is unknown and a leakage time of 10 minutes could be used for a chemical dangerous to human health. In a risk assessment, an important term is the worst-case scenario (within reason) so that all necessary safety precautions are taken if this scenario was to take place. Thermal radiation intensity values generated in calculations and CFD simulations for a hydrogen leak must be less than 3 kW/m^2 if the exposure time is greater than 2 minutes or a thermal radiation dose of 600 TDU (thermal radiation units) to avoid the possibility of causing irreversible effects to human anatomy. A thermal radiation intensity of 1.5 kW/m^2 can be used to assess a safe distance for humans – the minimum distance at which people will be out with the dangerous zone of thermal radiation. Levels of thermal radiation can be reduced at a certain distance from the leakage source if methods such as “water curtain, radiation shielding or fire-resistant materials” are used. These methods are often implemented in industrial areas as a safety precaution and are particularly useful for tightly-built sites where there is limited space [24].

There is a large number of chemical hazards associated with an accident. These include: thermal radiation, pressure waves, health effects and environmental effects. As a result of these hazards, it is important that chemicals are stored at a safe distance away from buildings, people and wildlife in the surroundings of the chemical storage site to minimize the consequences of an accident. This is described in the Chemical safety act: “When designing the location of production facilities for the manufacture, handling or storage of dangerous chemicals or explosives, the operator shall take into account that the facility is located at a distance from [buildings, transport, etc.] so that foreseeable explosions, fires and chemical releases do not pose a risk of personal injury, damage to the environment or property” [24].

The chemical storage site must be located far away enough from people in the vicinity of the chemical accident that in the case of a chemical accident, no person would suffer serious, long-term effects. In order to minimise the effects of an accident, humans must be at a certain distance away from the source of the leakage so that the concentration and exposure time of the leaked chemical are sufficiently low. The biological risk of a chemical leakage on a person depends on a number of factors such as: “substance properties, concentration, rate of spread, exposure time, individual sensitivity, protection and elimination conditions” [24]

European standards must be adhered to for technical production processes and services and therefore play a principal role in hydrogen gas storage and therefore this research. As previously mentioned in section 2.1.4, static electricity poses a huge threat to explosive gas clouds and European standard EN 1127-1 describes how explosive atmospheres are realised through static electricity [27]. Furthermore, this standard describes explosion prevention, protection and the basic concepts and methodology associated with such. Similarly, EN 13237 highlights important concepts and definitions of important factors that should be considered in “potentially explosive

atmospheres” [28]. While this investigation considers a potential worst-case hydrogen leakage scenario where explosion safety systems and methods of suppression are assumed to fail, there are key standards which also govern such systems. For example, EN 14373 describes the basic requirements for design and application of explosion suppression systems and assesses the efficiency of such systems, should an explosion occur [29]. In the scenario explored in this investigation, a type IV pressure vessel (further described in section 2.2.7) is selected as the storage container for hydrogen gas. This vessel will be governed by standards such as EN 14460 – Explosion resistance equipment, which provides the calculation methodology for design pressure of vessels and is applicable to situations where deflagration may occur [30]. EN 15089 describes the requirements for explosion isolation systems - systems which prevent explosion pressure waves and/or flames from propagating through system components and across sites such as the one analysed here [31]. This plays an important role to this research, covering the criteria for various test methods which should be carried out to certify the efficacy of explosion isolations. As this is a safety analysis, standards concerning safety assessments should be mentioned. As such, standard EN 15233 sets out a clear methodology for execution of a safety assessment for protective systems for potentially explosive atmospheres [32]. Just as this investigation provides methods to determine values of overpressure from hydrogen gas explosions, so too does the standard EN 15967 test method detail how to measure explosion pressure as well as explosion pressure rise [33]. Two other types of test method are explained in standard EN 1839, allowing for determination of explosion limits and limiting oxygen concentration for flammable gases and vapours [34]. International standards were considered as well as European. ISO/TR15916 provides guidelines and basic considerations for safety in hydrogen systems and gaseous hydrogen storage [35]. Therefore, this standard should be kept in mind for the applications which rely on hydrogen, outlined in section 3.0.

2.2.4 Hydrogen Storage and Leakage Risks

Safe usage and storage of hydrogen is vital to reduce the risk of a hydrogen leakage accident with disastrous consequences and is interesting to understand how leakage can occur in the first place. Leakage is of particular concern as it is one of the most likely causes of hydrogen accidents [36] This leakage can then form a vapour cloud which can be dangerous when it contains hydrogen within the flammability limits of 4-75%. Investigation into previous Vapour Cloud Explosions (VCEs) instances have shown that even small quantities of hydrogen in a leakage can cause explosions with severe overpressure that leads to significant damage [36].

Hydrogen can pose a risk of asphyxiation if a large leakage takes place as it can displace oxygen in the air. This should be considered as a risk for indoor, enclosed storage whereas this is a negligible risk when stored in open, outdoors surroundings due to hydrogens density and dispersion characteristics [9].

Since gaseous hydrogen molecules are very small, particular care has to be taken when selecting the material used for a container to store the gas. The small size of the molecules means they are able to diffuse through many materials which would otherwise be considered airtight for a lot of other gases. Hydrogen embrittlement should also be considered in storage container selection as this can deteriorate certain material's properties and lead to possible leakage or catastrophic failure. Hydrogen embrittlement is dependent on a vast number of factors [9]. Hydrogen embrittlement is further explained in section 2.4 and the testing regarding this is mentioned in section 2.2.7.

2.2.5 Hydrogen Leakage Detection

Hydrogen is not toxic or poisonous, however it should still be treated with caution as it can be dangerous in certain circumstances. As mentioned in section 2.2.1, hydrogen is an odourless gas. It is often the case that odorants are added to odourless gases to create an artificial smell in order to make them safer. However, odorants don't tend to be used with hydrogen as it is difficult to find one with similar density and dispersion characteristics compared to hydrogen [10]. Pure hydrogen flames have a low radiant heat. Despite this, the flame itself can be as hot so should be approached with caution [37]. Pure hydrogen also burns with a light blue flame which can appear almost invisible in daylight. These factors combined make the detection of a leakage more difficult than other gases so certain methods and tools should be applied for improved and earlier detection of leaks [10]. For example, the use of thermal imaging cameras can be useful in hydrogen leak detection [37]. Thermal hazards and pressure effects are two important safety concerns when dealing with hydrogen leakage scenarios resulting in detonations and deflagrations. Thermal and pressure values were plotted against distance using a variety of numerical methods and machine learning techniques, further discussed in sections 4.4 and 4.5.

2.2.6 Hydrogen Safety Mitigation & Prevention Technology

As a safety precaution for hydrogen used in cars, emergency valves can be used to quickly dispense hydrogen from a container so in the event that the gas does ignite, the flame will be rather controlled as opposed to surrounding the vehicle completely. An advantage of hydrogen's properties in terms of safety is that it rises and quickly disperses away from the container it is stored in. This is in contrast with gasoline which spreads outwards in a pool and can engulf a vehicle in flames in a matter of seconds once ignited [9].

All equipment used with hydrogen storage should be thoroughly grounded due to hydrogen's low electroconductivity. Therefore, movement of hydrogen can generate electrostatic charges in certain scenarios which can result in sparks and possible explosions as mentioned in section 2.1.1 [9]. Hydrogen has been used in space applications such as rocket fuel for decades due to its favourable combination of low weight and high energy output – both vital in the space industry [38]. NASA (National Aeronautics and Space Administration) have many years of experience in this sector and continue to learn effective solutions to reduce potential risks and hazards arising

chemicals and materials in industry. There is a potential of ignition from static charge when gases are used in vent stacks. NASA implemented solutions to reduce the severity of the fire caused by this ignition. One solution was having closing valves and purging the system with nitrogen gas to remove unwanted fuels present. Another solution was installing a lightning (fibreglass) rod next to the vent system with its tip above the flammable gas to air mixture as a method of grounding – an important method previously discussed. Pressure release devices can also be effective safety measure to limit overpressure resulting from the expansion of confined hydrogen [38].

Equipment and protective systems should for operational purposes in a potentially explosive environment should test against whether they meet the requirements of the Ignition Hazard Assessment (IHA). Two of the main requirements they must pass in this assessment are the systems must be sufficiently protected against the effects of an explosion and must be unlikely to become an ignition source. Passing this test means that the systems satisfy the health and safety requirements outlined by ‘ATEX’ (Explosive atmospheres) EU regulations which are designed to protect workers from potential explosion hazards and risks [39].

In the event of leakage from damaged pipes or pipe connection, there is usually a self-acting valve in the tank system which limits the leakage to one group of cylinders – other cylinder groups may not empty as a result of the failure. Other methods for mitigation and prevention technology other than valves for a potentially explosive environment include; explosion venting systems, water deluge and fog-nozzles, flame arresters and chemical barriers [40].

2.2.7 Storage tank types and material properties

Several material tests can be useful to ensure the safety of the gas storage container. One example of this is to test that the embrittlement of the storage material is low. This can be checked using a tensile test, fracture mechanism tests or a disc test. Charpy impact test is another material test which can be useful to check the brittleness of the storage container due to cold. The type of storage pressure vessel in the case being investigated is a type IV. This type of pressure vessel is mainly intended for portable applications, for example hydrogen fuel for transportation hence their lightweight nature. They tend to be made from a polymeric liner which is fully-wrapped with a fibre-resin composite. Permeation is a possible problem when using type IV vessels which can occur in some situations when gas comes into contact with polymers. As a safety check, a permeation measurement can be done on a vessel to prove permeation is below a specified rate ($1\text{cm}^3/\text{l/h}$) [41]. Potential reasons for hydrogen leakage from the vessel are discussed in section 2.4.

The pressure vessels in the scenario investigated here, manufactured by Umoe Advanced Composites (UAC) use fibre glass and epoxy resin materials which make them lightweight, robust, highly durable to fatigue and can cope with a wide range of temperature and offer increased safety most importantly [42].

2.3 Safety Analyses and Prior investigations

2.3.1 Fuel Cell Vehicles and Fuelling Stations

Several journal articles and research papers concerning hydrogen fuel cell vehicles (FCV) and ships were consulted in an effort to arouse greater appreciation for the practical applications of hydrogen storage and the study at hand. The use of hydrogen as a fuel source in future travel industries is perhaps the greatest motivation behind this current research. However, before this modern technology becomes readily available the appropriate safety measures and risk assessments must be rigorously considered. This is an area which has - in more recent years - generated much interest and a number of studies concerning the safety aspects of hydrogen usage in industries have been carried out as a result.

One such paper investigates leakage related accidents at hydrogen fuelling stations in both Japan and the USA, in a comparative study [43]. In this research by Sakamoto et al, different types of hydrogen leakage are categorised under 6 different types of incidents or accidents e.g., Leakage I, Leakage II ... Leakage VI. Through this investigation data was extrapolated from the High-Pressure Gas Safety Act Database - concerning incidents in Japan - and the Hydrogen incident reporting database (HIRD) - regarding incidents in the USA. The report also makes reference to the Hydrogen incident and Accident Database (HIAD) - a global database. The report found that design error and human error were 2 considerable factors which resulted in hydrogen Leakages and more specifically highlights that "safety measures should be developed". While that investigation may not specifically discuss safety concerns related to hydrogen storage, it does address the need for greater hydrogen safety measures to be investigated and put in place. Furthermore, the leakage classification system created through this report will play a useful role going forward and may prove as a useful scaling method in future studies.

One experimental study by Hao et al analysed hydrogen leakage of fuel cell vehicles in confined spaces [44]. This provides useful insight into hydrogen gas behaviour in closed spaces, conversely to the present investigation which will look at a hydrogen leakage in a large semi-unconfined site. Both scenarios are interesting, and it is useful to analyse the role that different environment's play in the dispersion of hydrogen gas. Hao et al also draw attention to some existing standards of test methods and hydrogen safety regulations. Like Sakamoto et al, the study by Hao et al agrees that further improvements in hydrogen safety testing are required.

2.3.2 Confined/Unconfined Scenario

While Hao et al explored hydrogen leakage from FCV in closed spaces, Malakhov et al carried out an experimental study of hydrogen leakage in a semi-closed space by means of CFD simulation, with the express purpose of risk mitigation [45]. The study appropriately states, "The ability to predict all the physical phenomena that may occur following an accidental hydrogen release is mandatory for future safety studies on an industrial or urban scale"

which further emphasises the need for the present investigation of hydrogen leakage safety analysis as well as future studies surrounding this topic.

After consultation of studies which investigate hydrogen leakage scenarios in closed and semi-closed spaces, it was necessary to look at studies which considered a leak in unconfined/open spaces. A CFD evaluation of unconfined hydrogen explosion by Edlia et al is useful as a reference to both hydrogen explosion characteristics (earlier described in section 2.1.4) as well as leakages in unconfined spaces [46]. The paper provides recommendations of safety distances which will be interesting to compare to the safety distances calculated in section 7.5. Particular attention is given to concepts such as the Coandă effect (the phenomena where a fluid flow attaches itself to a nearby surface) and deflagration to detonation transition (DDT) which makes this study useful as an introduction to the topic of hydrogen explosions.

2.3.3 Fuel Cell Ships Investigations

Hydrogen gas has huge potential as a source of power in the shipping industry as well as the automotive industry. These practical applications further explain the need for the work at hand. As the aforementioned studies have suggested, it is ever more apparent that hydrogen usage in shipping and the associated safety concerns require greater research and through researching the topic a number of reports pertaining to hydrogen fuel cell ships have been consulted. "A study on a numerical simulation of the leakage and diffusion of hydrogen in a fuel cell ship" by Li et al investigates safety of hydrogen fuel cells on a ship through CFD methods and explores solutions to hydrogen gas dispersion within cabins and other areas of the ship [47]. This investigation provides recommendations on sensor layout and ventilation conditions – two very important considerations which may prevent fatal accidents onboard such ships in the future. This evokes great appreciation for CFD models and how they may be used by safety experts to select the appropriate tools and devices to mitigate fatal accidents as a result of hydrogen leakage.

A similar study by Mao et al also considers a hydrogen fuel cell ship and explores hydrogen leakage and explosion behaviours using ANSYS Fluent software [48]. This is of great use to the current study which also utilises ANSYS Fluent software to investigate a hydrogen dispersion scenario. In line with the aims of the current research, the paper appropriately points out that simulations of these types of incidents will allow us to create and design more efficient safety management and escape systems. Mao et al also explain in detail the physical and theoretical models used in their investigation, the corresponding grid characteristics and calculations employed. Overpressure damage and high temperature damage were reported as the main consequences of hydrogen explosions demonstrating that these are valid areas of concern which should be analysed.

2.4 Potential Leakage Sources

While this investigation is concerned with the effects of hydrogen gas leakage and the associated safety implications of such, it is important to

analyse how leakage from hydrogen storage may occur in the first place. Analyses of potential leakage sources will become more important as hydrogen demand increases over the coming decades. With greater amounts of hydrogen produced and stored, the higher the chances of leakage and therefore, potential fatalities. An estimated 558 million tonnes will be required by 2050 to support the rollout of clean energy applications [49].

Pressure vessels are primarily used for storage of compressed hydrogen gas and are the most advantageous method for transportation of the gas. One potential cause of failure of these vessels - leading to a leak - is hydrogen embrittlement. This is the process by which a metal material (in this case, the pressure vessel) becomes brittle during service as hydrogen diffuses into the metal. This effect can be enhanced by increasing vessel pressure. Furthermore, heat affected zones (HAZ) of storage vessels such as welded zones and similar areas of high residual stress are regions which host a higher concentration of hydrogen. As a consequence, these regions have a higher risk of fracture during service – this fracture may also be referred to as hydrogen induced cracking [50].

The forming technique of autofrettage is highly favourable for vessels and pipelines which use compressed gas in operation. Through autofrettage – a material fabrication method - the durability of a tubular metal component and resistance to stress corrosion cracking are increased as a result of inducing compressive residual stresses into the material. As demonstrated in a number of studies, autofrettage can have an enormous impact on material limits. For example, one investigation found that the endurance limit of non-propagating cracks was increased by 130% compared to components which did not undergo the process of autofrettage [51].

2.5 Shockwaves & Overpressure

2.5.1 Characteristics

Shockwaves are defined as waves possessing a very sudden and significant change in the properties of the gas they are travelling through [52]. The most significant property is a sudden, large increase in pressure. Immediately after the wave passes, the properties - including pressure - rapidly decay and return to their ambient state. The only exception to this decay is entropy, which remains increased - the amount of which is proportionally related to the energy of the wave and therefore also the distance from the origin, as the wave loses energy as it propagates outwards [52].

This behaviour of the shock wave as it passes and “leaves the ambient gas in a state of radially decreasing entropy” [52] infers that there is no way to fully describe the thermodynamic process mathematically. As a result, the time history of the properties, such as temperature or density, of the gas cannot be directly calculated from a measurement of the pressure-time history with a pressure gauge at a fixed point in space. This also infers that there is no direct way to calculate the spatial characteristics of the wave, such as the peak pressure-distance behaviour of the wave as it travels. This means that measuring or estimating the properties of a gas subject to a shockwave is a significant challenge.

The peak overpressure generated by shockwave or blast wave from an explosion of hydrogen is dependent upon the peak flame speed of the mixture's combustion [53].

2.5.2 Overpressure Investigations

While most initial research was mainly concerned with existing hydrogen standards and the areas where hydrogen storage safety is important, the success of the present investigation would ultimately depend on the methods selected for calculation of safety distances, overpressure values, heat fluxes and other associated hydrogen blast parameters. Numerous papers were consulted in order to establish the most useful and applicable methods to the specific scenario of an open-air hydrogen VCE. The consulted articles – although similar in nature – differ significantly in their approach, outcomes and results.

Overpressure is of equally important consideration to this research and will be a determining factor in the calculation of appropriate safety distances from hydrogen storage facilities. In researching different methods of calculation of overpressure, 'The Yellow Book' proved to be of great use and is a comprehensive overview of a variety of methods [54]. The report also features example scenarios with step-by-step guides on how these methods may be applied to different scenarios. Chapter 5 and 6 detailing vapour cloud explosions and heat flux from fires respectively, were especially useful.

One investigation by Dorofeev evaluates the safety distance from an unconfined hydrogen vapour cloud explosion as a function of the flame speed and presents three scenarios of obstacle density surrounding the release location [55]. It is highlighted that the level of congestion has a huge impact on blast effects. This notion welcomes investigations where explosions are analysed relative to a congested area. This links to the model created within the current research, further described in section 5.2. Similar investigation such as a vapour cloud explosion analysis by Baker et al features more in depth discussion on the associated effects of obstructions, confinement, and obstacle parameters [56].

One method which is frequently mentioned in literature is the TNO Multi-Energy method (TNO-ME). Several studies utilise this particular method for calculation of overpressure values at varying distances from a VCE. Similar in many ways, the Baker-Strehlow-Tang (BST) method may be used as an alternative and is described in greater detail in section 2.5.9. Many investigations utilise this method as opposed to the TNO-ME however research by mélani et al reviews both, which was useful in aiding in the understanding of the two methods [57]. That particular study uses data from 6 articles and aims to recreate the data using both calculation methods. In the results for overpressure values, it was found that both methods were in good agreement, providing similar correlation – especially with increasing distance from the explosion. However, the study emphasises that TNO-ME provided a better approximation for the overpressure values and concluded that BST methods are not applicable for scenarios involving hydrogen.

To assess the validity of these claims, further research into both TNO and BST methods was carried out and other investigations conferred. One piece of research points out the two methods have their separate advantages and disadvantages yet can be said to be methodically similar and equally make use of so-called “blast curves” [58]. A third method discussed in that research – The TNT (Trinitrotoluene) Equivalence Method – also utilises blast curves and has been used as a popular method for calculation of overpressure from vapour cloud explosions. From that investigation, the BST Method has been revised and a new flame speed table was produced by means of experimentation. Going forward, this table should be referred to in future implementation of the BST Method and will be particularly useful in section 4.

More details of the TNT equivalence method were provided in an analysis by Zulkifli et al which provided a different evaluation of the method - contrary to the earlier claims of Pieroranzio - stating that the TNT equivalence method is proven to be particularly useful in far field damage assessments [59]. This highlights why it is necessary to consider a variety of studies in the background research of any topic.

Furthermore, this TNT method has been described as useful as a means of calculating safety distances in worst case scenario in an investigative analysis by Lopez, further demonstrating its applicability to the problem studied here [60].

2.5.3 Scaling Law

In the early 1900's, Carl Cranz [61], and Bertram Hopkinson [62] both independently defined and published a similarity rule while in the process of their work relating to explosions, blast waves, and ballistics, which became known universally as the Cranz-Hopkinson Scaling Law. The relation can be applied to spherical explosive devices and substances producing spherical, radially propagating blast waves.

The scaling law states that the properties observed at a distance R_1 , for an explosion of energy E_1 , can be scaled to an explosion of energy E_2 , allowing for the calculation of the distance R_2 for which the same properties can be observed. The relation is shown below [63].

Equation 5:

$$\frac{D_2}{D_1} = \left(\frac{E_2}{E_1}\right)^{\frac{1}{3}}$$

Where:

D = Distance (m)

E = Explosion Energy (J)

The ratio of energy in the above scaling equation can be substituted for the mass of the explosive substance, provided the explosions are of the same substance. This allows for more accurate results, since the portions of energy used to generate the blast wave are not always accurately known, as some

energy is released in other forms such as; heat, the disturbance of ground material, or in the motion of debris ejected from the blast area. This relation is sometimes also referred to as the “cube root scaling law” [63] as the equation above implies.

In 1944, a paper by Sachs further developed the scaling law to include difference in ambient pressure and temperature between the two blasts, as well as incorporating the time of arrival of a shockwave into the relation [64]. The updated formulae are shown below[63].

Equation 6:

$$\frac{D_2}{D_1} = \left(\frac{W_2}{W_1}\right)^{\frac{1}{3}} \left(\frac{P_{a1}}{P_{a2}}\right)^{\frac{1}{3}}$$

Equation 7:

$$\frac{t_{a2}}{t_{a1}} = \left(\frac{W_2}{W_1}\right)^{\frac{1}{3}} \left(\frac{P_1}{P_2}\right)^{\frac{1}{3}} \left(\frac{T_{a1}}{T_{a2}}\right)^{\frac{1}{3}}$$

Where:

W_n = Mass of explosive substance (kg)

P_{an} = Ambient pressure (Pa)

t_{an} = Time of arrival of shockwave (s)

T_{an} = Ambient temperature (K)

(Subscript n = 1 or 2)

The above relations have been tested and validated against experimental data from blasts including TNT explosions [65]. It is important to note that this relation does not allow for a workaround of the multivariate nature of the blast wave problem. It does not allow for the calculation of properties at any distance, simply the scaling of known properties for a known measurement distance to alternative explosion sizes.

2.5.4 Mach Stems

Shockwaves behave differently depending on the physical environment they are propagating through. In a free-air scenario with no obstructions, they propagate from the centre, radially in all directions. Although in a surface-blast scenario, the wave will reflect off the ground surface, forming a Mach stem at the surface that propagates along the ground with the reflected wave, as shown in figure 6 [66]. As shockwaves possess the same behaviours described in simple wave theory, a Mach stem formed by the wave addition of the initial and reflected wave, has the potential to create overpressures much greater than that of the initial wave alone.

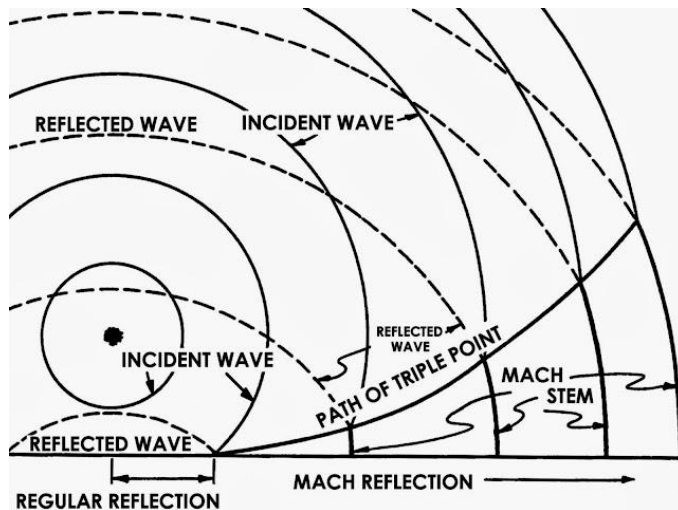


Figure 6: Propagation of Shockwaves.

2.5.5 Measurement

Measurements of physical properties of a gas subject to a shockwave are most commonly done with either specially designed measurement gauge devices, or high-speed photography. Gauges are installed at known measured distances from the shock origin, and record data as the wave passes. There is a limit to gauge measurements, as the devices have a high likelihood of succumbing to the destructive power of the shockwave, and most likely the explosion that caused it. While thermal imaging camera can be used in detecting leakage (previously mentioned in section 2.2.5), high-speed photography is commonly used from a very far distance and is able to capture wave properties through distortions in the images, smoke tracer lines are often used alongside photography to visualise the behaviour of a wave.

2.5.6 Modelling

It is not possible to describe a shockwave or blast wave with a fully analytical solution, as the nature of shockwaves in 3 dimensions make for a multivariate problem that has continuously varying parameters in both space and time. However, many solutions have been derived previously using purely empirical and partially empirical methods that describe only certain parameters. Most often this is the peak shockwave overpressure as a function of distance from the origin of the wave, as this is commonly regarded as the most useful and important quantity in relation to shockwave damage and safety. Some of the most notable and relevant methods for estimating blast wave overpressures are described in the following sections.

2.5.7 TNT Equivalency Method

The past century has seen a vast amount of explosive testing with an array of different destructive devices such as nuclear, chemical, and conventional bombs, the most common of which is TNT (Trinitrotoluene). The consistency and repeatability of this explosive substance allowed for the creation of empirical equations that, combined with experimental data from controlled explosive experiments for other substances such as hydrogen, have been used to construct a TNT equivalency model. The method is able to provide an estimation of the overpressure as a function of distance by approximating

the energy release from a hydrogen cloud explosion to an equivalent amount of TNT. The equation to calculate the amount of TNT for an equivalent blast is shown below [67].

Equation 8:

$$m_{TNT} = \frac{m_{cloud} \Delta H \cdot \eta}{\Delta H_{TNT}}$$

Where:

M_{TNT} = Mass of equivalent TNT (kg)

M_{cloud} = Mass of hydrogen cloud (kg)

η = Explosion efficiency

ΔH = Lower heat of combustion of hydrogen (MJ/kg)

ΔH_{TNT} = Lower heat of combustion of TNT (MJ/kg)

While the equation to calculate the distance required to experience a certain overpressure is [67]:

Equation 9:

$$D = 0.3967 m_{TNT}^{\frac{1}{3}} \times e^{[3.5031 - 0.7241 \ln(P) + 0.0398(\ln(P))^2]}$$

Where:

D = Distance from origin for the given overpressure (m)

P = Overpressure (psi)

The TNT equivalency method has been found to overpredict overpressure values for hydrogen cloud explosions due to its inability to account for the hydrogen concentration in the flammable cloud mixture, as well as poorly fitting sets of experimental data [68]. The method is deemed “inadequate when it comes to the estimation of overpressures resulting from hydrogen” [68] however given the popularity of this method, it is useful to investigate these claims which will be evaluated in section 8.

The field of safety engineering often uses this method for explosion investigations and does so based on the fact the TNT explosions are so well documented and researched thus if one can obtain TNT equivalent values, explosion values for countless explosions may be easily evaluated. For example, nuclear explosions are often approximated using the TNT equivalent method which can be used to calculate overpressure values. As stated in the study by Lopez et al the TNT equivalent model can be used for analysis of “high pressure hydrogen cylinder explosions” and furthermore, accounts for the effects of Vapour Cloud Explosion (VCE) [60]. In the investigation by Lopez et al, the use of the TNT equivalent model was found to be in good agreement with other experimental and numerical data, concluding that the model may play a useful role in the calculation of safety

distances, making it highly appropriate as method of investigation for the presented study.

2.5.8 TNO Multi-Energy Method

This overpressure estimation method is based on the level of confinement of the explosion, consisting of a set of 10 overpressure-distance curves. Each curve approximates a level of confinement, allowing for the very rough estimates of hydrogen explosions in a variety of geometrical settings. Comparisons to experimental data of hydrogen explosions has found that the method does not provide any high level of accuracy for unconfined, unobstructed explosions, however, is still a worthy method for the purpose of approximation [68]. An example of these curves is shown below in figure 7 [69].

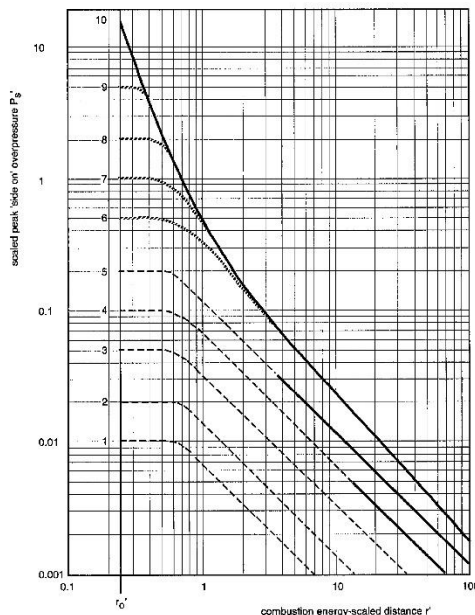


Figure 7: Overpressure vs. Scaled Distance Curves for TNO Multi-Energy Method.

The TNO method was modernised and converted to analytical form with sufficient accuracy by F. Alonso et al [70]. The original curves were fitted to a power curve equation and conditional logic was applied to produce an easy to implement, accurate analytical system that can be used within a digital environment. This allows for the TNO method to be applied quickly and with little repetition.

The appropriate confinement or “explosion strength” curve is selected based on table 2 below which classifies the level of ignition energy, shockwave obstruction density, and level of confinement. This system of guidelines for curve choice was proposed by Kinsella [71].

Table 2: Guidelines for Choosing Class Number of Explosion Strength for TNO Method [71].

Ignition energy		Obstacle density			Confinement		Strength
Low	High	High	Low	No	existing	no	
	x	x			x		7 - 10
	x	x				x	7 - 10
x		x			x		5 - 7
	x		x		x		5 - 7
	x		x			x	4 - 6
	x			x	x		4 - 6
x		x				x	4 - 5
	x			x		x	4 - 5
x			x		x		3 - 5
x			x			x	2 - 3
x				x	x		1 - 2
x				x		x	1

2.5.9 Baker-Strehlow-Tang (BST) Method

The Baker-Strehlow-Tang method, published in 1994 uses a function of chemical potential, obstruction density, and physical geometry layout to approximate the explosion flame speed, and produce a set of 27 overpressure-distance curves, each for a unique Mach number of a shockwave. While this method was implemented in the "Guidelines for consequence analysis of chemical release" for the American Institute of Chemical Engineers in 1999 [72], it has been shown to be inaccurate at estimating unobstructed hydrogen explosions specifically. Moreover, like the TNO energy method it is better suited to lower accuracy estimations where more variables, like obstruction shape and density, are to be considered [68]. Below is an example of the set of Mach number overpressure-distance curves developed with this method [69].

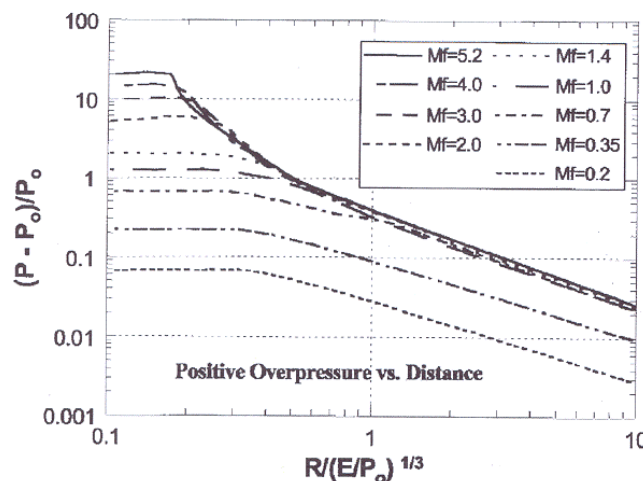


Figure 8: Mach Number Overpressure-Distance Curves.

As explained in the literature, the BST method is an improvement on the original curves presented in the 1970's as part of the Baker-Strehlow method.

2.5.10 Experimental Data Curve Fitting Model

A hydrogen cloud explosion-specific method was developed in 2018 using a wide variety of experimental results from hydrogen explosion tests [68]. The data was curve fitted using a variety of different basic equations until an optimal fit with the lowest error was found. This first method was developed by Mukhim et al, who set out to create a method of predicting overpressure resulting from unconfined, open-air hydrogen vapour cloud explosions. The authors conglomerated the data from many different previous experimental studies, and were able to establish a set of estimation equations that can approximate the overpressure at any distance from a hydrogen cloud explosion, given the volume of the cloud and the hydrogen volume fraction. This was achieved by a traditional regression analysis, fitting to a power curve equation.

This particular curve method was described in the authors' research as over-predicting overpressure which is more desirable from the perspective of a safety analysis. The power curve fitting estimation method is highly applicable for the present investigation as it is intrinsically linked with the central goals of this investigation – predicting overpressure from at various distances from hydrogen explosions.

2.5.11 Ideal Waves with the Friedlander Equation

Real-world measurement datasets of blast waves are often imperfect due to a variety of factors, such as; signal noise, measurement error, and the physical testing setup deviating from the assumptions and idealisations made during the theoretical design stage of the experiment. The behaviour of a wave can also undergo change when encountering obstructions and obstacles as it propagates. An example of this is shown below in figure 9, the complex pressure-time profile of an external blast wave measured from inside a vehicle [73].

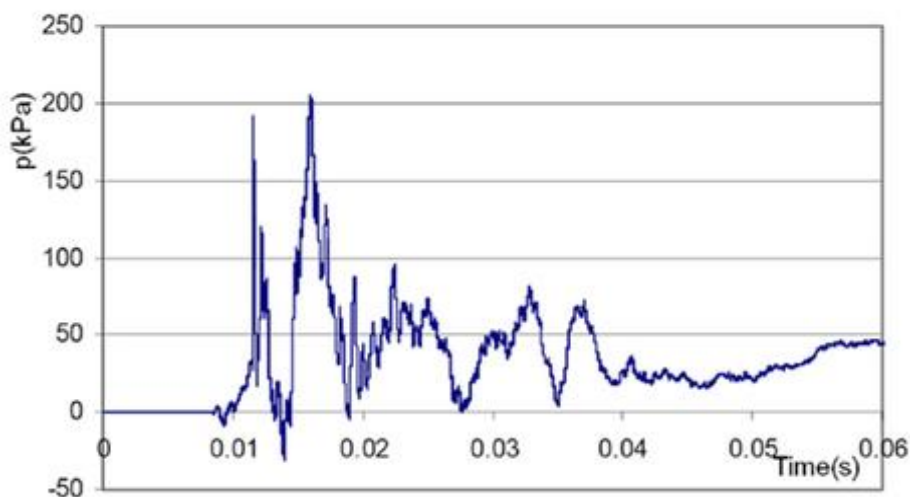


Figure 9: Pressure-Time Graph of a Blast Wave measured from inside a Vehicle [73]

The Friedlander waveform, devised by the late Frederick Gerard Friedlander in 1946 while investigating the protection offered by walls from blast waves, offers a simple method to describe an idealised theoretical blast wave [74].

The waveform equation is regarded as the most simplistic form of a pressure-time relationship for an unobstructed blast wave [74]. The equation has been tested against experimental data and has been confirmed to accurately describe an unobstructed blast wave [75]. The wave equation and an accompanying graph showing the pressure curve's decaying profile are shown below [76] [74]. The equation captures the initial spike in pressure, followed by a quick decay to a small negative pressure, before returning to ambient conditions.

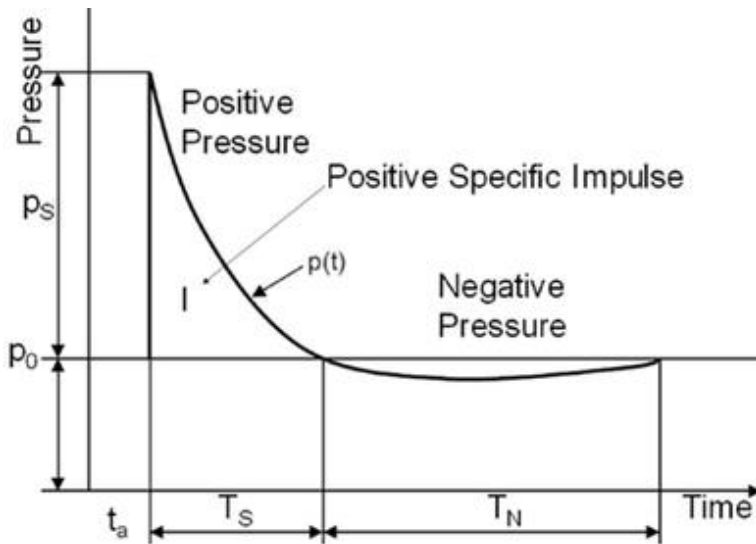


Figure 10: Decaying Profile of a Pressure Curve.

Equation 10:

$$P = P_s e^{-\frac{t}{t^+}} \left(1 - \frac{t}{t^+} \right)$$

Where:

P = Pressure at specified time (Pa)

P_s = Peak positive overpressure (Pa)

t^+ = Duration of positive pressure phase (s)

t = Time at which the pressure is evaluated (s)

2.5.12 Damaging effects

While the flame temperature of hydrogen is relatively high (2480K), its radiant heat transfer with its surroundings is relatively low, lowering the risk of damage due to thermal radiation significantly. A much more probable cause of damage or injury from a hydrogen explosion is from the shockwave and resulting overpressure it will subject upon its surroundings. The blast wave is commonly regarded as the most important factor when considering hydrogen explosion damage. Numerous experiments have catalogued and categorised

the resulting damage for certain values of blast wave overpressure. The positive impulse, from the positive overpressure phase of a wave is regarded as having the most significant impact on the amount of damage caused [70].

2.6 Thermal Heat Flux Models

While overpressure effects from an explosion are of primary concern to this study, heat flux effects are also considered. However, in the earlier research stages of this project, it was found that few methods for calculation of heat flux at various distances from explosions exist. More specifically, there was found to be a significant lack of documentation related to calculation of heat flux from a hydrogen vapor cloud explosion. Two methods described in the literature showed potential and have been employed for the remainder of this report.

2.6.1 Solid Flame Model

The methodology explained in a study by Ustolin and Paltrinieri can be used for the calculation of radiative heat flux values at a distance from boiling liquid expanding vapour explosions (BLEVEs) [76]. As part of a consequence analysis study, this source describes how the “solid flame model” works in a step-by-step approach and states the corresponding assumptions. In doing so, the paper has potential to act as a reference point for the creation of codes and standards for hydrogen safety practices – particularly related to the resulting heat flux from an explosion. The same method is also utilised in other analyses [77]. Further details and the associated equations for this method are explained in section 4.

2.6.2 BLEVE Model

Another source which was important in the investigation of heat flux calculations specifically looks at estimation methods for calculating radiant heat flux from different types of fires – particularly in large open spaces [78]. Furthermore, this source provides substantial background detail as to the concept of heat flux before presenting different methods of heat flux calculation for several fire types. The method which will be of use to the present investigation is explicitly constructed for “Radiation Due to BLEVEs with Accompanying Fireball”. This method is explored further in section 4.

2.7 Machine Learning Regression Models

2.7.1 Relevance

The potential of machine learning systems in the form of regression models has long been recognised as a solution to solving multivariate regression problems using an extensive dataset of experimental results or data. Moreover, machine learning overpressure prediction is perhaps the most common alternative method to empirical models [79]. With empirical estimation models often considering only the mass or size of the explosive substance, they are often somewhat inaccurate, and are not sufficient to fully describe the complex relationship between the nuanced characteristics of a hydrogen leakage explosion and the blast overpressure, as such factors as ambient conditions, geometrical layout, explosive cloud mixture contents, and ignition source - among others - contribute to the nonlinear relationship with

overpressure. This has led to artificial intelligence (AI) and machine learning (ML) models being studied and implemented in a variety of designs due to their ability to distinguish trends and describe nonlinear relationships present with experimental data [79].

2.7.2 Previous Research

A wide selection of model designs and approaches have been implemented to predict overpressure, most commonly for open-cast mine explosions. One study in 2005 developed an artificial neural network model to predict overpressure for this case, with the resulting model predicting results with far superior accuracy than traditional empirical methods. The neural network model displayed a coefficient of determination or “score” of 95.7%, while the traditional method used for comparison in the study showed scores of just 38.1%. Despite the blast overpressure being dependent on a variety of factors, the features used for prediction by the model were the same as those used for calculation via the traditional empirical method, those being the explosive charge mass, and the target distance [80]. The concept of neural networks is discussed further in section 2.9.3.

Attempts at including more features in the dataset of a machine learning overpressure prediction model - again for an open-cast mine explosion - have been made, in an attempt to better describe the complex relationship and its reliance on the various influencing factors. A study from 2015 successfully created an overpressure prediction model using an adaptive neuro-fuzzy interference system (a design of an artificial neural network system - the description of the inner workings and design of which is beyond the scope of this research). The model was trained using a larger dataset containing five features as opposed to the above model which used only two, in an attempt to better describe the nonlinear relationships, present within the data. The study found via sensitivity analysis that the explosive charge size, the explosive substance, and the distance from the blast, were the most influential factors for the resulting overpressure. The study also demonstrated the potential for very high accuracy in the prediction results, with a score of 97.1% during testing, and a comparison with a similar artificial neural network model, as well as more traditional prediction methods, showed the neuro-fuzzy model to be the most accurate [81].

Further increases in dataset size and complexity, have shown similar results from machine learning and artificial intelligence models, with a 2018 comparative study successfully producing a neural network model with a score of 96.1%. This finds it to be superior to the other model types when tested and compared [82]. Other studies have also shown that heuristic algorithms can successfully be implemented to optimise the predictions of a neural network model for blast overpressure, with a study in 2016 using the imperialist competitive algorithm in tandem with a neural model to produce correlation scores of 96.9% during testing [83].

2.7.3 Considerations of Model Design

The algorithm choice, alongside the tuneable parameters of the algorithm are critical for the performance and accuracy of the results from a machine learning model [82].

Within machine learning model parameters there exists a general function of complexity of the model. For example, a random forest model's complexity may be measured by the number of trees within the model, and an artificial neural network's complexity may be measured by the number of layers and number of neurons within the model.

Controlling the complexity of a model is of very high importance as this has a direct correlation to how well the model is fitted to the training data [79]. If the model is not sufficiently complex enough it may not be capable of fully capturing the desired non-linear trends within the data. This is known as underfitting. Conversely, if the model is too complex it may lead to both underfitting or overfitting and will struggle to produce accurate predictions when new testing data is introduced that differs from the training dataset. It is also important to note that increasing the complexity of a model will increase the computational time [79].

2.7.4 Training Data Considerations

The quality of the input dataset for machine learning models is of upmost importance and is a defining factor for the effectiveness and performance of the model, due to the fact that this is the sole source of information for an otherwise empty model. The features of a dataset represent the number of different input variables.

Various techniques are often employed to take advantage of nuances in different datasets such as model choice, as some models tend to perform to a higher level with a large dataset. On the other hand, some models may only require a smaller set before reaching a level of diminishing returns in terms of prediction performance. Model choice can also be governed by sparsity of data. When poor quality data or a lack of sufficient data is available, models may have to be excluded from use.

With this being said, Random Forest models and other decision tree-based algorithms have been found to perform well with small and lacking datasets.

Data cleaning is also often performed, whereby noise in the data is filtered out, and outliers are removed to aid in accuracy.

Data scaling is often performed whereby the numerical values are scaled to a mean value of 0, and a variance of 1, although this is not always necessary. It can help improve model accuracy and prevent overfitting, so it can be regarded as a somewhat necessary step when working with artificial neural network models. It is important to note that the exact scaling procedure must be recorded, as the model's output predictions must be reverse scaled using this procedure to reveal truly meaningful results.

2.8 “Decision Tree” Machine Learning Algorithms

2.8.1 Decision Tree Learning

The concept of a decision tree has been implemented within the field of machine learning and artificial intelligence in many forms and has become a cornerstone of the field [84]. A decision tree can be used to make predictions and learn trends from data in cases of both regression and classification, as well as being a concept that is easy to visualise, making it ideal for the implementation of simple prediction models [84].

The concept is extended further when multiple decision trees are trained and combined to improve the accuracy of a model. This concept revolves around the assumption that the combined effect of many weak learned trees can produce a final strongly learned result, with robustness and accuracy when applied to different prediction scenarios through the injection of randomness and a variety of techniques [85]. This has been shown to be not only viable but extremely successful technique when applied to both classification and regression problems [87].

2.8.2 Random Forest Model

A “Random Forest” model is known as an ensemble method due to the nature of its construction which constitutes the learning of a large number of decision trees to construct a hypothetical “forest”, as opposed to a single tree. The forest can provide significantly more accurate results and has been used previously in blast overpressure prediction with a wide variety of datasets, resulting in highly accurate results [88]. This proves the models worth and relevance to the present investigation. Additionally, the random forest algorithm has been shown to be robust against overfitting, and an excellent general purpose prediction model [87]. The final prediction result in the case of regression is the average prediction from each tree in the forest.

The Random Forest algorithm constructs the ensemble of decision trees using a method known as bootstrap aggregating or “bagging”, where each tree is constructed using random subsamples from the training dataset. There are many specific data selection techniques within the general concept of bagging, such as the random subspace method whereby subsets are randomly chosen from the training data’s features, as opposed to its samples [89]. Bagging in general refers to the splitting of the dataset when training predictor algorithms for an ensemble method. Bagging is beneficial to prediction accuracy, as it can reduce the variance in the prediction results significantly [90].

2.8.3 Extremely Randomised Trees Model

The extremely randomised trees or “Extra Trees” model is very similar to the random forest but differs in how the model is trained. The name is representative of the difference between a random forest model and the extremely randomised model as the level of randomness “goes one step further” [86]. Bagging is still implemented to randomly distribute the dataset amongst individual trees. However, when “nodes” or “branch splits” are met in a decision tree, rather than searching for the definitive best split threshold

(the technique of a random forest), several random thresholds are generated and the best value of these is selected. This has the benefit of further reducing the variance in the model, however this can also increase overfitting [86]. The extremely randomised trees algorithm can be thought of as a variant of the random forest algorithm.

2.8.4 Gradient Boosting Models

Gradient boosted decision trees are another approach to decision tree-based ensemble learning methods, however are more suited to large-scale applications with very large datasets and are employed when the dataset is missing some sample data. This is because the gradient decent algorithm is capable of dealing with missing data [91]. The difference present within tree boosting algorithms is that the individual trees are built iteratively in series, rather than in parallel as in the methods above. Each tree attempts to reduce the error from the previous one, resulting in a model with great accuracy built from an ensemble of weak individual trees [92].

Gradient boosting methods do not typically use bagging techniques to split the dataset and subsample the data for each tree (although it is possible to use bagging with boosting methods), rather each successive tree learns from a modified version of the original dataset based on the residuals from the previous learner tree [92]. Boosting methods also possess a tuneable parameter other than the number of trees used, known as the “learning rate”. This is a value between zero and one that controls the magnitude of the influence of each tree, effectively controlling the rate at which the model learns. It is generally the case that models trained with more trees and a smaller learning rate are more generalised and robust. However, a high number of trees can lead to overfitting [86].

Many popular variations of gradient boosted tree algorithms exist and are in use today, one of which named “Adaboost” [93] (short for “adaptive boosting”), won the Gödel Prize in 2003, an award for exceptional papers in the field of computer science theory [94].

2.9 Alternative Machine Learning Algorithms

2.9.1 K-Nearest Neighbours

Neighbour's algorithms belong to the family of simple algorithms, as they do not include any complex computation or algorithmic technique. In this case, the neighbour's prediction method is based on computing the average value of the nearest “neighbouring” data points, to predict an unknown point. This neighbour's prediction technique can be applied with a variety of differences, such as the radius-neighbours method, where all the datapoints within a given radius are used for prediction, as well as varying the number of neighbours considered in the nearest-neighbours approach [95]. This type of method was first proposed in 1951 and has been improved upon and modified in various ways, multiple times as available computational power and techniques have evolved over the years [96]. Neighbour's algorithms can be applied to both classification and regression problems.

Weighting of the neighbour data points is often implemented, with the most common weighting metric being the distance of the neighbour point to the query point [95]. Despite the relative simplicity of the neighbour's-based algorithms, they have been shown to be capable of producing useful results with high accuracy and have been combined with a neural network model in a case of overpressure prediction from mining explosives with a performance score of 95% [97].

2.9.2 Support Vector Regression

A support vector regressor (SVR), also referred to as a support vector machine (SVM, for the use case of classification), is a type of machine learning algorithm that involves the use of a predefined function, known as the kernel. Common kernel functions include a sigmoidal function, or a polynomial function. Before the support vector predictive process can be undertaken, first the choice must be made on what variation of the support vector algorithm (this depends on the problem and desired outcome of the system). The choice is related to the desired accuracy of the model, between the ϵ -SVR, and v-SVR models, the former of which utilises the ϵ parameter as a value of acceptable error or allowable margin, while the latter seeks to minimise the error ϵ to achieve the most accurate predictions [98].

A support vector machine aims to classify data by constructing a "hyperplane", a plane that exists in a higher dimensional space, where the number of dimensions is defined as the number of features in the dataset for the given problem. The hyperplane is optimised using the value of the distance from the plane to the nearest data points, these points closest to the plane are often termed extreme points, as they lie close to the boundary of their parent classes. The hyperplane that maximises the distance to all of the closest extreme points is known as the plane with the best margin. To extend this concept to the problem of regression, the same process followed. The hyperplane is constructed using the predefined kernel function, fitting the function to the dataset. Conversely to classification, the margin from the hyperplane aims to include as many data points as possible in the case of a predefined allowable margin and including all datapoints within the margin in the case where the maximum error is to be calculated [99].

Due to the nature of the data-inclusive margin, support vector regression is somewhat sensitive to outliers in the dataset, as outliers must be included within the margins also. On the contrary, SVR is less sensitive to concentrated clusters of nearby data points. This can be somewhat counteracted by the use of data scaling, a process which is recommended for SVR and SVM models, as they are not scale invariant [100].

2.9.3 Multi-Layer Perceptron

A Perceptron belongs to a class of machine learning algorithms known as "neural networks" that are modelled to replicate the connected neural structure of a brain. These models can be implemented with any arbitrary number of neurons and groups of neurons (called layers), although these parameters are adjusted as a way to test and improve model performance, ensuring the model accurately captures the trends of the dataset without

overfitting. A Perceptron refers to a model with only an input and output layer of neurons, whereas a multi-layer Perceptron refers to a model that contains at least one “hidden” layer between the input and output layers of the model, as illustrated below in figure 11. The number of input layer and output layer neurons are representative of the number of input features and output variables the model is implemented with respectively. As illustrated in figure 11, each neuron in each layer is connected to every neuron in its adjacent layers.

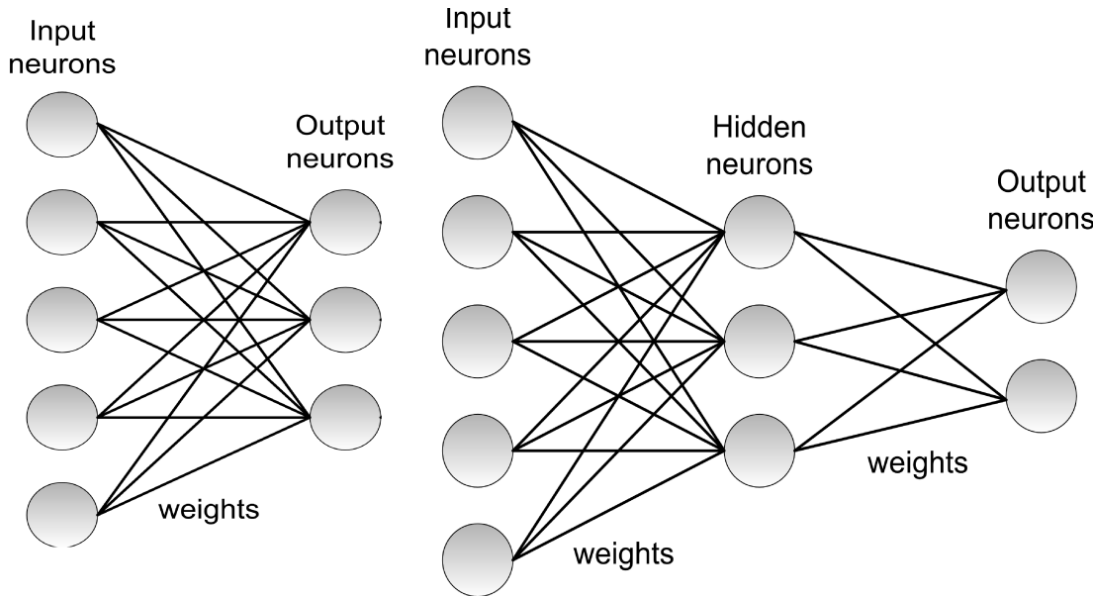


Figure 11: Illustration of Perceptron (left) and Multi-Layer Perceptron (right) Neurons and Layers [101].

The use of hidden layers of neurons inside the model allows for the learning and capture of complex and non-linear relationships present within a dataset, as a regular Perceptron is only capable of capturing linear relationships.

Predictions are calculated inside a Perceptron model by propagating the input feature values through the layers of neurons, with each connection between a neuron in an adjacent layer applying a weighting parameter that is tuned during the training of the model, in addition to weights, a bias can also be added at each layer, the value of which is tuned during training. The output of each neuron is defined with an “activation function” that acts on the weighted sum of the outputs of every connected neuron from the previous layer.

Neural network models including multi-layer Perceptron's have been implemented with great success for predicting blast overpressure from embedded mining explosives in an unobstructed, unconfined environment, with the multi-layer Perceptron exhibiting the best performance and accuracy with a coefficient of determination of 96.1% during testing [83].

2.9.4 Model Performance Metrics

Measuring the performance of machine learning-based estimator models is a well-documented and thoroughly researched topic. As the nature of the problem is data based and numerically based in the case of regression,

various well-established traditional methods for quantifying accuracy and performance can be easily applied. As briefly mentioned previously, the coefficient of determination, or “R²” scoring metric is most often used to simply quantify the performance of a prediction model, providing a universally comparable value within the range of zero and one where one is a perfect fit and zero represents a model that is input invariant, resulting in predictions always equal to the mean. It is possible for a model to be worse than random predictions, in this case the score will be negative, however the quantity will always be dimensionless [102]. Overall, this metric indicates how well the predicted results of a model fit the experimental data and is defined as follows.

First, the sum of squares of the residuals is calculated.

Equation 11:

$$SS_{res} = \sum_i (y_{a\ i} - y_{p\ i})^2$$

Secondly the total sum of squares is calculated.

Equation 12:

$$SS_{total} = \sum_i (y_{a\ i} - y_m)^2$$

Finally, the coefficient of determination is calculated.

Equation 13:

$$R^2 = 1 - \frac{SS_{res}}{SS_{total}}$$

Where:

R² = Coefficient of determination

SS_{res} = Sum of squares of residuals

SS_{total} = Total sum of squares

y_m = Mean value of the actual values from the test dataset

y_a = Actual values from the test dataset

y_p = Predicted values from the model

i = Iterator for the number of predictions made

The R² metric is a valuable tool for understanding the goodness-of-fit of a model and is the most common reference used to describe the performance of an estimator [102]. In comparison to ranged metrics such as the mean square error (MSE) or mean absolute error (MAE), is it more easily compared and is more informative [103]. It has also been proven to be more robust

compared to the similarly intuitive symmetric mean absolute percentage error (SMAPE) [103].

It is also important to have a high level of confidence in an estimator model, therefore multiple metrics are often used to provide different perspectives on the quality of results obtained. The R^2 cannot fully validate the accuracy of a model or evaluate its usefulness alone [102]. Therefore, additional alternative metrics can be used alongside of R^2 to further investigate the predictions from a model.

The MSE and MAE metrics, conversely to R^2 , possess the units of the quantity being estimated and exhibit a range dependent on the data involved in the system. Despite not being very comparable due to the reasons above, these metrics, especially MSE and additionally root mean squared error (RMSE) have been used in the evaluation of a large number of machine learning-based studies [103]. The MSE, MAE, and RMSE metrics are defined below.

Equation 14:

$$MSE = \frac{1}{n} \sum_{i=1}^n (Y_{a i} - Y_{p i})^2$$

Equation 15:

$$MAE = \frac{1}{n} \sum_{i=1}^n |Y_{a i} - Y_{p i}|$$

Equation 16:

$$RMSE = \sqrt{\frac{1}{n} \sum_{i=1}^n (Y_{a i} - Y_{p i})^2}$$

2.9.5 Model Validation Techniques

In addition to evaluating the performance of a model with statistical metrics, it is of great importance to ensure that an estimator provides meaningful results when asked to perform predictions on previously unseen data, for example, once the model is deployed for use in the real world. This can be ensured using a “train – test split” of the dataset, whereby the whole dataset available for the problem is split into two subsets, for training and testing the model independently. It is of the utmost importance that the test set is withheld from view from the model during training stage whereby the training set is used to train the model. Otherwise, the model will be biased when asked to provide prediction results for comparison against the test set, as it will have in essence, seen the correct answer beforehand [104]. Following the train – test

methodology is universally agreed upon as the go-to method for development of machine learning systems [104].

In addition to independently testing the model using the withheld test set, the concept of cross validation is almost universally employed as a method of strong validation of model performance. This consists of partitioning duplicates of the dataset in multiple ways and iteratively training and testing a model to evaluate the consistency of the performance across different splits of the dataset [104].

The most common cross validation method is known as k-fold cross validation, whereby the dataset is randomly shuffled and split according to a chosen integer, k (most commonly 5, 10, or 20) [104]. The dataset is split into k equally sized subsets at random, $k-1$ of which are used for training, with the remaining subset being used for testing. This process is repeated k times, with the resulting performance metrics evaluated using each test set averaged to provide a final set of cross validated scores with high confidence [104].

A k value of 10 is most commonly used when developing machine learning systems to provide a high enough level of confidence in the performance of the model, it is often the case that stratified sampling is also used to preserve the original distribution of the dataset [104]. A visualisation of the data splitting methodology of 10-fold cross validation is shown below in figure 12.

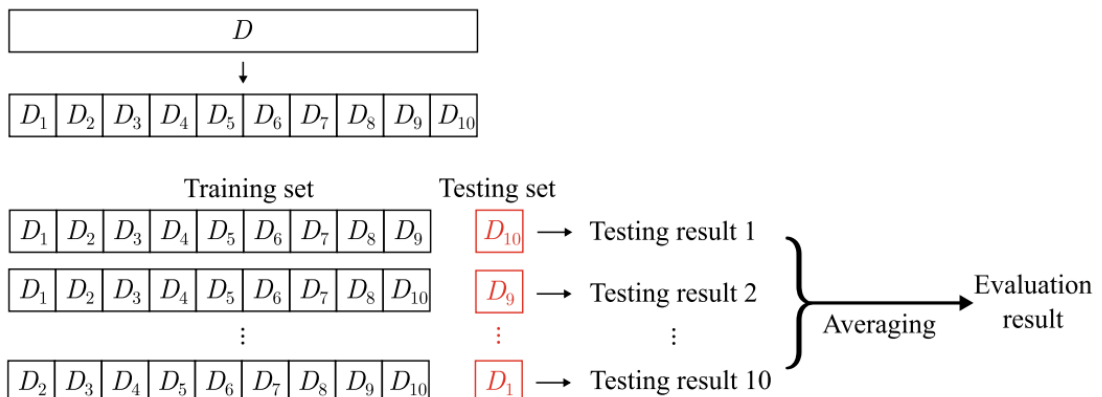


Figure 12: Visual Representation of 10-fold Cross Validation Dataset Train/Test Splitting [104].

2.10 CFD Governing Equations

While CFD remains a secondary part of this research which is primarily concerned with the various methods of overpressure and radiation calculation, CFD is used as a tool to provide the input variables which are utilised within these calculation methods.

ANSYS Fluent software was selected to model the hydrogen gas leakage scenario under investigation and provides values of the flammable hydrogen cloud volume (m^3) and hydrogen volume fraction related to this scenario.

More details of the CFD geometry, mesh and setup are described in section 5.

The software solves conservation equations of mass and momentum for various flows.

2.10.1 Conservation of mass

Equation 17:

$$\frac{\partial \rho}{\partial t} + \nabla \cdot (\rho \vec{v}) = S_m$$

This is the general form of the mass conservation equation (continuity equation) which is valid for both compressible and incompressible flows. The term S_m on the right-hand side of the equation denotes the source [105].

2.10.2 Conservation of momentum

Equation 18:

$$\frac{\partial}{\partial t}(\rho \vec{v}) + \nabla \cdot (\rho \vec{v} \vec{v}) = -\nabla p + \nabla \cdot (\bar{\tau}) + \rho \vec{g} + \vec{F}$$

Equation 18 (above) describes the conservation of momentum equation in an inertial reference frame where p is static pressure, ρg and F are body forces and τ is a stress tensor given by the following, equation 19:

Equation 19:

$$\bar{\tau} = \mu \left[\left(\nabla \vec{v} + \nabla \vec{v}^T \right) - \frac{2}{3} \nabla \cdot \vec{v} I \right]$$

The term μ is the molecular viscosity, I is the unit tensor and ∇ is the effect of volume dilation [105].

2.10.3 Conservation of energy

The conservation of energy is described by equation 20:

Equation 20:

$$\frac{\partial}{\partial t}(\rho E) + \nabla \cdot (\vec{v} (\rho E + p)) = -\nabla \cdot \left(\sum_j h_j J_j \right) + S_h$$

Where the following describes the transport of enthalpy due to species diffusion [105]:

Equation 21:

$$\nabla \cdot \left[\sum_{i=1}^n h_i \vec{J}_i \right]$$

2.10.4 Species Transport Modelling

The leaked hydrogen gas mixes with air in the atmosphere as it is ejected through a jet stream from the storage container and is modelled using a species transport model. Fluent solves conservation equations for each gaseous species in the model and in doing so, simulates the mixing and transport of the species.

For species transport modelling, the convection-diffusion equation is used which predicts the local mass fraction of species Y_i for the i^{th} species. ANSYS Fluent was used to model the mixing and transport of chemical species in order to solve conservation equations for diffusion, convection and reaction sources for each species. Hydrogen and oxygen were both two important elements involved in this particular project with their particular concentrations inserted as inputs at different regions of the model.

Equation 22:

$$\frac{\partial}{\partial t} (\rho Y_i) + \nabla \cdot (\rho \vec{v} Y_i) = -\nabla \cdot \vec{J}_i + R_i + S_i$$

Where R_i is the net rate of production by chemical reaction for a species, i . S_i is the rate of creation by addition from the dispersed phase plus any user-defined source. This is solved for $N - 1$ where N is the number of fluid chemical species in the system.

Equation 23:

$$\vec{J}_i = - \left(\rho D_{i,m} + \frac{\mu_t}{Sc_t} \right) \nabla Y_i - D_{T,i} \frac{\nabla T}{T}$$

J_i is diffusion flux for a species i , $D_{i,m}$ is a species' mass diffusion coefficient, $D_{T,i}$ is the thermal diffusion coefficient, Sc_t defines the turbulent Schmit number which is 0.7 by default [105].

2.10.5 Turbulence Modelling

The realisable $k-\epsilon$ model was selected to model turbulence. In equation 24 below, k represents a kinetic energy transport equation. Equation 25 is a transport equation involving the dissipation rate, ϵ in the model.

Equation 24:

$$\frac{\partial}{\partial t} (\rho k) + \frac{\partial}{\partial x_j} (\rho k u_j) = \frac{\partial}{\partial x_j} \left[\left(\mu + \frac{\mu_t}{\sigma_k} \right) \frac{\partial k}{\partial x_j} \right] + G_k + G_b - \rho \epsilon - Y_M + S_k$$

And,

Equation 25:

$$\frac{\partial}{\partial t}(\rho \varepsilon) + \frac{\partial}{\partial x_j}(\rho \varepsilon u_j) = \frac{\partial}{\partial x_j} \left[\left(\mu + \frac{\mu_t}{\sigma_\varepsilon} \right) \frac{\partial \varepsilon}{\partial x_j} \right] + \rho C_1 S_\varepsilon - \rho C_2 \frac{\varepsilon^2}{k + \sqrt{v_\varepsilon}} + C_{1\varepsilon} \frac{\varepsilon}{k} C_{3\varepsilon} G_b + S_\varepsilon$$

Where:

$$C_1 = \max \left[0.43, \frac{\eta}{\eta + 5} \right], \quad \eta = S \frac{k}{\varepsilon}, \quad S = \sqrt{2S_{ij}S_{ij}}$$

Where, G_K is the generation of turbulence kinetic energy due to the mean velocity gradient, G_b is the turbulence kinetic energy generated as a result of buoyancy, S_M represents fluctuating dilatation contribution overall dissipation rate for compressible turbulence, σ_K and σ_ε are turbulent Prandtl numbers for K and ε , C_2 and $C_{1\varepsilon}$ are constants. The remaining terms, S_ε and S_K are user-defined source terms.

The constants correspond to the following values for this model of: $C_{1\varepsilon} = 1.44$, $C_2 = 1.9$, $\sigma_K = 1.0$ and $\sigma_\varepsilon = 1.2$. Buoyancy is an important and distinctive feature of hydrogen gas, represented by equation 26:

Equation 26:

$$G_b = \beta g_i \frac{\mu_t}{Pr_t} \frac{\partial T}{\partial x_i}$$

Where β is the coefficient of thermal expansion, g_i is the gravitational component in the direction i and Pr_t is the turbulent Prandtl number for energy which is given a default value of 0.85 for realisable k- ε models.

There are two key differences between the standard and realisable k- ε model. Standard and realisable contain different formulations for the turbulent viscosity. They also differ in the transport equation they use for dissipation rate, ε . The realisable model is based on the dynamic equation of the mean-square vorticity fluctuation. ‘Realisable’ means that “the model satisfies certain mathematical constraints on the Reynolds stress, relevant to turbulent flow physics” [105].

2.11 Hydrogen Leakage Safety Analysis Software

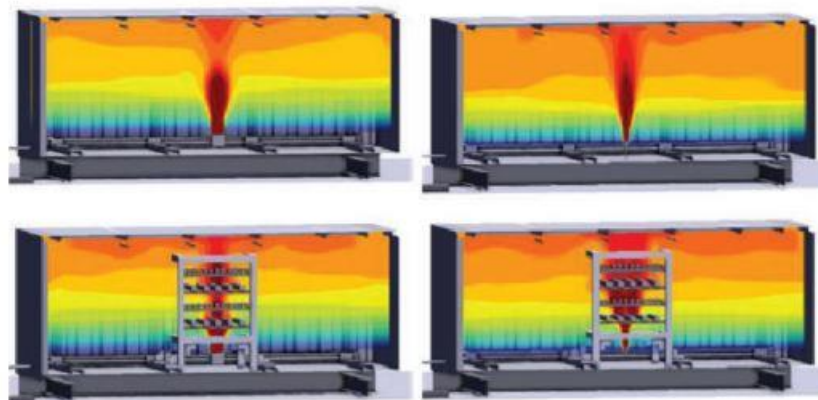
Due to various properties of hydrogen outlined throughout section 2.1, it is vital that the way hydrogen is stored is carefully considered to ensure its safe use. Safety analysis software’s which often use CFD can be very useful tools in hazard awareness and risk analysis, which allows precautions to be taken and mitigation of leakage consequences. They can help in designing a safe and reliable hydrogen storage system.

2.11.1 PHAST

DNV (Det Norske Veritas) are an organisation that specialises in assurance and risk management. DNV are a world leader in health and safety digital solutions and have a software, PHAST which can be used for managing risk and enhancing safety within an industrial environment. [106] The Process Hazard Development Software (PHAST) is the most comprehensive process hazard analysis software system in the world and is used by more than 1000 organisations globally. [107] It can model an accident scenario from the initial leakage to the dispersion of large volumes of spreading gas. This software can model; leaks, ruptures, dispersion and flammable hazards and also has 3D explosion modelling capabilities. [107] The 3D explosion modelling software appears to be useful for investigating gas leakage scenarios and very relevant to the project. The software can analyse VCEs and can use either the Baker Strehlow Tang or Multi-Energy methods to investigate the impact of the flammable cloud in 3D when congestion is considered. Crucially, this software can calculate blast loads such as overpressure for a given scenario. This software also considers the effect of wind [108].

2.11.2 Gexcon Software Including FLACS – CFD

Gexcon are another leading company in the safety and risk management sector. Gexcon have experience in many hydrogen safety projects in a number of applications including hydrogen plants and filling stations. More specifically some of the hydrogen work Gexcon have done includes estimation of safe distances which is central to this investigation. They have experience in dispersion, explosion and fire simulations – all key areas in hydrogen leakage safety analyses and they develop and market software's which have tools that are used for these analyses. These include; consequence modelling tools, quantitative risk analysis tools and pre-incident planning tools. FLACS (Flame Acceleration Simulator) CFD can be used to effectively model accidental hydrogen releases and explosions and the company also do their own hydrogen explosion testing to validate their software. Gexcon studies also include the structural response of a hydrogen storage container to an explosion using Finite Element models [109].



Modeling of an accidental release of hydrogen in a container with FLACS-CFD

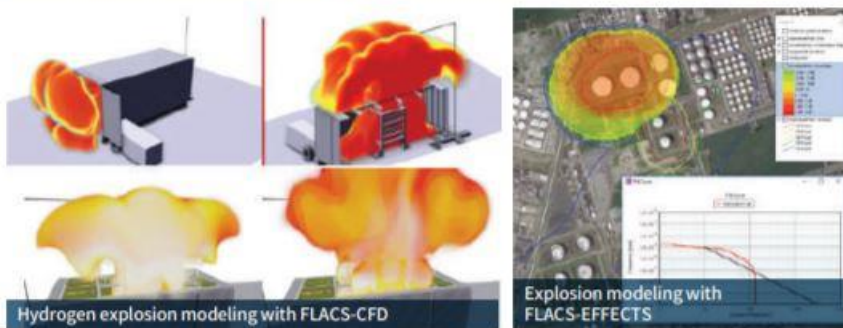


Figure 13: Example Images of Hydrogen Release and Explosion CFD Modelling Using FLACS Software [109].

3 Applications

As with any new, developing technology, a safety analysis is highly necessary to ensure safe usage of the product in the future, highlighting possible risks and recommendations for risk mitigation. Without rigorous safety analysis of hydrogen storage facilities, the rollout of hydrogen powered technologies and other applications of hydrogen gas would be impossible. This emphasises the importance of hydrogen safety research such as this study which future hydrogen technologies may heavily rely on. A variety of the applications where this research plays an important role are mentioned throughout section 3.

Hydrogen is a viable alternative as an energy storage solution, the clean power generated from renewable sources can be used to generate and store the gas for later consumption, and the process of production from water is emission-free. Hydrogen can be used as a replacement for traditional batteries in technology such as hydrogen fuel cell powered vehicles and can also be used as an alternative fuel in existing internal combustion engines with little modification [110]. Fuel cells also have the capability of being twice as efficient as combustion engines. These fuel cells combine oxygen and hydrogen in an electrochemical reaction which generates electricity that can be used to power a motor to drive a vehicle. Hydrogen fuel cells are currently in use to power many forms of vehicle, including cars, buses, trucks and forklifts. Hydrogen has also been used as a fuel for rockets for several years with its high energy density an advantage over traditional fuels for applications such as rocket launchers [111].

One current limitation with the use of hydrogen as a fuel is that despite having a high energy content per mass, the density of hydrogen remains low even when stored at high pressures or liquified which results in expensive energy storage [112].

3.1 Better than Batteries

In more recent decades, society has observed a global shift from fossil fuels as a means of energy generation, to clean alternatives such as solar and wind power. Traditional batteries, while an effective energy storage solution, cannot scale to meet the needs of humankind as a sole solution without considerable advancement in energy density and charging technology. Their large carbon footprint during production is cause for concern and something most people forget about or do not even realise is associated with battery technology. Therefore, batteries are not the only answer to all CO₂ related problems, and this is where hydrogen fuel comes in. Hydrogen storage is imperative for the technologies which rely on hydrogen as a fuel.

3.2 Shipping Industry

Hydrogen fuel and its associated storage techniques are of particular interest to the maritime industry on their quest to decarbonise and go green. Hydrogen has already proven to have a promising future in the industry. This is evident from a number of ongoing projects across the globe which are looking to integrate fleets of hydrogen ferries and establish if such a concept

would be a viable alternative to the majority diesel and petrol ferries that 2.1 billion people use every year [113].

Scotland's Orkney islands are set to become home to the first hydrogen powered sea-going ferry in Europe which uses hydrogen produced entirely from local renewable energy sources [114]. This completely zero emissions Hyseas III project unveiled concept ferry designs in October 2021 and is undergoing string testing to validate the main power train components [115]. While the hydrogen may be produced locally in the vicinity of the proposed routes, ferry ports will require hydrogen storage facilities which in turn demand safety analyses.

Power2AX is a similar project which involves both the production and use of green hydrogen in ferries in the Åland archipelago of Finland. Hydrogen is planned to be produced from a wind farm in the Åland archipelago due to excellent wind conditions and used in fuel cell ferries in the region. This generation and usage of clean energy in a system in what is described as a "full sector coupling approach" provides the opportunity to develop 100% renewable systems in the future. Flexens are the company behind this project along with the government of Åland, engineering consultancies Elomatic and Deltamarin. The earliest set operation date for this technology is 2024 [116].

Norway is renowned as a leading producer of clean energy and is also one of the largest energy exporters in the world. As a nation with a vast coastline and over 1000 fjords, ferries play a huge role in Norway's transport infrastructure. The MF Hydra – hailed as the world's first liquid hydrogen ferry – was delivered to Norwegian ferry operator Norled in July 2021. This hydrogen fuel cell ferry will reduce carbon emissions from its predecessor by a substantial 95% [117].

The launch of Switch Maritime's Sea Change ferry labelled the first commercial ferry powered entirely by 100% hydrogen fuel cells underwent trials in the San Francisco Bay Area of California, starting August 2021. Unlike the MF Hydra, Sea Change is a completely zero emissions ferry [118]. Major changes are set to take place in the future of the shipping industry as the potential of hydrogen fuel is now being realised through efforts such as Sea Change and MF Hydra.

The technology also has potential in existing natural gas ships which may be retrofitted with hydrogen fuel cells. This concept is being developed as part of the Havyard Group's FreeCO2ast project who will integrate a 3.2MW fuel cell into an existing sea vessel [119].

While the ferries store hydrogen onboard in liquified form, hydrogen gas is the product of electrolysis. Ultimately without this process and hydrogen gas storage, the applications which so depend on hydrogen would be impossible to maintain, stressing the relevance of this investigation and future research into this area.

3.3 Fuel Cell Vehicles

The year 2013 saw the first commercially available hydrogen fuel cell vehicle on the market – the Hyundai ix35 FCEV. This marked the new age of clean, zero emission transport solutions. Now, less than a decade later, significant progress is being made in the FCV industry with major automotive companies such as Toyota, Honda, Hyundai, Audi and BMW pursuing this area, holding a majority market share. In 2018, the hydrogen fuel cell market was valued at \$651.9 million. This is projected to increase to a value of over \$42 billion by 2026 [120]. The investment in this area comes as greater efforts are made to tackle the climate crisis along with business and government initiatives, pledging to reduce their carbon footprint.

Cellcentric - a new joint venture by automotive leaders Volvo and Daimler Truck AG – announced in April 2021, will be a first for the industry as a global manufacturer of hydrogen fuel cells particularly for applications in long-haulage trucks [121]. Hydrogen fuel cells are predicted to be a highly favourable alternative to electric motors for heavy goods vehicles in the future and Cellcentric hope to lead the way in this niche market.

Germany have already established a strong network of hydrogen refuelling stations for passenger cars. However, further work is needed in this area as it is not currently cost effective in towns with smaller populations [112].

Hydrogen fuel cells also have a promising future within construction equipment and other industrial applications so much so that Volvo Construction Equipment (CE) have opened a test laboratory in Eskilstuna, Sweden in May 2021 for this express purpose [122].

While the technology has many advantages, it is not without its limitations. There is an EU wide demand for truck specific fuelling stations to be constructed and targets of 300 and 1000 stations to be built by 2025 and 2030, respectively [123]. Safety investigations will play a crucial role in meeting these targets and are an essential step in the planning and construction of these refuelling stations.

3.4 Space Industry

Hydrogen fuel cell applications have been at the forefront of the space industry for many years now, having been used as far back as 1963 which saw the first successful in-flight burn of a liquid-hydrogen/liquid-oxygen engine of the Centaur rocket. Hydrogen storage, detection systems and other associated applications have been a major focal point for NASA research and development and remain as such to this day [124]. Hydrogen is highly advantageous to the industry as it can be produced and recycled in space thus reducing the cost and intricacy of future missions. This will be of particular use on long, remote missions where payload is limited. For example, if water is attainable on the surface of Mars, hydrogen can be generated through the process of electrolysis and go on to be used as a source of power for potential return missions.

4 Methodology

4.1 Method Aim

The methodology implemented in the following section provides a rigorous and systematic process of producing “ballpark” estimate values for the positionally safe distances of hydrogen storage systems in an industrial environment. These safe distances are calculated when given the desired safe values of pressure and thermal radiation from ignition of a vapour cloud as a result of hydrogen gas dispersion.

4.2 Safety Limits

The methodology for calculation of safe distances takes into consideration a safe shockwave overpressure limit, as well as a thermal radiation limit. Both conditions must be satisfied for the distance limit to be considered “safe”.

4.2.1 Safety Limits for Overpressure

Overpressure	Damage
0.5 psi (≈ 3 kPa)	Windows shattered, limited minor damage to house structures.
1 psi (≈ 7 kPa)	Partial demolition of houses; corrugated metal panels fail and buckle; skin lacerations from flying glass.
5 psi (≈ 34 kPa)	Wooden utility poles snapped.
10 psi (≈ 69 kPa)	Probable total building collapse. Lungs hemorrhage.

Figure 14: Overpressure Values for Expected Damages to Buildings and Structures [125].

From the table above, it is evident that the overpressure at a certain distance away from the point of a hydrogen explosion must not exceed 3 kPa in order to avoid expected minor damages to building structures and shattering of windows.

Effect	Overpressure, kPa
Temporary threshold shift [57]: “no harm” threshold for hazard distance (evacuation perimeter)	1.35
1% probability of eardrum rupture (chosen as “injury” threshold) [58]	16.5
1% probability of fatality-lung haemorrhage (chosen as “fatality” threshold) [58]	100

Figure 15: Effects Observed at Various Overpressure Values [126].

Damage	Overpressure, kPa
Minor damage of the house	4.8
Partial demolition of the house-remains inhabitable	6.9
Almost total destruction of the house	34.5-48.3

Figure 16: Damage Observed at Various Overpressure Values [126].

The effect of various overpressures on human health can be observed from figures 14 and 15 above. The “no harm” overpressure value of 1.35 kPa in figure 14 can be used to find a safe distance for humans from the explosive point. As 1.35 kPa is declared as a no-harm threshold, overpressure vs distance curves produced using the various methods can be used to specify the safe distance. The method which is found to be the best or most accurate can be used to find a final safe distance estimation.

Table 3: Effects of a pressure wave [24].

<u>Overpressure, kPa</u>	<u>Impacts on buildings and people</u>	<u>Possible construction or building types</u>
30	Collapse of load-bearing structures, possible accident risk of expansion	Industrial equipment and structures
15	Partial collapse of houses, risk of permanent injury	Buildings and structures for which this is acceptable for justified reasons upper limit, such as pressure resistance dimensioned industrial buildings
5	Minor damage to house structures Risk of injury	Buildings and areas where people normally stay

A visual representation of table 3 above is shown in Figure 17 below, showing the damage effects at various overpressure values which decrease further away from the point of explosion:

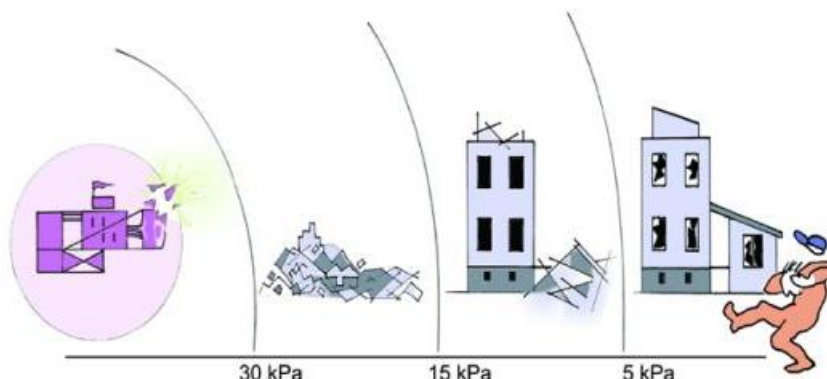


Figure 17: Pressure Wave Effects at Various Overpressure levels (kPa) [24].

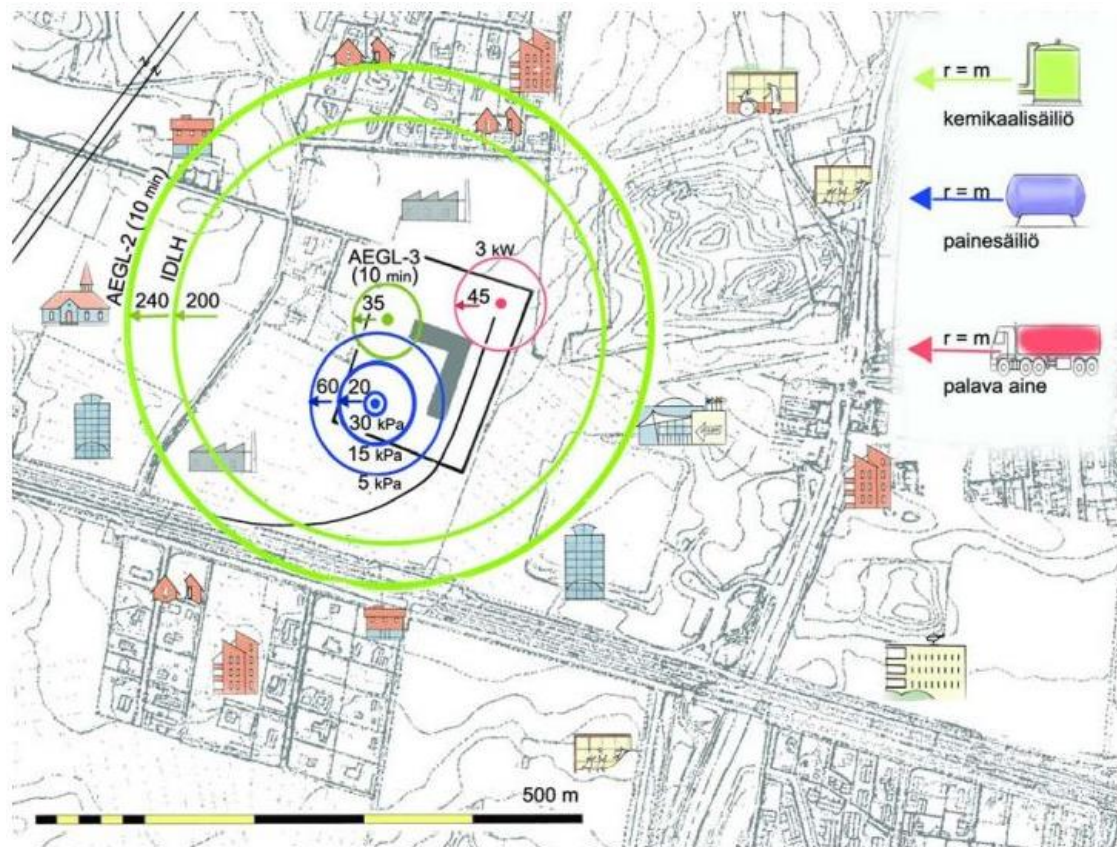


Figure 18: Map of Health, Radiation and Pressure Effects [24].

The green radii in Figure 18 represents a distance for different AEGL values (explained in section 2.2.2) concerning chemical storage. The pink radius represents a combustible storage distance. The circle and distances which are of greatest interest to this study are displayed in a blue colour and illustrate estimated safe distances for pressure vessels. Distances of 20m and 60m correspond to an overpressure of 15 kPa and 5 kPa respectively.

As discussed with the stakeholders a value of 10 kPa would be the crucial limit for overpressure at a site border for the leakage scenario relevant to this project. From this overpressure limit, importantly a safe distance could be obtained using implemented methods which are described throughout section 4.

4.2.2 Safety Limits for Thermal Radiation

The effects of thermal radiation, like overpressure are important safety considerations in an industrial setting. Thermal radiation has previously been discussed in section 2.2.3 where effects of thermal radiation over a given time duration and industrial methods for reducing levels of thermal radiation were mentioned.

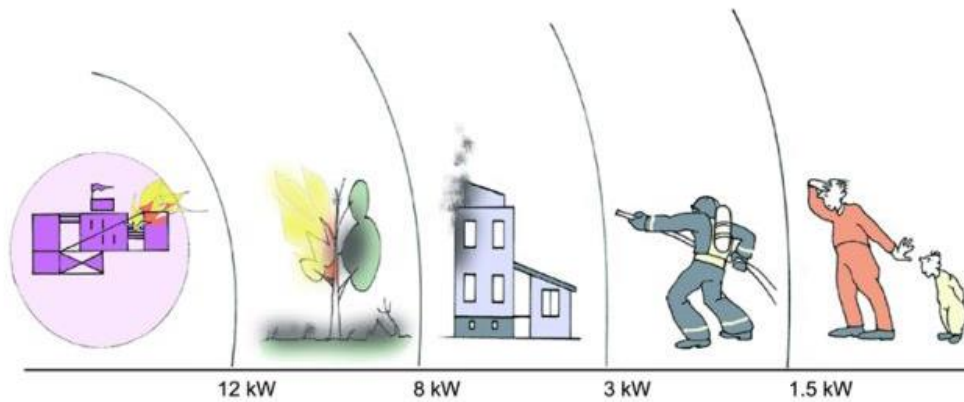


Figure 19: Varying Thermal Radiation Effects Diagram [24].

Above, Figure 19 demonstrates that (fire) rescue operations can progress up to and including the distance where heat flux is 3 kW/m^2 , and bystanders are safe up to and including the distance where heat flux reaches 1.5 kW/m^2 . As discussed with project stakeholders, 8 kW/m^2 would be the main limit used for thermal radiation for the purposes of the investigation which involves a leakage scenario in an industrial setting.

4.3 Hydrogen Leakage: Possible Worst-Case Scenario

The scenario investigated in this project was constructed based on recommendations from project stakeholder, Elomatic. These recommendations include specifications regarding site layout and boundary conditions. A hydrogen leakage can result in various different outcomes depending on a number of factors. The main outcomes resulting from an accidental hydrogen release are summarised in the following diagram:

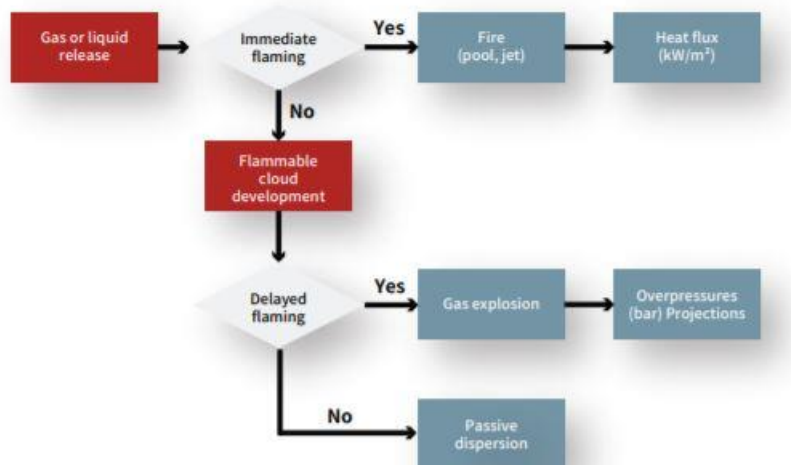


Figure 20: Potential Outcomes of an Accidental Hydrogen Release [109].

As seen in figure 20, the main scenario involved in this investigation involves a hydrogen release which forms a flammable cloud which then results in an explosion after ignition.

In the event of a sudden rupture of a high-pressure hydrogen storage vessel, resulting in the rapid release of hydrogen into the atmosphere, the aggressive expansion of the gas can form a shockwave that will radiate out from the rupture location, carrying with it an overpressure effect. However, while this event would be very destructive, it is incredibly unlikely to occur, as the pressure vessel would need to be impacted in such a manner that would result in a rupture orifice with size sufficient to pose little or no restriction to the escape and expansion of the gas. This scenario would require an excessive amount of impact force on the vessel, or require it to undergo internal structural failure, perhaps due to filling to a pressure far beyond the rated working pressure, or due to manufacturing defects that would almost certainly be detected during testing and quality control. Other potential reasons for failure were described in earlier section 2.4.

In the event of a leakage from a hydrogen container, there is a high possibility of a flammable hydrogen-air cloud forming around the leakage site, which will most likely be ignited from some source (given certain conditions as outlined in section 2.1.1). Preventative measure to reduce the likelihood of ignition are given in section 2.2.6. This explosion will also produce a shockwave – the effects of which are realised through blast wave overpressure - as well as exposing the surroundings to a significant amount of thermal radiation. The overpressure and thermal heat flux radiation are central to this investigation and the methodologies of calculating such are described in this section.

4.3.1 Layout of hydrogen storage facilities

For the purposes of the scenario in question, the container gas cylinders are connected with piping in groups so that the maximum hydrogen release is limited to a couple of containers in the event of a failure. The worst-case leakage is dependent on how many cylinders are connected per group. Self-acting valves are usually installed in this type of tank system arrangement and will close in the event of a breach.

The scenario central to this investigation is concerned with a leak of hydrogen gas from the end face of a cylindrical storage vessel. The storage vessel is positioned in an outside, semi-obstructed atmosphere. The location can be described as “semi-obstructed” as 2 buildings are positioned in the surrounding region where the hydrogen vapour cloud forms. These could represent office buildings or warehouse spaces at a hydrogen gas storage or production facility. More details and figures of the proposed scenario location are provided in section 5.

High winds are known to result in substantial dispersion of gas from gas leaks meanwhile slight gusts or no wind conditions can result in the largest cloud volumes and therefore the worst cases of explosion. Due to computational time and project scope, the scenario investigated here analyses gas dispersion with a “no wind” condition. It was expected that very high wind speeds would disperse the gas cloud and reduce the severity of the accident, so therefore the worst-case leakage would be a result of very low wind speeds or no wind at all. Due to time limitations and project scope,

the effects of varying wind speed were not investigated. However, the effects of wind could be a useful area for future work as further explained in section 10.

4.3.2 Pressure vessel data

Umoe Advanced Composites pressure vessels were selected to store the hydrogen gas for this specific case. Data associated with these type IV pressure vessels was provided by Elomatic and includes hydrogen storage details relevant to this scenario - highlighted in the table below [42]. Details on the type of pressure vessels used in this scenario are provided in earlier section 2.2.7.

Standard type IV pressure vessels

Working pressure (bar)	Water volume (liter)	Length (mm)	Diameter (mm)	Hydrogen capacity (kg)
200	1 650	5 720	708	24
250	1 650	5 720	728	31
300	1 650	5 720	739	35
350	1 650	5 720	750	40
200	1 700	5 860	708	25
250	1 700	5 860	728	31
300	1 700	5 860	739	37
350	1 700	5 860	750	41
200	1 925	6 600	708	28
250	1 925	6 600	728	36
300	1 925	6 600	739	41
350	1 925	6 600	750	46

Figure 21: Pressure Vessel Data Relevant to the Selected Hydrogen Storage (highlighted in the red box) [42].

The release rate of a gas is dependent on the size of the pipe used and cylinder pressure. The flow rate from gas production to the storage is 126 kg/h and from the storage to use 1800 kg/h under normal operating conditions. However, when a pipe is broken, this flow rate can be expected to be much higher. This information was provided by Elomatic. The equivalent mass flow rate values for hydrogen at the leakage point is shown in table 11 (section 5.4). These values were provided by Elomatic, for two different working pressure values: 350 bar and 35 bar. 350 bar was selected as it was the highest pressure considered for this hydrogen storage scenario and will therefore result in a worst-case leakage accident as this will discharge the most gas. 35 bar is equivalent to the pre-tank pressure, from the electrolyser. In addition, the resulting flow from a 35-bar burst was easier to simulate using CFD as it is significantly less computationally intensive than the higher pressure of 350 bar.

Since the hydrogen capacity of a singular cylinder is 46kg (figure 21), it is reasonable that a sudden release of this amount could occur from a serious failure such as severe damage to the top connection of the cylinder or in the cylinder structure.

4.3.3 Surroundings and Environmental factors

In reality, surroundings and environmental factors can have an impact on the leakage from hydrogen storage. Some important and commonly investigated factors in gas leakage are wind effects and obstructions such as surrounding buildings.

An assessment can be made whether wind gusts are beneficial or detrimental to the risks associated with the spread of gas in the particular leakage scenario being modelled. The concentration of hydrogen would be expected to drop but the gas cloud would be expected to spread over a larger area with greater wind [11]. Any nearby obstacles have to be carefully considered in the event of a gas release. Similar to wind, obstacles can have a negative or positive effect on the severity of gas leakage consequences. A positive effect could be that obstacles can reduce the hazardous area of the gas cloud which is spreading. On the other hand, many obstacles or walls surrounding the leakage can cause the gas cloud to accumulate, leading potentially to a catastrophic explosion such as was the case in the Stockholm incident [11].

4.4 Traditional Methods for Overpressure Calculation

Research into calculation methods was of paramount importance to the present study and so a number of other reports into these methods were analysed and discussed earlier in sections 2.5 and 2.6. The methods which were researched and found to be valuable to the aims of this research are presented in greater detail in the following section.

4.4.1 Curve Fitting Estimation Method

The curve fitting estimation method is the first of four methods used to obtain overpressure vs distance curves. The main aspect of this method - as this name suggests – is curve fitting. Following the study presenting this method, power and exponential trends provided the highest correlation coefficient values and so polynomial, and logarithmic trends were disregarded. After parity plots were generated to evaluate the suitability of power and exponential plots, it was concluded that the power curve expression was the most suitable for hydrogen overpressure prediction. Furthermore, this method was found to be the most reliable when compared with an existing model and other experimental results proving its value to this research.

The resulting estimation formulae are shown below [68].

Equation 27:

$$A = 0.0000006948(V \times C)^3 - 0.0000807(V \times C)^2 + 0.002943(V \times C) + 0.02095$$

$$B = -0.7072$$

Equation 28:

$$P' = \frac{\Delta P}{Pa}$$

Equation 29:

$$Z = \frac{D}{(E/Pa)^{\left(\frac{1}{3}\right)}}$$

Equation 30:

$$E = V \times C \times H_c$$

Equation 31:

$$\text{Scaled overpressure} = A * \text{Scaled distance}^B$$

Where:

P' = Scaled overpressure

ΔP = Overpressure (Pa)

Pa = Ambient pressure (Pa)

Z = Scaled distance

D = Distance from ignition point in cloud to transducer recording pressure from blast wave (m)

V = Volume of the H-A mixture (m^3)

H_c = Heat of combustion (J/m^3)

E = Energy of the explosion (J)

C = Hydrogen volume fraction in the cloud

A and B = Coefficients

4.4.2 TNT Equivalency Method

The TNT equivalence method is capable of evaluating overpressure by approximating the energy release of one particular explosion - in this case a hydrogen vapour cloud explosion - to that of a TNT explosion. In order to do this, the equivalent mass of TNT must first be calculated.

The equivalent mass of TNT can be calculated using following equation 32:

Equation 32:

$$M_{TNT} = \frac{M_{cloud} \Delta H \cdot \eta}{\Delta H_{TNT}}$$

Where:

M_{TNT} = Equivalent mass of TNT (kg)

M_{cloud} = Mass of hydrogen in the cloud (kg)

ΔH = Lower heat of combustion of hydrogen (130800 kJ/kg)

ΔH_{TNT} = Lower heat of combustion of TNT (4520 kJ/kg)

η = Efficiency of explosion

(η is usually between 0.01 to 0.1 for an unconfined vapour cloud explosion)

The safe distance to a specified pressure level may be calculated using equation 33:

Equation 33:

$$D = 0.3967 M_{TNT}^{\frac{1}{3}} e^{[3.503 - 0.724 \ln P + 0.0398(\ln P)^2]}$$

And rearranged for pressure:

Equation 34:

$$P = e^{\frac{0.7241 - (0.1592 \ln(2.52079D) - \frac{0.1592}{3} \ln(M_{TNT}) - 0.033372711)}{0.0796}}$$

Where:

P = Peak overpressure (psi)

D = Distance (m)

M_{TNT} = Equivalent mass of TNT (kg)

4.4.3 TNO Multi-Energy Method

As outlined in earlier section 2.5.8, the TNO Multi-Energy has been widely documented as a method for predicting overpressure resulting from vapour cloud explosions and as such is useful to this research. The method evaluates overpressure based on various curves corresponding to levels of explosion confinement. There are 10 curves in total, however only 4 are related to the type of vapour cloud explosion considered in this investigation.

Conveniently, the traditional, paper-copy blast curves outlined for the TNO method, have been modernised and converted to analytical form as previously mentioned in the literature review. This modernised method takes the form of a power curve as shown below in equation 35.

Equation 35:

$$P' = aZ^b$$

Where:

P' = Scaled Overpressure

Z = Scaled Distance

a, b = Fitted Equation Coefficients

The coefficients a , and b , can be found from the paper describing the new modern versions of the TNO method curves [70], and are shown below in table 4.

Table 4: TNO method fitted power curve coefficients [70].

Explosion level	Interval for R'	a	b	Interval for R'	a	b
1	$0.23 \leq R' < 0.6$	10^{-2}	0	$0.6 \leq R' \leq 7$	6.40×10^{-3}	-0.97
2	$0.23 \leq R' < 0.7$	2×10^{-2}	0	$0.7 \leq R' \leq 12$	1.32×10^{-2}	-0.98
3	$0.23 \leq R' < 0.6$	5×10^{-2}	0	$0.6 \leq R' \leq 30$	6.05×10^{-2}	-0.99
4	$0.23 \leq R' < 0.5$	10^{-1}	0	$0.5 \leq R' \leq 70$	6.44×10^{-2}	-0.99
5	$0.23 \leq R' < 0.6$	2×10^{-1}	0	$0.6 \leq R' \leq 90$	1.17×10^{-1}	-0.99
6	$0.23 \leq R' < 0.6$	5×10^{-1}	0	$0.6 \leq R' \leq 100$	3.01×10^{-1}	-1.11
7	$0.23 \leq R' < 0.5$	1	0	$0.5 \leq R' \leq 100$	4.06×10^{-1}	-1.20
8	$0.23 \leq R' < 0.5$	2	0	$0.5 \leq R' < 1$	4.76×10^{-1}	-2.08
	$1 \leq R' < 2$	4.67×10^{-1}	-1.58	$2 \leq R' \leq 100$	3.18×10^{-1}	-1.13
9	$0.23 \leq R' < 0.35$	5	0	$0.35 \leq R' < 1$	4.87×10^{-1}	-2.03
	$1 \leq R' < 2$	4.67×10^{-1}	-1.58	$2 \leq R' \leq 100$	3.18×10^{-1}	-1.13
10	$0.23 \leq R' < 1$	4.41×10^{-1}	-2.39	$1 \leq R' < 2$	4.67×10^{-1}	-1.58
	$2 \leq R' \leq 100$	3.18×10^{-1}	-1.13			

The scaled pressure and scaled distance are calculated as defined in the curve fitting estimation method above, using equation 28 and 29 respectively.

4.4.4 Baker-Strehlow-Tang (BST) Method

BST method requires selection of the maximum flame speed, on the basis of the combined effects of the following factors: congestion, fuel reactivity and confinement.

For our hydrogen case, congestion levels are low, area blockage is < 10% and the number of obstacle layers is 1 or 2. Hydrogen has high reactivity and the confinement is 3D – almost completely unconfined volume. Therefore, reading from Table 10.20 in the BST literature source discussed in section 2.5.9, the flame speed Mach number is 0.36. Calculation of distance or associated pressure is done by reading the appropriate blast curve for the chosen Mach number, and using the same equations 28 and 29 shown for the curve fitting method, the scaled values from the curve can be converted to real results.

4.5 Traditional Methods for Heat Flux Calculation

Section 4.5 describes the two methods which were utilised to calculate heat flux radiation at various distances from the modelled explosion. The results of these calculations can be considered alongside guidelines and recommended maximum heat flux values to find the safe distance from the explosive scenario investigated. Although overpressure is of greater

importance, heat flux limits should still be considered, despite the little existing data and few methods that exist for calculating such.

4.5.1 Solid Flame Model

The first of two methods used to acquire values for radiation heat flux at various distances is termed as the “solid flame model” which was developed primarily for calculation of heat flux in worst cases. The instant of hydrogen cloud ignition and explosion is assumed as a solid flame fire which is approximated as a sphere. The resulting thermal radiation is also assumed to diffuse from the sphere surface and is calculated using the following equations:

Equation 36:

$$D_F = 7.93 \times \sqrt[3]{(V_c \rho_c)}$$

Equation 37:

$$D = \sqrt{Z_p^2 + R^2}$$

Equation 38:

$$F_V = \left(\frac{D_f}{2D} \right)^2 \times \cos \theta$$

Equation 39:

$$E = e(5.67 \times 10^{-8})(T_F^4)$$

Equation 40:

$$\tau = 2.02 \left(P_W \left(D - \frac{D_F}{2} \right) \right)^{-0.09}$$

Equation 41:

$$q = \tau \cdot F_v \cdot E_s$$

Where:

q = Incident radiative heat flux from explosion (fireball) (kW/m^2)

τ = Atmospheric transmissivity

F_v = View factor

E_s = Surface emissive power (W/m^2)

V_c = Volume of hydrogen in the cloud (m^3)

ρ_c = Density of hydrogen at atmospheric conditions (kg/m^3)

θ = View factor angle (degrees)

D = Distance from fireball to centre of target (m)

D_F = Fireball diameter (m)

e = Emissivity factor ($0 < e < 1$) ($e=1$, black body emitter)

T_F = Fireball flame temperature (K)

P_w = Partial vapour water pressure at atmospheric conditions (Pa)

4.5.2 Radiation due to BLEVE's Model

While the second method for calculation of heat flux is primarily for BLEVEs, the method has been used here to approximate the resulting heat flux from a hydrogen vapour cloud explosion. The radiation received by an object at some distance from the cloud (approximated as a fireball) is calculated through the following equation:

Equation 42:

$$Z_p = 12.73 \times \sqrt[3]{V_c}$$

Equation 43:

$$D = \sqrt{Z_p^2 + Rh^2}$$

Equation 44:

$$q = \frac{828 (V_c \rho_c)^{0.771}}{D^2}$$

Where:

q = thermal radiation from the cloud (fireball) (kW/m^2)

Rh = Horizontal distance from the centre of the fireball to the target (m)

Z_p = Flame height (m)

V_c = Volume of hydrogen in the cloud (m^3)

ρ_c = Density of hydrogen at atmospheric conditions (kg/m^3)

D = Distance from the centre of the fireball to the target (m)

4.6 Machine Learning for Overpressure Calculation

4.6.1 Experimental Method Goals

For the purpose of this research, an attempt was made to develop and implement a new method for estimating the peak overpressure at a given distance from an unobstructed, unconfined hydrogen vapour cloud explosion. The implementation of this method revolved around the training of machine learning algorithms using the data acquired from experiments involving controlled hydrogen vapour cloud explosions, in order to form a regression model that can be used to predict resulting pressure values from input data. Building on the previous research in this field of using machine learning models to capture the complex relationships involving positive overpressure from unconfined explosions as mentioned in the literature review and applying a new approach to forming a regression model from the experimental data presented in the curve fitting estimation method [68].

4.6.2 Experimental Data

The experimental data was taken from the same research paper that presented the curve fitting estimation method [68], which used the data to perform a traditional mathematical curve fit which presented prediction results more accurate than older, non-hydrogen specific methods. The data is gathered from numerous experiments and covers a small array of hydrogen concentrations and cloud sizes. The dataset consists of 3 input features: cloud hydrogen volume concentration, cloud volume, and sensor distance from the origin of the explosion. There is a single target variable, the peak positive overpressure.

The dataset contains a total of 87 samples from 14 different experiments of different hydrogen concentration and cloud volume combinations, with overpressure values measured at a variety of different distances, all for unconfined hydrogen vapour cloud explosions. The dataset is attached in Appendix 1.

4.6.3 Machine Learning Model Selection

As the nature of the problem can be described as a multivariate regression, a variety of appropriate algorithms were selected and tested for performance and accuracy. The chosen algorithms are listed in table 5 below.

Table 5 - List of Considered Machine Learning Algorithms.

Random Decision Forest	Extremely Randomised Trees	Gradient Tree Boosting	k-Nearest Neighbours	Support Vector Machine	Multi-Layer Perceptron
------------------------	----------------------------	------------------------	----------------------	------------------------	------------------------

All of these models are capable of multivariate regression, and each possess their own preferred use cases and areas in which they may offer an advantage. In order to find the optimal algorithm for this problem, all the above-mentioned models were extensively tested, tuned, and validated to find the ideal solution to this problem case, while providing confidence in the results.

4.6.4 Model Hyperparameter Tuning

An exhaustive grid of hyperparameter values were iterated through in order to determine the optimally tuned values for each model that produced the best performance. There is no shortcut to determining the best parameters for a model, therefore this extensive “trial and error” approach whereby the performance is measured after each iteration, was adopted. The range of values tested for each model is shown below.

Table 6: Parameter Tuning Grid for Random Forest and “ExtraTrees” models.

Parameter	No. of trees	Minimum no. of samples to split a node	Minimum no. of samples at a leaf node
Range	10-300	2-4	1-4
Step	5	1	1

Table 7: Parameter Tuning Grid for Gradient Boosted Trees Model.

Parameter	No. of trees	Minimum no. of samples to split a node	Minimum no. of samples at a leaf node	Learning rate	Maximum depth of each tree
Range	10-300	2-4	1-4	0.1-1	1-5
Step	10	1	1	0.1	1

Table 8: Parameter Tuning Grid for k-Nearest Neighbours Model.

Parameter	No. of Neighbours	Weighting	Leaf size
Range	1-10	Uniform/Distance	5-50
Step	1	-	1

Table 9: Parameter Tuning Grid for Support Vector Machine Model.

Parameter	nu	C	Kernel	Degree (polynomial only)
Range	0.1-1	0.5-3	Linear/Polynomial/RBF/Sigmoid	2-5
Step	0.1	0.5	-	1

Table 10: Parameter Tuning Grid for Multi-Layer Perceptron Model.

Parameter	Hidden Layers	Hidden Layer Neurons	Activation Function
Range	1-6	2-8	ReLU/Tanh/Logistic
Step	1	1	-

4.6.5 Model Validation

As the models were tested and tuned, k-fold cross validation was implemented to ensure that the results are accurate and repeatable, and to give confidence in the performance of the models and the results produced. A 10-fold cross validation system utilising a 90:10 train/test split of the dataset was implemented and invoked at each iteration of the hyperparameter tuning process. The fold splits of the dataset were chosen randomly to eliminate possible bias in the model training stage.

4.7 Implementation

4.7.1 Implementation Of Estimation Methods

All methods described in this research were implemented in Python 3 using a robust and flexible approach to the design of the implemented code, allowing for the produced system to be universal, and accept any input parameters desired.

The standard format of double precision present within Python was believed to be more than sufficient for computational accuracy for this system, as accuracy and precision to a very high number of decimal places were not of any importance in the results, with the level of accuracy associated with the assumptions and design of the estimation methods being of far greater importance.

The standard Python math libraries, alongside the NumPy library were used to assist in the implementation of the system of the traditional methods, while the popular “Scikit-Learn” [127] machine learning library was used to facilitate the implementation of the machine learning estimation models, providing easy access to a number of algorithms and relevant model performance analysis and validation tools.

4.7.2 Considerations

Numerous implementation platforms were considered for this project, among the most relevant were: Python, MATLAB, and Excel for the implementation of the ballpark methods, with Python being chosen as the platform of choice due to the vast selection of open-source libraries and wide array of community-based support, and with the platform itself being open and free to use. The ability for this system to be used by anyone was of considerable importance due to the project relating heavily to the field of safety. It was deemed that MATLAB’s commercial nature may inhibit the ease of use of the finished system, as well as possibly hinder the development with a lack of available community libraries.

For the implementation of the CFD models, ANSYS Fluent was recommended by Elomatic as their currently used in-house software solution for CFD, offering their assistance and skilled experience and advice from many years of use alongside. Thus, ANSYS Fluent was used to perform the CFD simulations shown in this project, as the expertise and advice of the engineers at Elomatic was considered invaluable to the success of the project. It should be noted that other CFD software solutions such as OpenFOAM, SimScale and CobaltCFD, were also considered.

5 CFD

While traditional methods and machine learning methods for calculating overpressure and heat flux at various distances are the primary aspect of this research, CFD is a secondary area which was employed to provide the inputs for these calculation methods. With limited resources, CFD hydrogen explosion scenarios are notoriously difficult to simulate successfully from a design point of view and are computationally intensive. It can take several months to simulate a full leakage and explosion from start to finish as a high number of elements are often required in the model. However, this study has successfully managed to simulate a potential worst case leakage scenario using CFD, forming the basis of what is required to calculate safety distances, should ignition and explosion occur.

5.1 CFD Model

ANSYS fluent was chosen as a CFD software to simulate a hydrogen storage leakage situation. The purpose of CFD in this project is to better understand how a leakage of hydrogen gas from a storage container disperses in air and use results from the simulation as input values for the pressure and heat flux estimation methods. Therefore, although potential explosions are an important part of hydrogen leakage safety analysis, CFD was not used to simulate the explosive event, rather used to simulate the formation and dispersion of the gaseous cloud resulting from a hydrogen leakage. The cloud volume and average volume fraction of the hydrogen cloud are two results which can then be selected as inputs. Cloud volume and average volume fraction are dependent on parameters such as pressure of storage, leakage hole diameter and wind speed and direction.

The various aspects of CFD (geometry, meshing and set up) which were used in modelling the scenario in question are explained throughout the following section.

5.2 Geometry Design

Following discussions with project stakeholder Elomatic, 3 hydrogen gas storage cylinders were created in ANSYS Workbench Fluent geometry. The total size of the domain was a total of 180m x 80m x 200m in the x, y and z directions respectfully and the central cylinder was located at coordinates of 90m, 0.5m and 70m in the x, y and z directions respectively. The cylinders were created with a diameter of 0.75m, length of 6.6m and separation of 2m at the nearest point on the outside faces of the cylinder and Type IV cylinders manufactured by Umoe Advanced Composites.

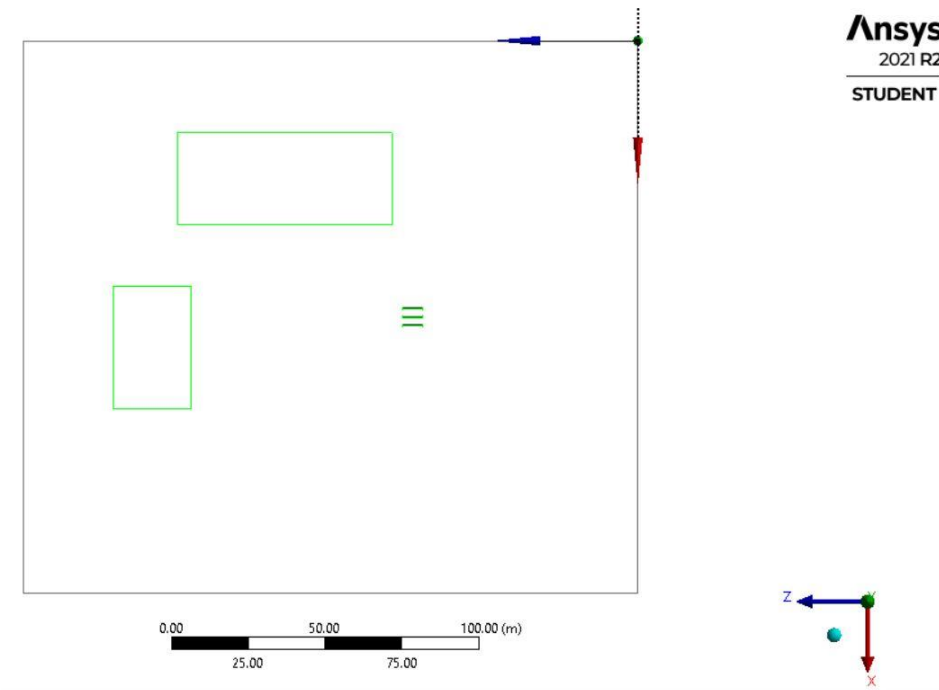


Figure 22: Aerial View of the Storage Facility CFD Model. 3 Hydrogen Gas Cylinders and 2 Buildings can be Observed.

The cylinders at either side of the central cylinder were created using a linear, body pattern feature. A cylindrical extrusion of 0.01m was created on the front face of the central cylinder (the face further away from the origin) from a concentric sketch of a 0.02m diameter circle. The corresponding mass flow rates out of this inlet for different storage pressures are shown in table 11 in section 5.4. This models the orifice which hydrogen leaks from.

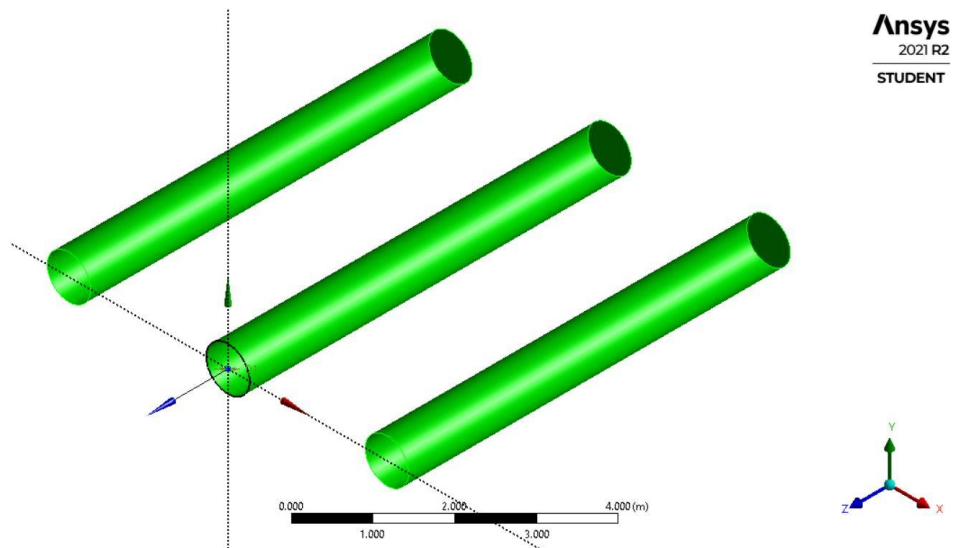


Figure 23: Enlarged Isometric View of the 3 Cylindrical Hydrogen Gas Storage Vessels. The Leak Orifice is Located at the Origin.

A ‘Boolean – subtract’ was then introduced to “remove” 5 bodies (set as tool bodies). These 5 bodies are comprised of the 3 storage cylinders and 2

buildings from the total domain size (set as target body). This is done in order to create 1 part and 1 body.

One of the buildings was placed with its nearest face 30m away from the inlet in the x direction and the other one located with its nearest face 70m away in the z direction (direction of gaseous mass flow rate from the orifice in this case). The boxes which represented the 2 buildings were extruded 15m vertically (y direction). The two buildings can be observed in figure 24 below:

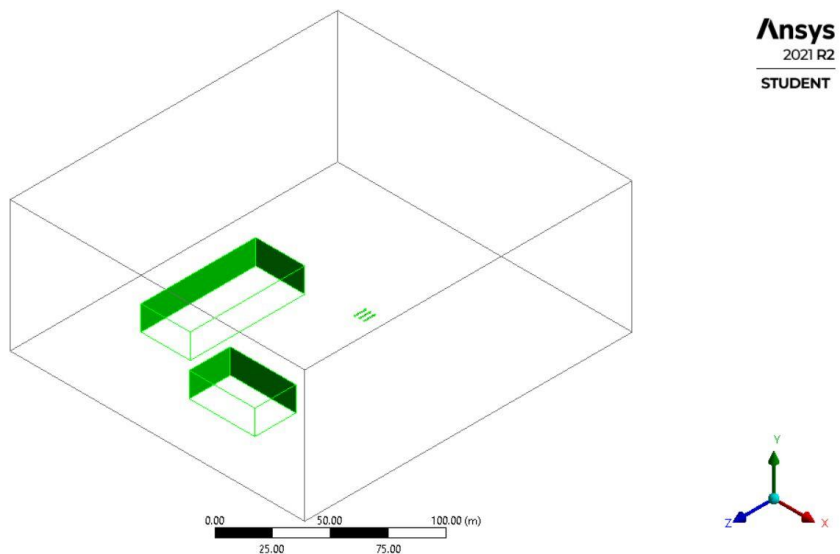


Figure 24: Isometric View of the 3 Hydrogen Gas Cylinders and 2 Buildings.

Named selections were created on appropriate faces. The outer face of the cylindrical extrusion from the middle storage cylinder was named “inlet”. 5 faces of the outer walls of the domain were named pressure outlet with the remaining outer wall selected as wind inlet which is parallel to the inlet face and starts at the origin. All 10 faces of the geometry resembling buildings were named “buildings”.

The creation of this geometry allows for the simulation of a potential worst-case leakage scenario. The next step involved in the creation of a simulation was creating an adequate mesh.

5.3 Mesh Design

Due to the nature of the hydrogen leakage scenario being investigated and the relative size of the orifice in comparison to the enormity of the total domain, creating a suitable mesh was not without its challenges. The domain had to be large to capture the full physical formation of a vapour cloud from the gas as it leaked from the small orifice at a high mass flow rate and rapidly dispersed.

As explained in section 2, hydrogen’s properties also allow it to disperse rapidly and so a relatively large cloud is capable of forming even within seconds of initial release – another reason for the large domain. The mesh element size was required to be highly refined at the orifice diameter to

capture the physics of the flow of gas as accurately as possible at the point of release from the storage tank.

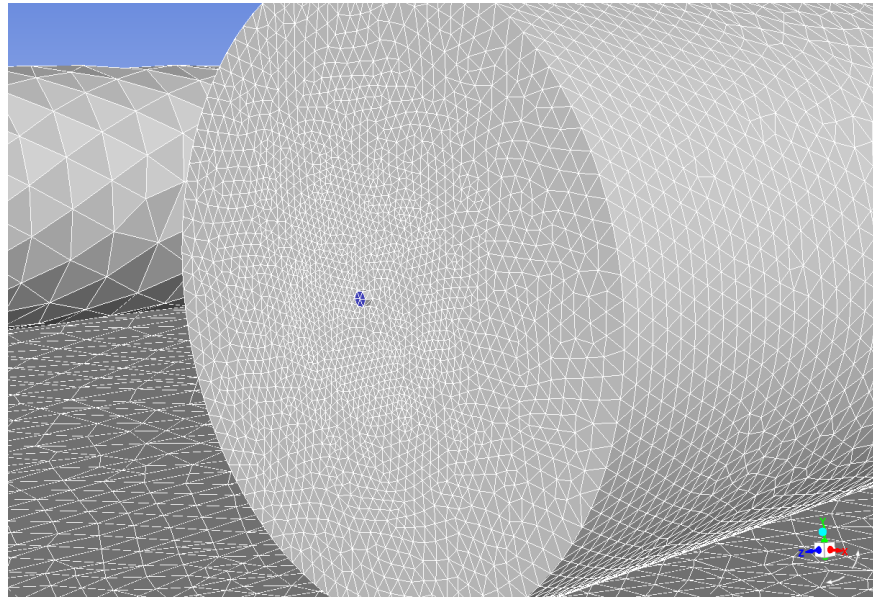


Figure 25: Close-up view of Pressure Vessel Leakage hole in CFD Mesh.

Increasing the maximum available number of elements presented the opportunity to significantly improve the growth rate from our initial model and also reduce the element size at key regions of the model. This was advantageous as it created a more gradual increase in the element size from the orifice (inlet) to the outer walls of the domain (pressure outlet). A more refined mesh was desired at the region surrounding the orifice, where the cloud would form from.

The mesh was made using two spheres of influence, one with an element size of 0.01m at the leakage orifice diameter and the other with an element size of 0.5m positioned as shown in the following figure 26:

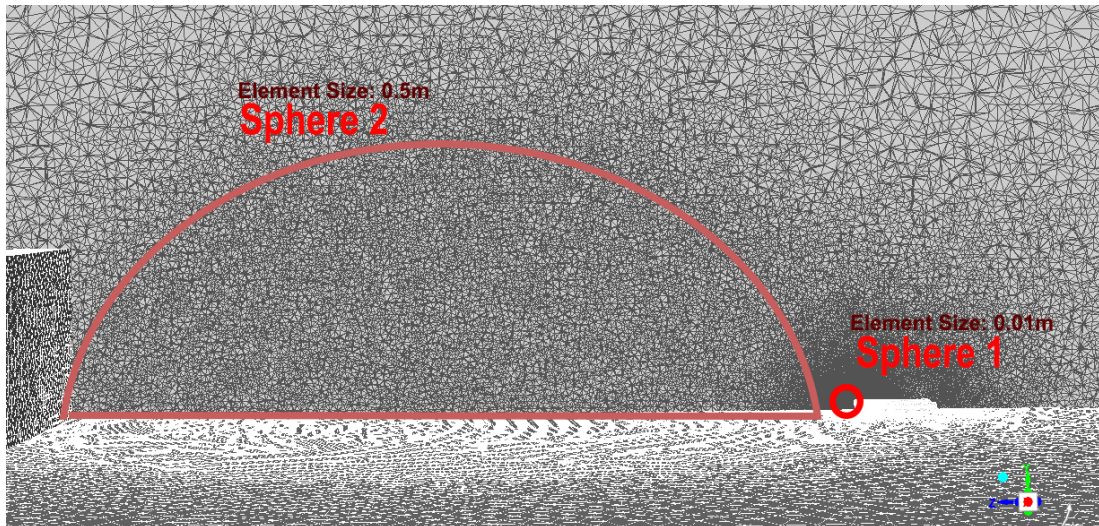


Figure 26: Vertical Cross Section view of CFD Mesh, Showing Spheres of Element Size Influence.

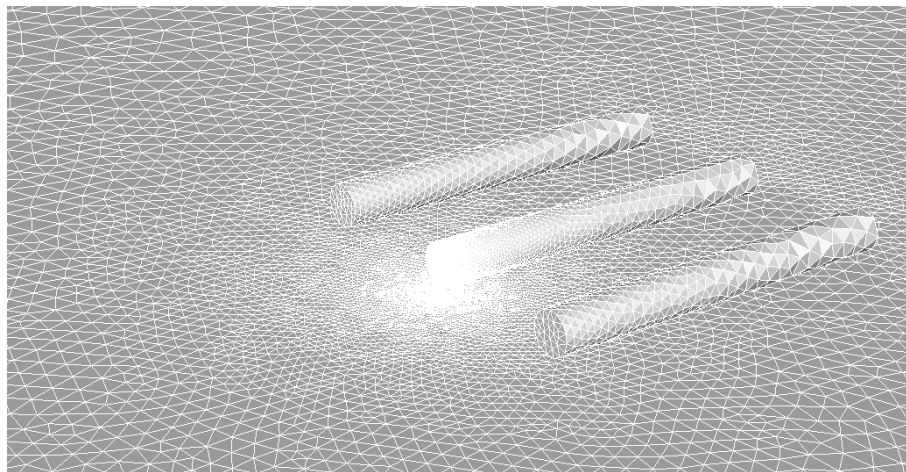


Figure 27: View of CFD Mesh around Pressure Vessel Geometry.

The final mesh utilised for the simulation involved 5,621,790 cells.

5.4 Setup

In the general section of the setup, gravity was set with a value of -9.81 m/s^2 in the Y direction. Multiphase modelling was not used as species transport model was used instead (the governing equations for species modelling are described in section 2.10.4). A realizable k-epsilon model (with the governing equations behind this model described in section 2.10.5) with standard near wall functions and full buoyancy effects selected. The selected species in the mixture template were hydrogen (H_2), oxygen (O_2) and nitrogen (N_2). With oxygen and nitrogen combined with appropriate concentration fractions to approximate ground level air of the atmosphere outside of the hydrogen storage container. The density of the gases was set to a Soave-Redlich-Kong real gas model.

In the boundary conditions set up, the ‘inlet’ was selected as a mass flow rate inlet. The species mass fraction at the orifice ‘inlet’ was set to 1 for hydrogen and 0 for Oxygen as hydrogen was the only species which would be leaking from the ‘inlet’. The use of a mass flow inlet was used to simulate the pressure burst where the mass flow rates that were used correspond to the orifice inlet diameter pressure under a choked flow assumption. The corresponding mass flow rates were provided as estimated values by Elomatic. These following mass flow rates assume constant pressure in a cylinder group:

Table 11: Mass Flow Rates for Different Pressure Values Using Choked Flow Assumption.

Temperature at 15 degC (288.15 K).

Pressure (bar)	D, hole (mm)	Mass flow rate (kg/s)
350	20	4.26
350	100	106.61
35	20	0.43
35	100	10.66

The species mass fraction at ‘pressure outlet’ was set to 0 for hydrogen and 0.22 for Oxygen.

A steady state simulation was run first to initialise the residuals. The simulation was resumed as transient once the residuals had settled which can reduce the overall computational time.

5.5 CFD Post

One plot which was produced in the results section of Fluent was an Isovolumne using the variable - H₂ mole fraction between manually inserted values of 0 and 0.75, representing the flammability limits of hydrogen, therefore the Isovolumne represents the flammable volume of the gaseous cloud. The flammability limits for a hydrogen-air mixture are between 4-75% as discussed in section 2.1.1 however a lower flammability of 0 was selected in CFD post as a conservative approach to obtain results with a margin of safety included.

Mole fraction is calculated as moles of species divided by the total number of moles in a mixture. The H₂ mole fraction was calculated using the following equation which was inserted as a custom-made formula within the expressions tab in CFD post:

Equation 45:

$$\frac{\frac{1}{2} H_2 \text{ Mass Fraction}}{\frac{H_2 \text{ Mass Fraction}}{2} + \frac{O_2 \text{ Mass Fraction}}{32} + \frac{N_2 \text{ Mass Fraction}}{28}}$$

Results were generated for both the volume of the hydrogen cloud and hydrogen mole fraction for various timesteps after the initial release of hydrogen gas. These results are presented in section 7.

6 Sensitivity Analysis

The sensitivity analysis was carried out to provide insight into how sensitive the methods of overpressure estimation are to small changes in the input values. Furthermore, a sensitivity analysis was used to validate how the estimation methods react predictively and produce results that do not vary wildly with small changes to the input values. Overall, this will provide confidence in the various methods to produce predictions that can be trusted and used in the context of real-world hydrogen safety problems.

6.1 Traditional Method Analysis

A Monte-Carlo simulation for sensitivity analysis of the estimation methods was conducted to explore the characteristics and response of each traditional method, as well as the best performing machine learning model, to a variety of input parameter values.

The leakage simulation was carried out assuming a uniform distribution of values for the cloud volume, and a uniform distribution of values for the hydrogen volume fraction, with a total variation of +/- 20% of the mean value of each (the mean values being the results from the CFD simulation). Results from the simulation were calculated for 1000 random samples of cloud volume (and 1000 total random samples of cloud volume and hydrogen volume fraction for the curve fitting estimation method which accepts these two inputs). A distance range of 5 to 100 metres was used for each iteration of the analysis.

6.2 Machine Learning Method Analysis

A similar Monte-Carlo simulation was carried out to conduct a sensitivity analysis of the machine learning model results for the best performing algorithm. The same setup parameters were used as described above, with a total of 1000 random samples of cloud volume and hydrogen volume fraction used as inputs for the machine learning models, and the same 5 to 100 metre distance range.

7 Results

This section reports all results from machine learning performance and sensitivity analysis (of traditional methods and ML methods) to CFD results (input values) and final safety distance predictions in terms of the distance to maximum tolerable overpressure or maximum heat flux.

7.1 Machine Learning Model Performance Scores

The final average R^2 scores and mean square error results of the 10-fold cross validation scheme, as well as the tuned hyperparameter values, are presented below for the best performing estimators in table 12, and visualised in figure 28 and 29. Wherever necessary, in the event of two differently tuned models exhibiting superior performance exclusively in one metric, the deciding metric used to select the best estimator was the mean squared error, while the R^2 score was also calculated and compared to provide additional confidence in the performance of the estimator. This decision was made as a lower mean squared error infers more strongly, the level of accuracy in the pressure predictions results, compared to the R^2 score.

This situation was only the case for the Extremely Randomised Trees, Support Vector Machine, and Multi-Layer Perceptron algorithms. In the case of the ExtraTrees model, the relative decrease in R^2 score was only 0.03% alongside an 8.3% relative improvement in mean square error, therefore the obvious choice was to use the best scoring MSE model in this case.

The Support Vector and Perceptron models showed no clear choice between model tuning parameters, with similar relative improvements across both metrics. In order to maintain consistency, the best MSE models were selected.

Table 12: R², M.S.E. Scores, and Hyperparameter Values of the Best Machine Learning Estimators.

Model (Best)	Random Forest	Extremely Randomised Trees	Gradient Boosted Trees	K-Nearest Neighbours	Support Vector Machine	Multi-Layer Perceptron
R² Mean Score	0.839	0.916	0.875	0.861	0.508	0.783
Mean M.S.E.	2.190	1.283	1.873	2.034	6.093	2.779
Hyperparameter Values	No. of trees: 10 Min_split: 2 Min_leaf: 1	No. of trees: 185 Min_split: 2 Min_leaf: 1	No. of trees: 210 Rate: 0.4 Depth: 3 Min_split: 4 Min_leaf: 1	No. of Neighbours: 2 No. of leafs: 5 Weights: distance	Kernel: Polynomial Degree: 3 Nu: 0.9 C: 3	Hidden layers: 3 Neurons/layer: 8,4,7 Activation function: ReLU

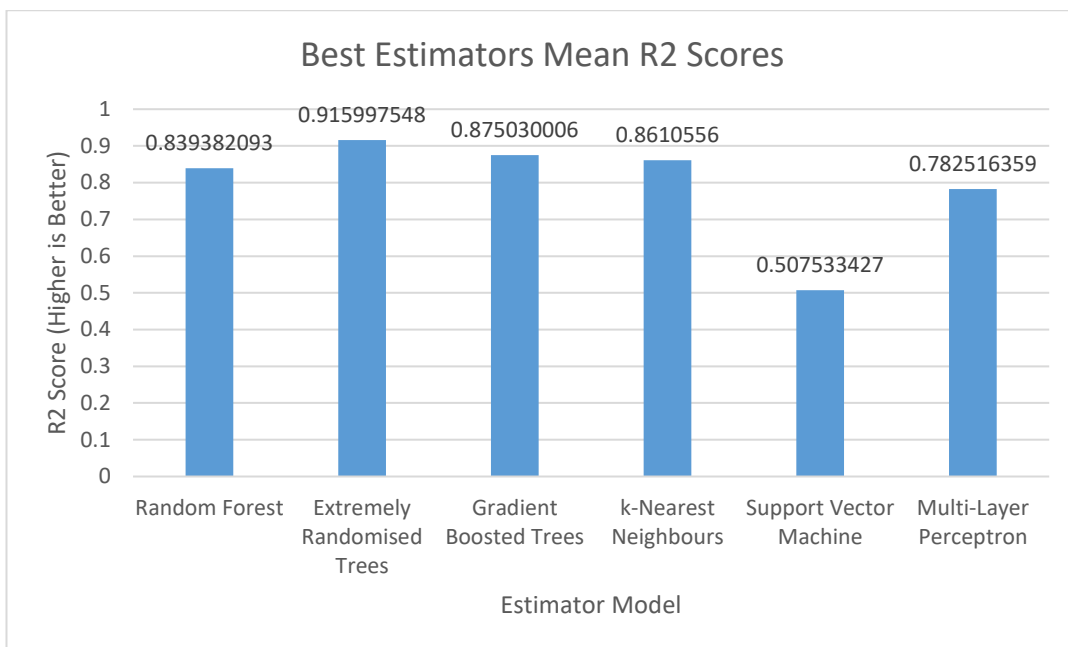


Figure 28: Graph of Best Performing Estimators R2 Scores.

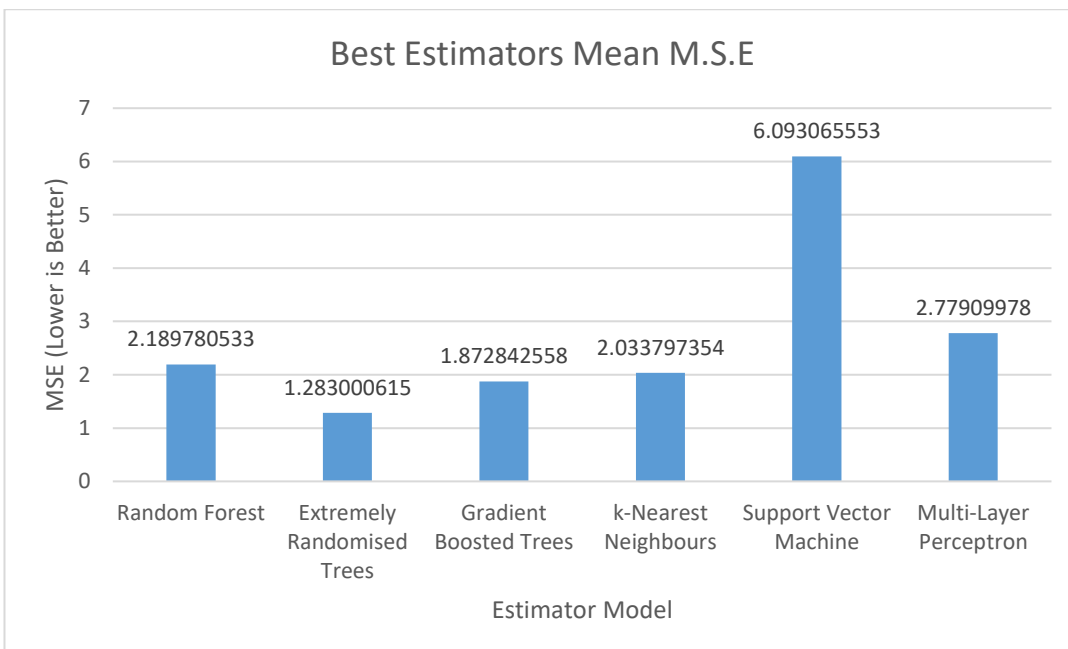


Figure 29: Graph of Best Performing Estimators Mean Square Errors.

As is shown in the performance results in figure 28 and 29, as well as table 12 above, the Extremely Randomised Trees exhibits the best estimator performance scores and lowest mean square error results when tested using the 10-fold cross validation scheme. Therefore, going forward only this best performing model will be considered for the prediction of results and machine learning model sensitivity analysis. It is also worth mentioning that the ExtraTrees model exhibited the lowest standard deviation and therefore the most consistency across the iterations of the cross-validation scheme.

7.2 Traditional Methods Sensitivity Analysis

The complete set of results from the Monte-Carlo sensitivity analysis for each traditional pressure estimation method, followed by the most probable, minimum, and maximum sets of results are shown in figures 30 and 31 respectively.

The most probable estimation is defined as the result calculated for the mean input values set as the output results of the CFD simulation, while the maximum and minimum estimations are defined as the results containing the maximum and minimum peak overpressure, respectively.

The values used as input parameters for the sensitivity analysis were taken from the CFD results and are shown below in table 13.

Table 13 - Sensitivity Analysis Input Parameters from CFD.

<u>CFD Simulation Time</u>	<u>Cloud Volume</u>	<u>Hydrogen Volume Fraction</u>	<u>No. of Samples</u>	<u>Maximum Variation of Cloud Volume</u>	<u>Maximum Variation of Volume Fraction</u>	<u>Cloud Volume and Fraction Distribution</u>
1.0s	170m ³	0.06042	1000	+ - 20%	+ - 20%	Uniform

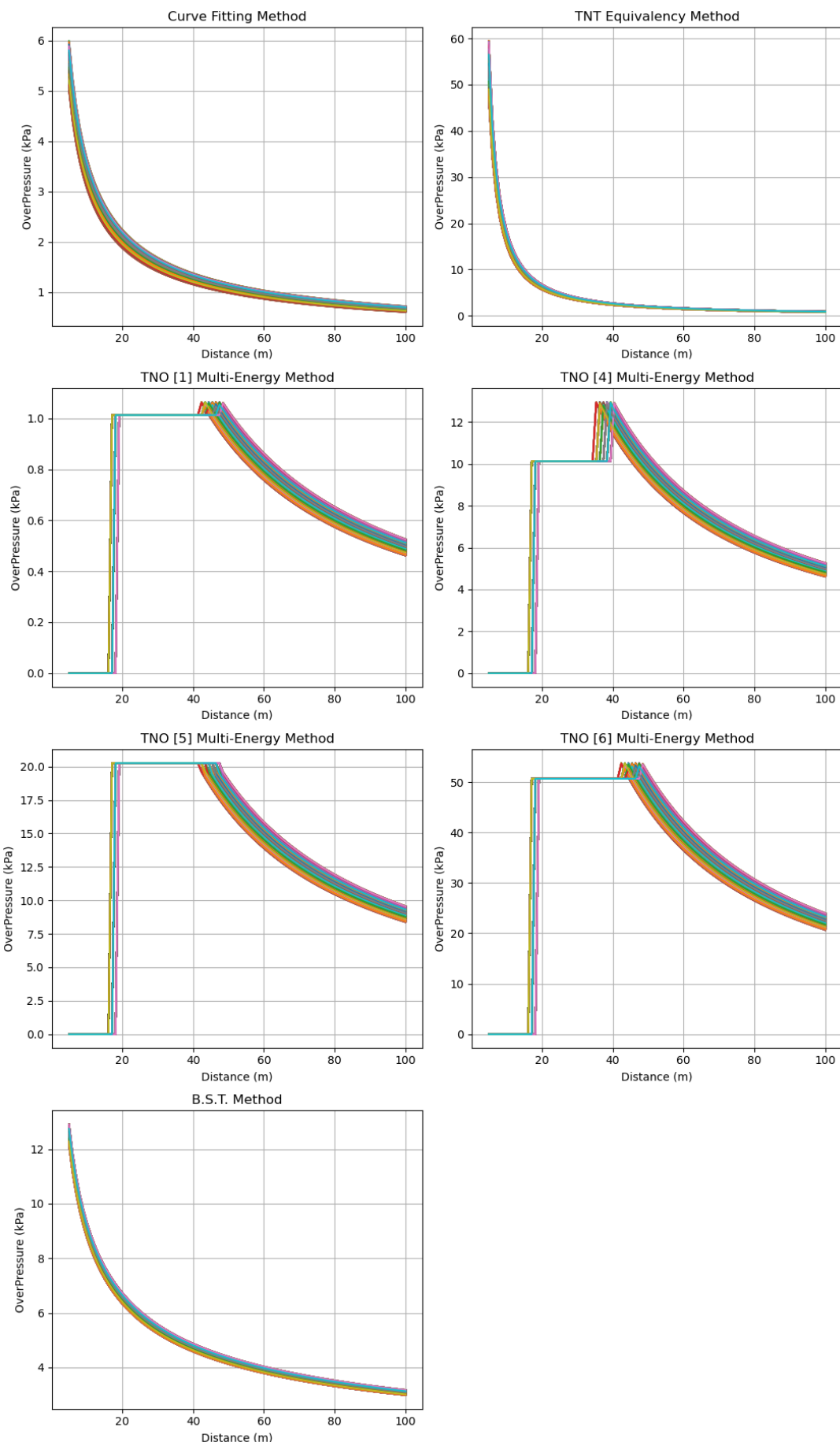


Figure 30: Traditional Methods Sensitivity Analysis - All Results.

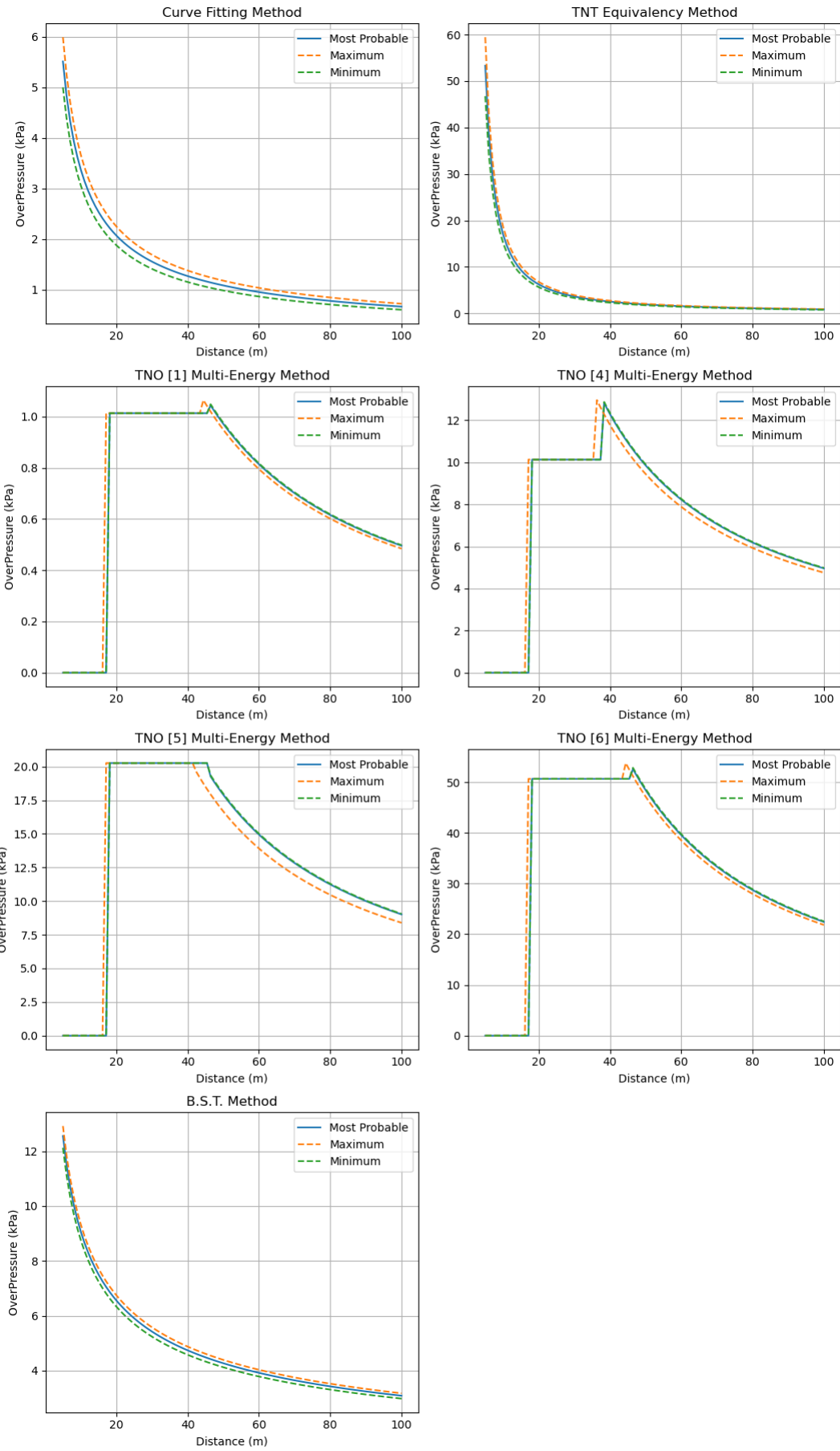


Figure 31: Traditional Methods Sensitivity Analysis - Mean, Maximum and Minimum Results.

7.3 Machine Learning Methods Sensitivity Analysis

The complete set of results from the Monte-Carlo sensitivity analysis for best performing ExtraTrees estimation model, followed by the most probable, minimum, and maximum sets of results are shown in figures 32 and 33 respectively. The most probable, maximum, and minimum results are defined as mentioned previously.

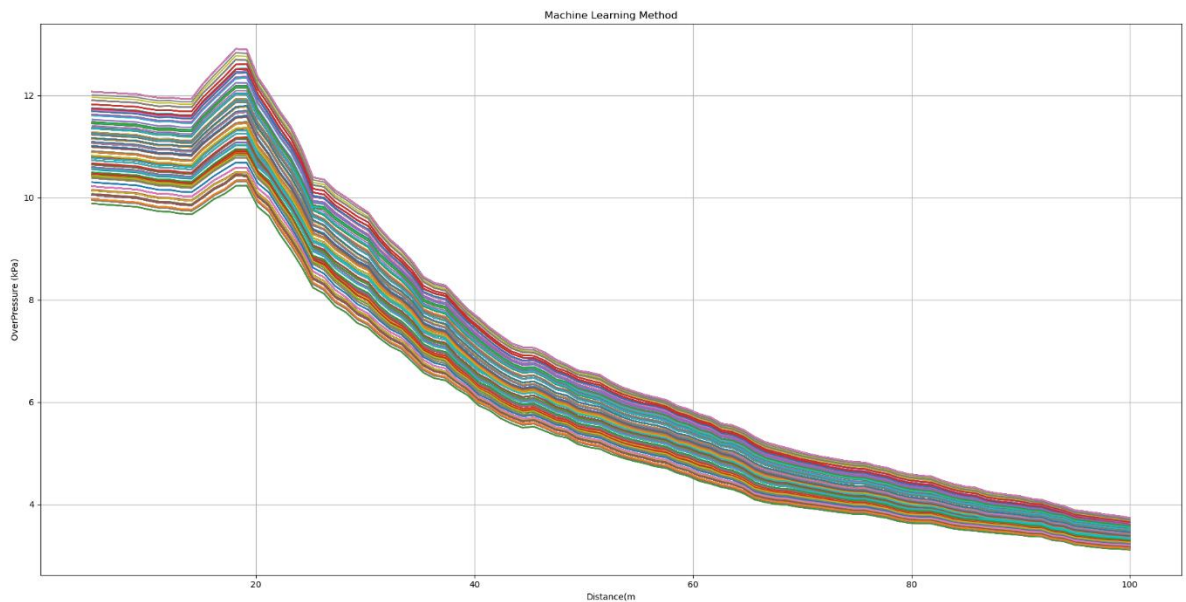


Figure 32: ExtraTrees Model Sensitivity Analysis - All Results.

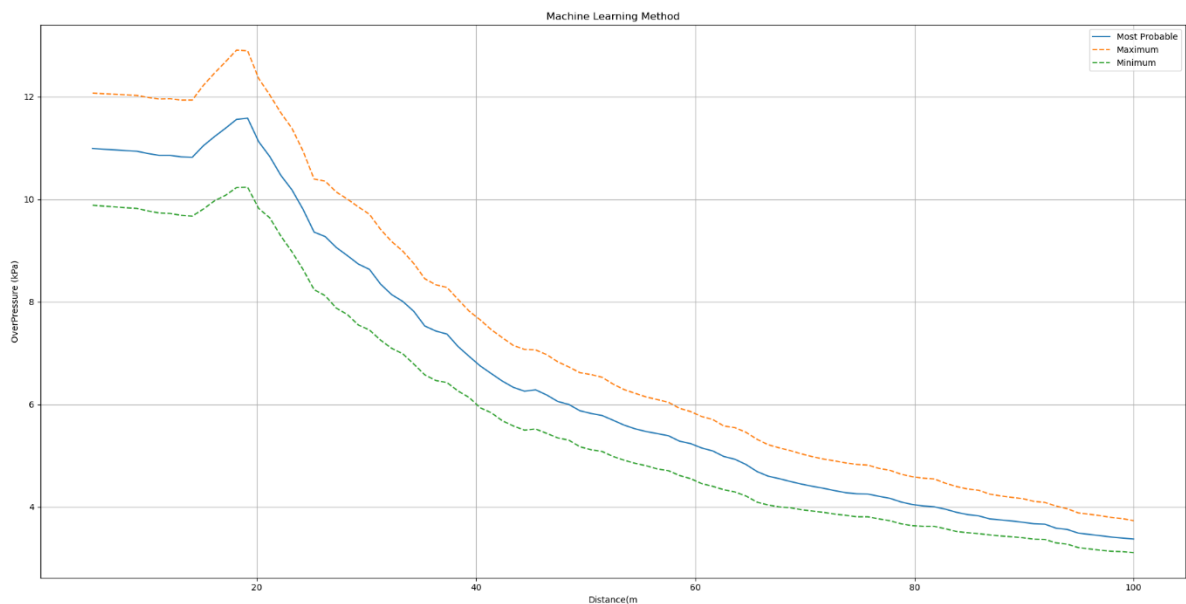


Figure 33: ExtraTrees Model Sensitivity Analysis - Mean, Maximum and Minimum Results.

7.5 CFD Results

The following results were produced through CFD (as explained in section 5.5) and describe the cloud volume (m^3) and hydrogen volume fraction ranging from 0 to 1 at regular timesteps of the leakage scenario. For the specified scenario, the results correspond to a cloud which has formed up to 15s after an initial leak from the gas cylinder. The following figures describe the various CFD results:

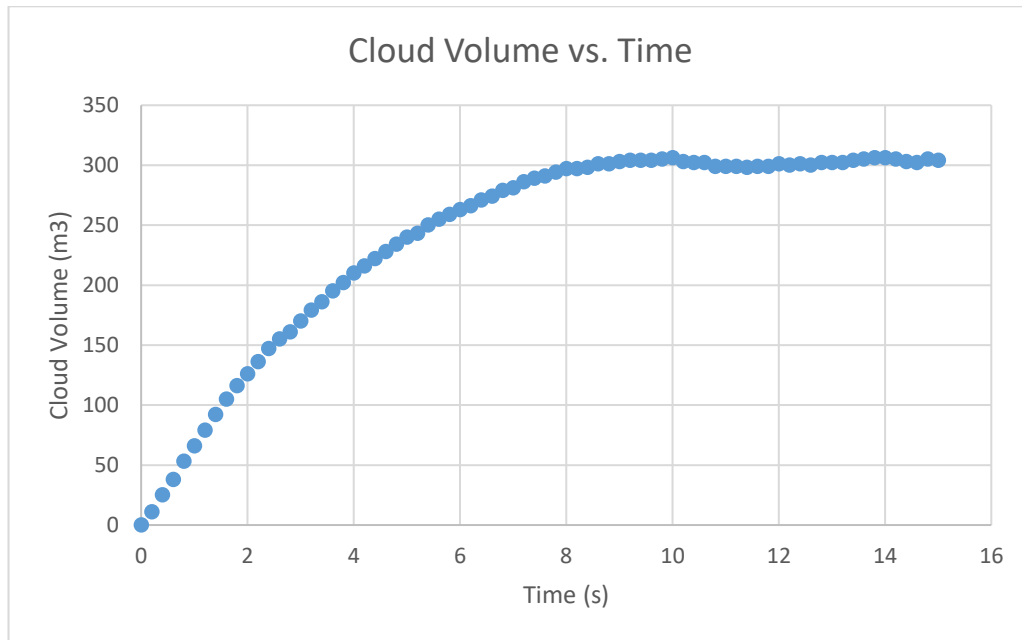


Figure 34: Cloud Volume vs. Time Plot from CFD Results.

Figures 34, 35 and 36 show that after approximately 10s, the cloud volume hydrogen mass and volume fraction remain almost constant. Should the gas continue leaking from the container for a period after this, the events that follow would be almost identical to that at approximately 10s after release.

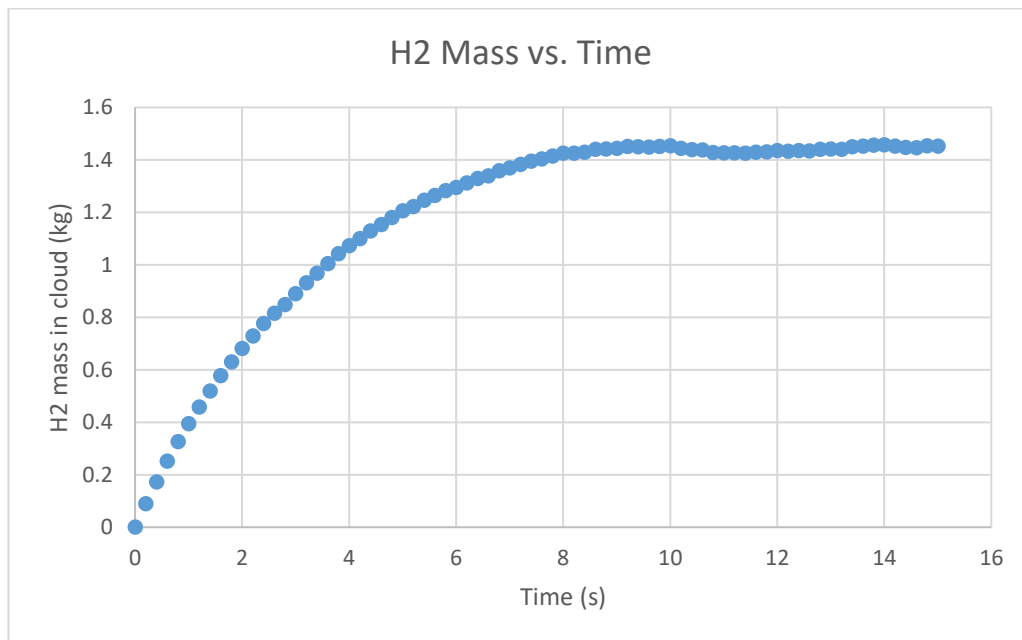


Figure 35: Mass of Hydrogen in Cloud vs. Time Plot from CFD Results.

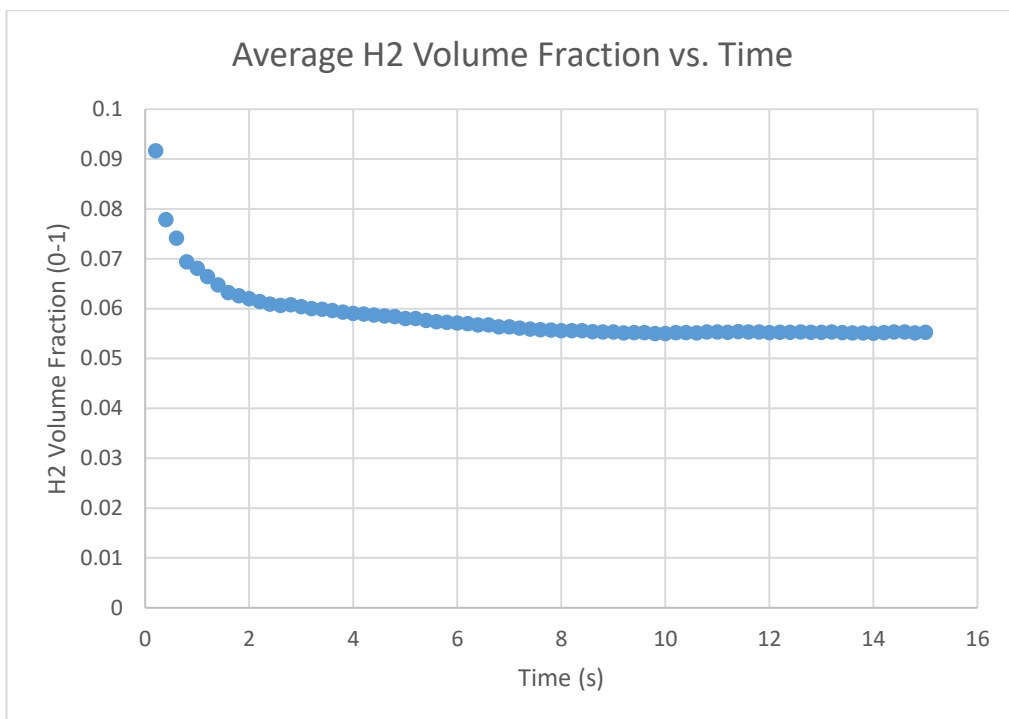


Figure 36: Average Hydrogen Volume Fraction vs. Time Plot from CFD Results.

A full set of results at instances from the moment of release up to 15s after release are provided in table 14, increasing incrementally by 0.2s between each row.

Table 14: CFD Post Results for Hydrogen Leakage at Various Times.

Time (s)	V (m3)	Average H2 mole fraction	H2 volume (m3)	H2 mass in cloud (kg)	Time (s)	V (m3)	Average H2 mole fraction	H2 volume (m3)	H2 mass in cloud (kg)
0.2	11	0.09171	1.00881	0.08941	7.6	291	0.05583	16.2465	1.40341
0.4	25	0.07788	1.947	0.1732	7.8	294	0.05571	16.3787	1.41508
0.6	38	0.07417	2.81846	0.25175	8	297	0.05558	16.5072	1.42517
0.8	53	0.06941	3.67873	0.32631	8.2	297	0.05564	16.5250	1.42528
1	66	0.06815	4.4979	0.39447	8.4	298	0.05563	16.5777	1.4288
1.2	79	0.06645	5.24955	0.45785	8.6	301	0.0554	16.6754	1.44009
1.4	92	0.06478	5.95976	0.51961	8.8	301	0.05538	16.6693	1.44163
1.6	105	0.06324	6.6402	0.57797	9	303	0.05534	16.7680	1.44461
1.8	116	0.0626	7.2616	0.6307	9.2	304	0.05516	16.7686	1.45072
2	126	0.06204	7.81704	0.68131	9.4	304	0.05522	16.7868	1.44963
2.2	136	0.06145	8.3572	0.72899	9.6	304	0.05521	16.7838	1.44871
2.4	147	0.06091	8.95377	0.77709	9.8	305	0.05505	16.7902	1.45082
2.6	155	0.06065	9.40075	0.81525	10	306	0.055	16.83	1.45335
2.8	161	0.06083	9.79363	0.84887	10.2	303	0.05522	16.7316	1.44397
3	170	0.06042	10.2714	0.88974	10.4	302	0.05523	16.6794	1.43933
3.2	179	0.06006	10.7507	0.93124	10.6	302	0.05517	16.6613	1.43827
3.4	186	0.0599	11.1414	0.96769	10.8	299	0.05538	16.5586	1.4276
3.6	195	0.05966	11.6337	1.00425	11	299	0.05532	16.5406	1.42742
3.8	202	0.05932	11.9826	1.04217	11.2	299	0.05531	16.5376	1.42752
4	210	0.05908	12.4068	1.07305	11.4	298	0.05539	16.5062	1.42571
4.2	216	0.05897	12.7375	1.09933	11.6	299	0.05533	16.5436	1.42939
4.4	222	0.05874	13.0402	1.1287	11.8	299	0.05535	16.5496	1.43004
4.6	228	0.05857	13.3539	1.15415	12	301	0.05525	16.6302	1.43557
4.8	234	0.05841	13.6679	1.17995	12.2	300	0.05531	16.593	1.43311
5	240	0.05807	13.9368	1.20604	12.4	301	0.0553	16.6453	1.43577
5.2	243	0.05804	14.1037	1.22148	12.6	300	0.05535	16.605	1.4339
5.4	250	0.05765	14.4125	1.24634	12.8	302	0.05526	16.6885	1.43995
5.6	255	0.05742	14.6421	1.26501	13	302	0.0553	16.7006	1.44203
5.8	259	0.0573	14.8407	1.28294	13.2	302	0.05536	16.7187	1.44092
6	263	0.05713	15.0251	1.29532	13.4	304	0.05521	16.7838	1.45002
6.2	266	0.05702	15.1673	1.31211	13.6	305	0.05517	16.8268	1.45217
6.4	271	0.05677	15.3846	1.32917	13.8	306	0.05514	16.8728	1.45601
6.6	274	0.05674	15.5467	1.33923	14	306	0.05512	16.8667	1.45767
6.8	279	0.05641	15.7383	1.35863	14.2	305	0.05522	16.8421	1.45267
7	281	0.05635	15.8343	1.36916	14.4	303	0.05533	16.7649	1.44755
7.2	286	0.05614	16.0560	1.38298	14.6	302	0.05537	16.7217	1.4464
7.4	289	0.05596	16.1724	1.39572	14.8	305	0.05519	16.8329	1.45406
					15	304	0.05527	16.8020	1.45302

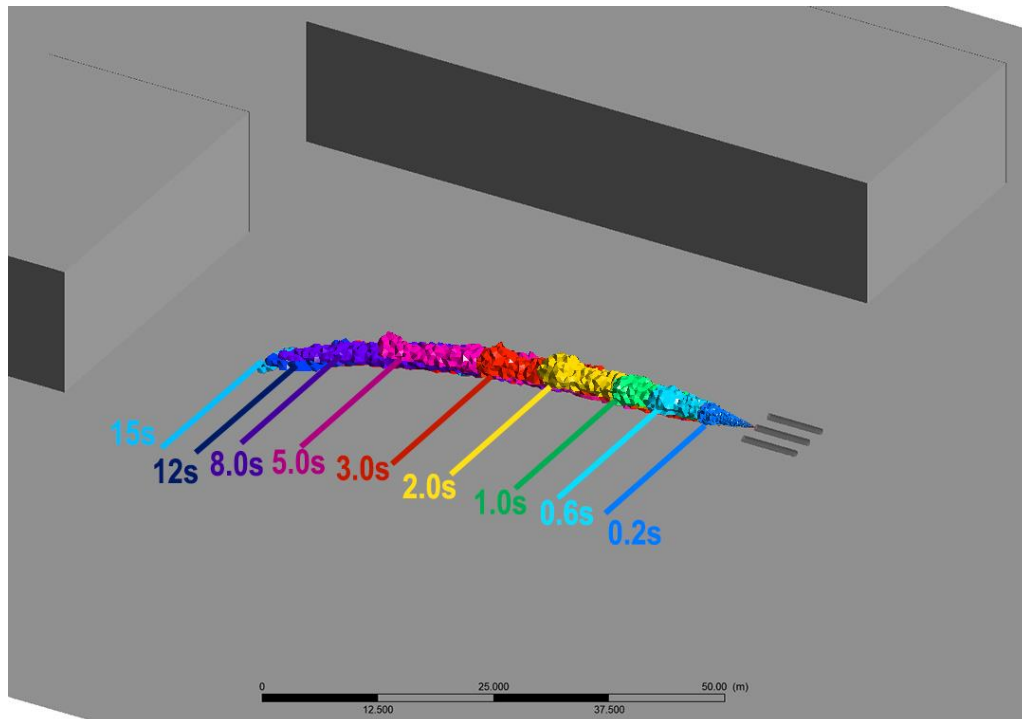


Figure 37: 3D Visualisation of CFD Hydrogen Dispersion at Various Timesteps (Growth of Cloud).

Corresponding to figures 34, 35, and 36 and the information displayed in table 14, figure 37 (above) shows the development of the flammable hydrogen cloud and how the size of the cloud increases with time - up to 15s after release.

7.6 Final Prediction Results

The results from the various traditional and machine learning methods are presented in the following tables and figures. In line with Finnish National (Tukes) standards guidance, the safety distances are estimated at various appropriate overpressure values. Note, the safety distances vary depending on the specific location of such storage facilities and are at the discretion of those who commission these facilities. In relation to the methodology of this report and the findings from the CFD results, prediction results have been included for hydrogen dispersion times of 0.2, 1, 5, and 10 seconds as this will provide a wide range of results for different ignition scenarios.

7.6.1 Overpressure Results

The results related to the various methods for predicting overpressure are displayed in table 15 and figures 38 to 41.

Table 15: Overpressure Results.

	Distance (m)	t = 0.2s			Distance (m)	t = 1.0s	
Limit	Curve Fitting	BST	Machine Learning		Curve Fitting	BST	Machine Learning
15kPa	0.36	1.37	2.55		0.92	2.5	6.15
10kPa	0.65	3.26	2.55		1.65	5.95	6.15
3kPa	3.5	42.56	2.55		8.97	77.36	55.52
1.35kPa	10.82	233.86	15.71		27.75	424.93	357.27
	Distance (m)	t = 5.0s			Distance (m)	t = 10s	
Limit	Curve Fitting	BST	Machine Learning		Curve Fitting	BST	Machine Learning
15kPa	2.35	3.85	26.45		2.7	4.16	42.7
10kPa	4.15	9.11	46.57		4.77	9.9	72
3kPa	22.7	118.93	222.41		26.16	128.96	327.57
1.35kPa	70.22	653.45	370.47		80.91	708.57	354.82

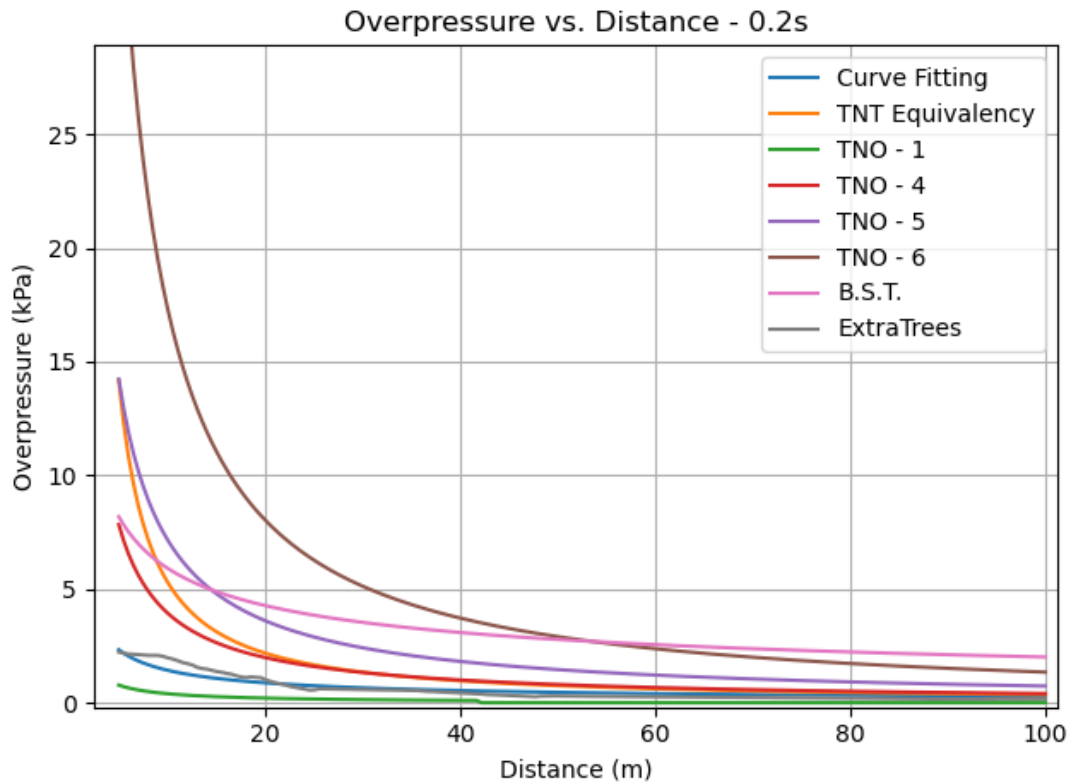


Figure 38: Overpressure vs. Distance Predictions for 0.2s CFD Hydrogen Cloud Data.

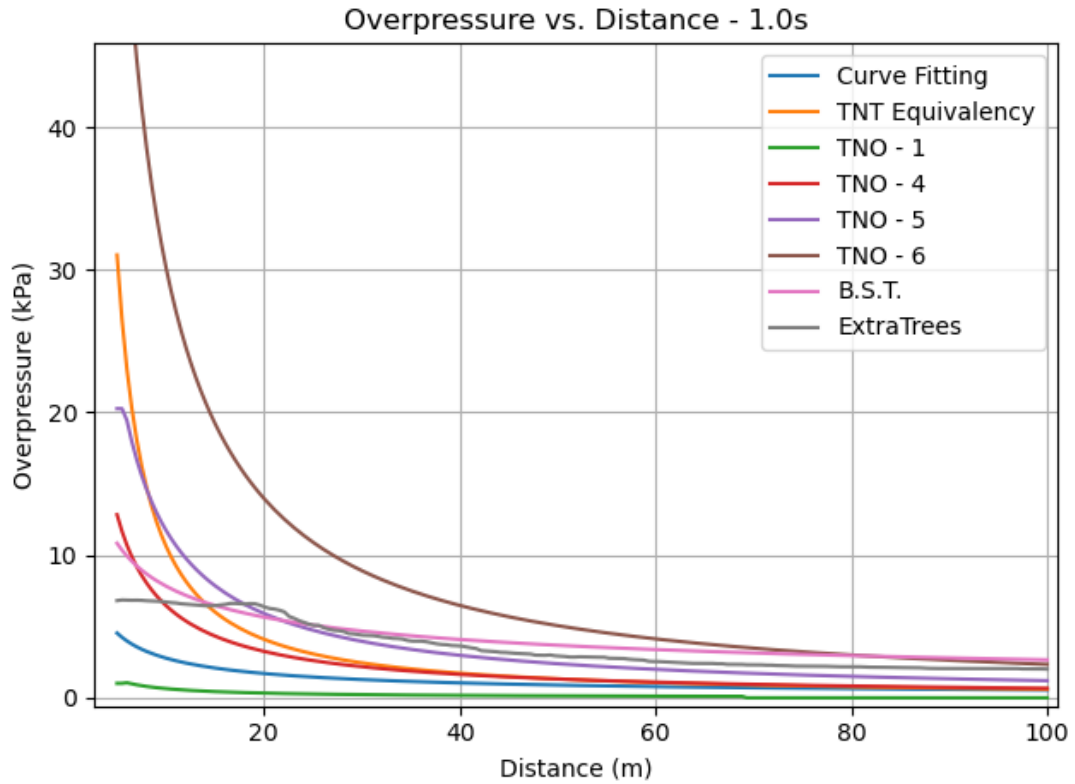


Figure 39: Overpressure vs. Distance Predictions for 1.0s CFD Hydrogen Cloud Data.

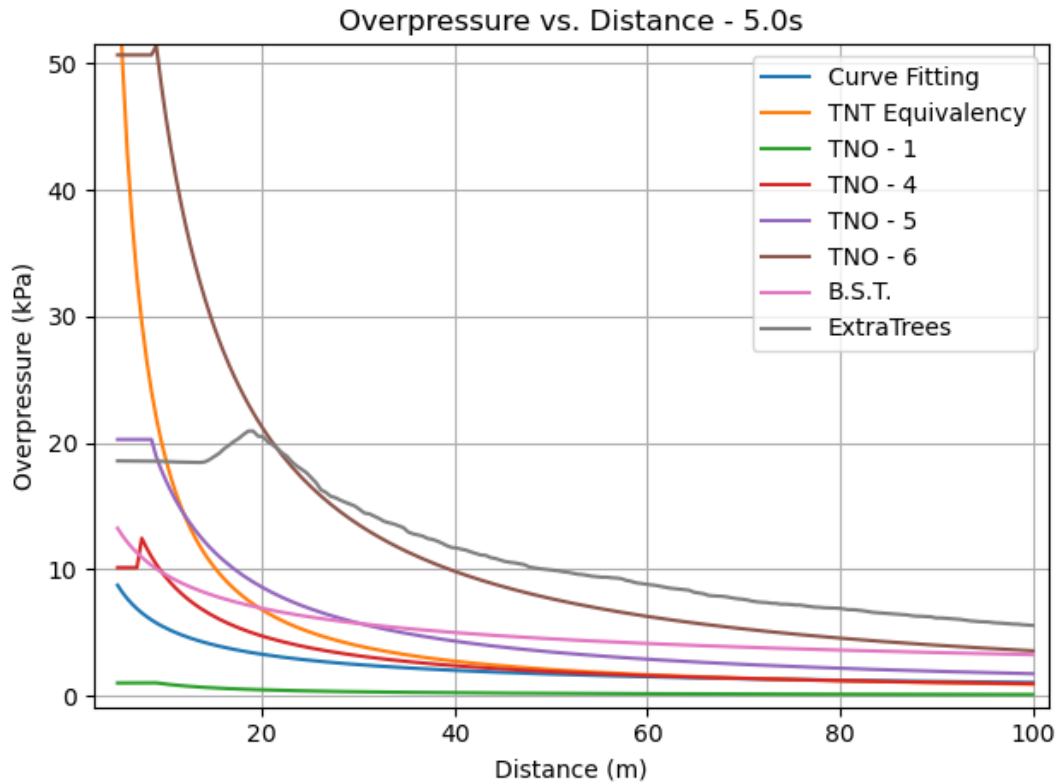


Figure 40: Overpressure vs. Distance Predictions for 5.0s CFD Hydrogen Cloud Data.

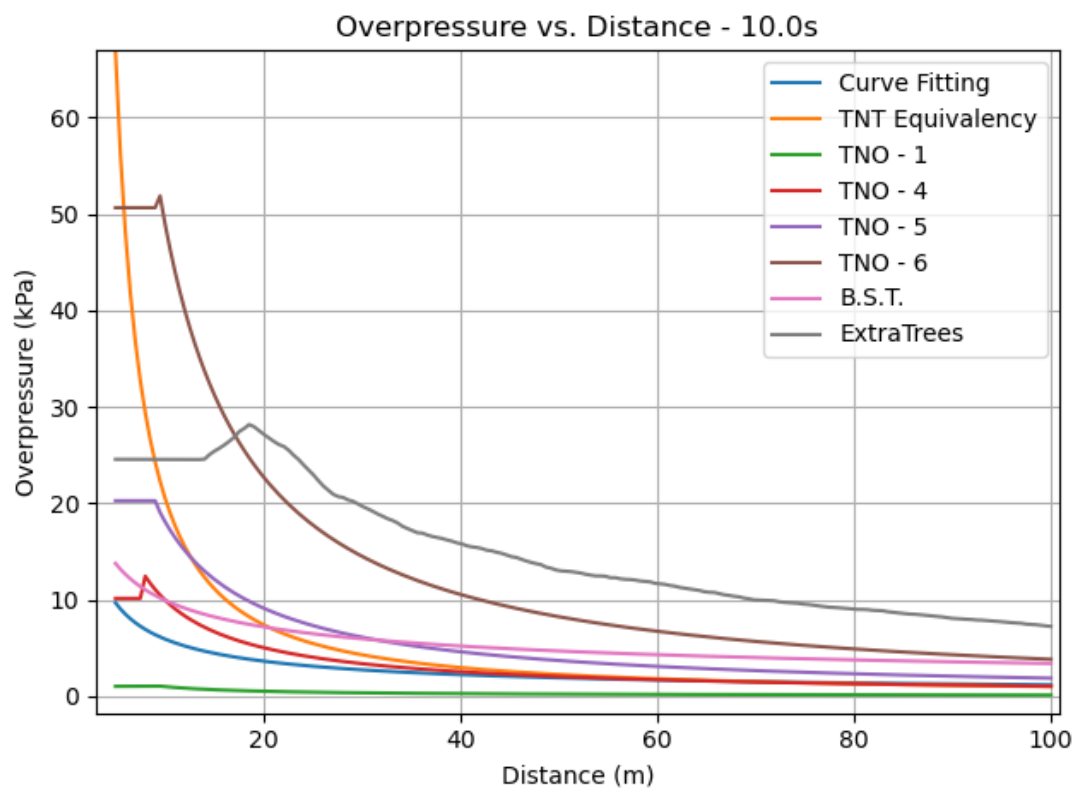


Figure 41: Overpressure vs. Distance Predictions for 10.0s CFD Hydrogen Cloud Data.

7.6.2 Heat Flux Results

The results related to the various methods for predicting heat flux are displayed in table 16 and figures 42 and 43.

Table 16: Heat Flux Results.

	Distance (m) t = 0.2s		Distance (m) t = 1.0s		Distance (m) t = 5.0s		Distance (m) Flux t = 10.0s	
Limit	Solid Flame	BLEVE	Solid Flame	BLEVE	Solid Flame	BLEVE	Solid Flame	BLEVE
8kW/m ²	16.35	3.07	26.3	5.71	37.7	9.1	40.02	9.8
3kW/m ²	26.45	5.95	42.5	10.7	61.05	16.65	64.82	17.95
1.5kW/m ²	36.95	8.75	59.51	15.65	85.36	24.28	90.66	26.12

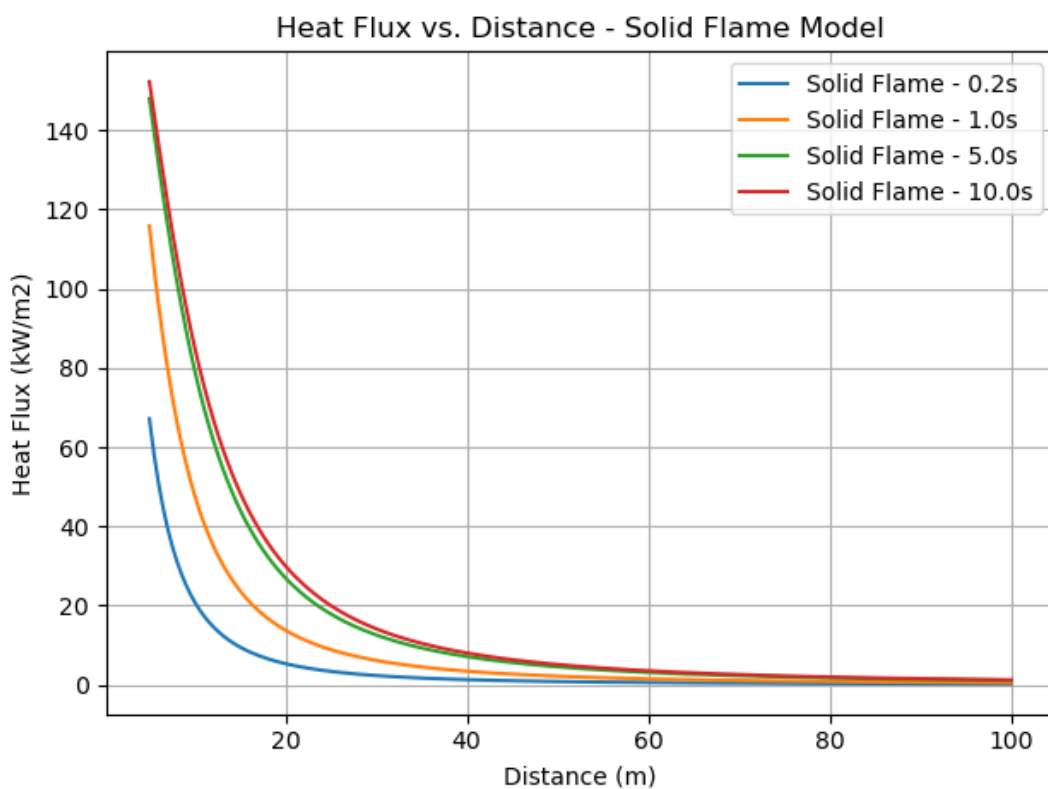


Figure 42: Heat Flux vs. Distance Predictions for Solid Flame Model.

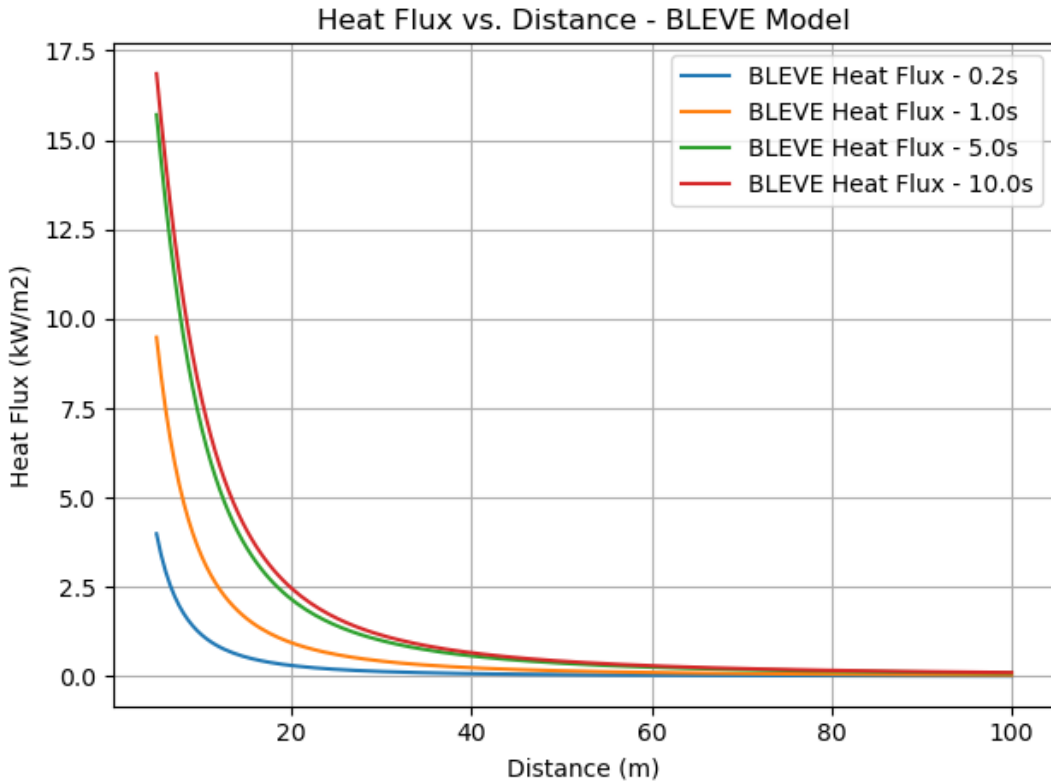


Figure 43: Heat Flux vs. Distance Predictions for BLEVE Heat Flux Model.

7.6.3 Overpressure Method Performance Scores

With the possession of experimental data for the overpressure of hydrogen vapour cloud explosions, it is possible to compare the accuracy of the blast pressure prediction methods. This was done using the average mean square error and R² score calculated from a 10-fold cross validation scheme using the dataset, for each pressure method. A traditional cross validation method was used for evaluating the machine learning model performance. Whereas to evaluate the performance of the traditional methods, the training set was simply discarded, and the testing set used to compute the results.

The best performing machine learning model was used in this comparison with the testing set used to evaluate the performance. The 10-fold splitting of the dataset was performed after a random shuffling of the set, however as the split was performed, the same train and test sets were used per iteration on each method, to ensure the results were comparable. Figures 44 and 45 present the mean square error and R² score results, respectively.

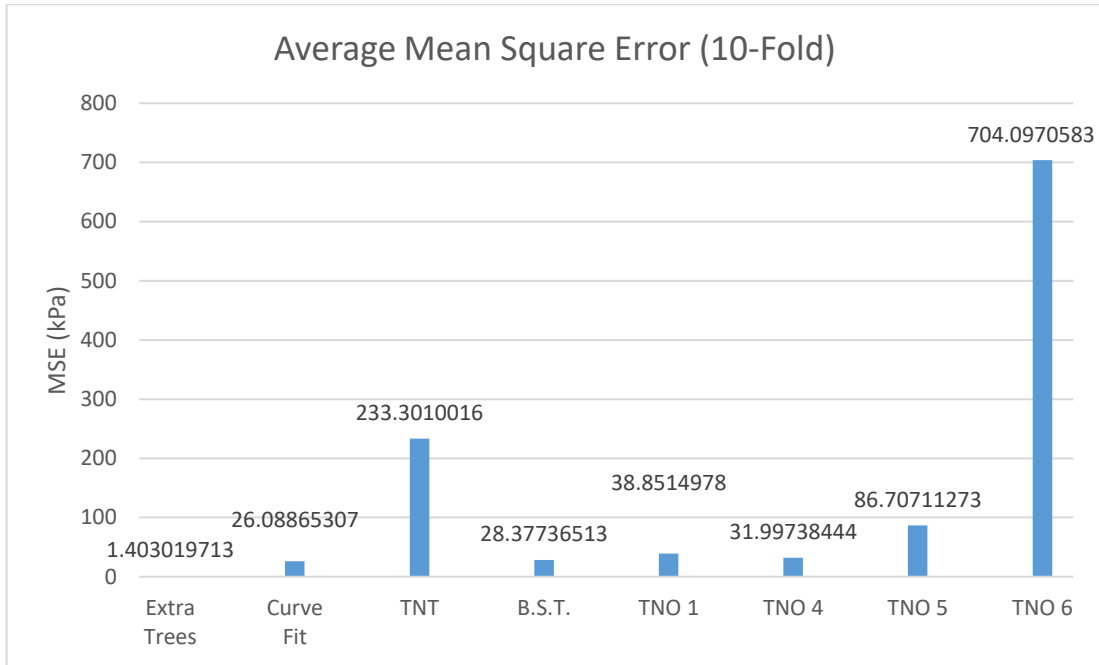


Figure 44: Comparison of Mean Square Error of Pressure Methods with 10-Fold Cross Validation.

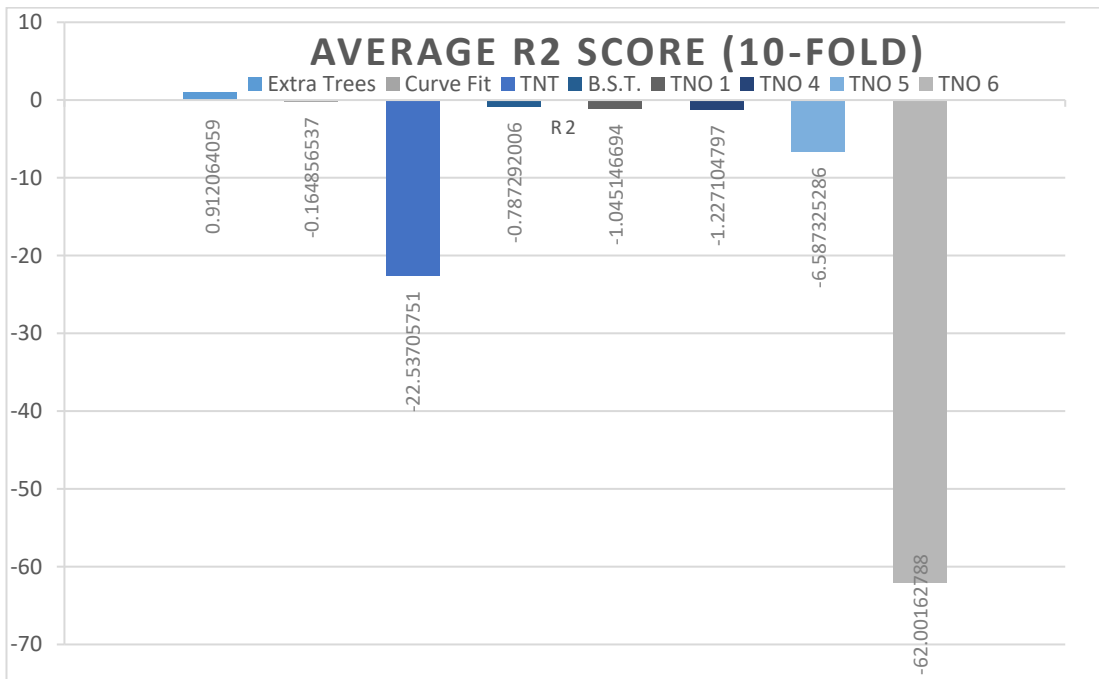


Figure 45: Comparison of R² Score of Pressure Methods with 10-Fold Cross Validation.

8 Discussion

8.1 Machine Learning Performance Comparison

Observing the R^2 scores and mean square error results of each of the machine learning methods presented in figures 44 and 45, it is clear that decision tree-based methods perform very well for this problem, with the Extremely Randomised Trees showing the best performance across both metrics. The nearest neighbours model also showed impressive performance considering the simplicity of the algorithm design. The support vector and Perceptron models show the worst performance - most likely a result of the small dataset and lack of variety in the dataset also, as these algorithms are more suited to larger scale problems with a large amount of data. Despite some tuned variations of the Perceptron model showing reasonable performance, it should be noted that in some configurations the model failed to converge during training on many occasions - an issue most likely also related to a lack of training data.

The unimpressive performance of the support vector model may also be a consequence of the fact that this type of algorithm is most commonly used and is much better for classification problems, as opposed to regression for which it is not commonly implemented. However, as expected with the size and complexity of the available data, tree-based algorithms showed the most promising performance and proved to be the most useful for this particular problem.

8.2 Pressure Methods Performance Comparison

Before comparison or analysis of the R^2 and mean square error results of the traditional pressure methods, it is important to consider what these performance metrics conclude. Regardless of on-paper performance, these metrics alone cannot decide how meaningful the prediction values are, or how useful the method is. Metrics are used here to compare the statistical performance and accuracy of the methods, only two of which are hydrogen specific.

Studying the mean square error results, it appears clear that of the energy levels considered (1,4,5, and 6), the TNO method using energy level 4 is the most suited to estimation for unconfined hydrogen cloud explosions of the considered volume, with similar performance to the BST method. The inaccuracy of the TNT equivalency method is particularly noticeable across both metrics, owing to significant differences between the explosion characteristics of hydrogen and TNT. In addition, the TNT method is suited to much larger explosions, as well as being quite conservative in regards to its predictions.

As is expected to be the case, the two hydrogen specific methods, curve fitting and machine learning, performed the best. However, when comparing statistical metrics, the machine learning method appears superior by quite a large margin. This is an unusual result as the same data was used for both traditional methods, with the testing data withheld from the machine learning model while the curve fitting method regression was conducted using the

entire dataset, therefore that method was being tested using the same data it was built from.

8.3 Sensitivity Analysis

The resulting graphs shown in figures 30 to 33 - presenting the results of the Monte-Carlo sensitivity analysis for traditional methods of overpressure - show the nuanced differences in the behaviour of each method. The most noticeable characteristic exhibited by the results is the way in which the TNO method handles the variation of input parameters with no variation in the values of overpressure - simply a change in the distance at which the pressure values occur. This is also the case for all TNO energy levels. The TNO method also displays a shortcoming in its ability to provide meaningful results for distances in the very near field. As a consequence of the design of the method, very small distances are outside the scope of the method's mathematical solutions.

The curve fitting, TNT equivalency, and BST methods all show similar behaviour in response to variation of input, with an appropriate and predictable response that shows small, regular changes in the results with similar small variation in input. All three of these methods also display similar sensitivity across the input variation range.

Overall, the sensitivity analysis showed that the curve fitting, BST, and TNT equivalency method are the most suitable for overpressure estimation in terms of confidence in the results, showing appropriate variations in estimated pressure.

8.4 CFD Results Analysis

The CFD hydrogen leakage and dispersion model provides some valuable insights and information on the appropriate parameters to use for estimation of overpressure and heat flux. The most notable inference of the CFD results, is an approach towards a steady state for the hydrogen vapour cloud as the leakage progresses in time. This is clearly visible from figures 34, 35 and 36 in the CFD results, where the values of cloud volume, hydrogen mass, and average hydrogen volume fraction all tend towards a constant value of steady state. Indicating that for this scenario, any leakage time beyond 10 seconds can be considered a worst-case scenario with maximum possible cloud size.

Observing figure 37 showing a superimposed 3D rendering of the hydrogen cloud across different timesteps, it is clear when considering the high buoyancy of hydrogen, that the immense release pressure has resulted in momentum driven flow from a turbulent high pressure hydrogen jet. The lack of increase in height of the flammable cloud volume shows this to be the case, with flammable cloud remaining mostly at ground level (until at least the point at which it is no longer a concern in terms of the flammability limits of hydrogen volume fraction). The leakage behaviour also shows that the ignition of the cloud would most likely result in ignition of the leakage jet. This would further result in a continuous jet flame from the leakage point, as the flammable cloud does not detach from the jet. The results also show the

cloud shape to be in no way approximate to that of a regular spheroid or similar shape that would hold as an assumption for a point source approximation for the origin of the explosion or resulting blast wave. This emphasises that more research would be necessary to evaluate safe distances for a leakage scenario on a case-by-case basis. This also hints at the importance of CFD or other similar methods for determining meaningful values in terms of the hydrogen cloud, for a given problem.

8.5 Pressure Methods Results Analysis

One most notable difference between the traditional pressure prediction methods and the machine learning prediction model, is the ability for the model to move past the approximation shapes of the pressure-distance curves of the traditional methods defined by their governing equations. Since the machine learning model is driven by real-world data, it is able to learn complex nonlinear trends that may not be accounted for in more simplistic approximation methods. The most obvious behaviour exhibited by the machine learning model is the capturing and reproduction of the effect of Mach stems on overpressure. Figure 46 below details the noticeable example from the results, showing the spike in pressure as the Mach stem forms quickly after explosion.

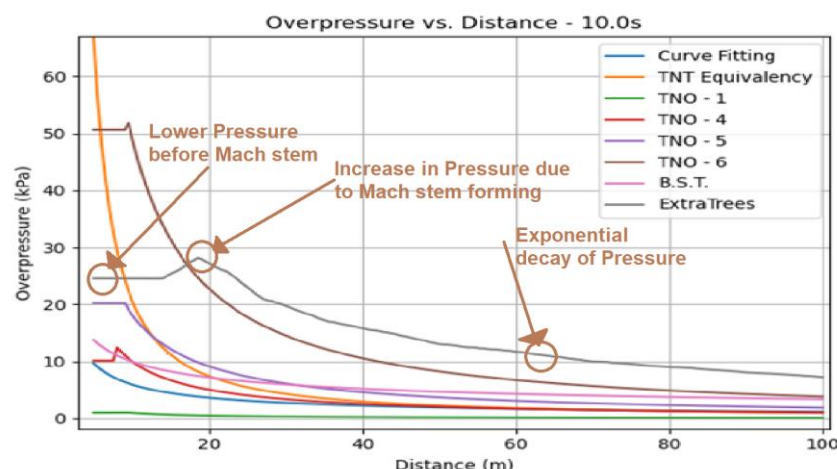


Figure 46: Overpressure vs. Distance Results Highlighting Machine Learning Behaviour.

In terms of the estimation results, it is clear that the TNT equivalency method is extremely conservative in its estimates to the point where it could be considered inaccurate for hydrogen cloud explosions. The TNO method curves are also proven to be somewhat inadequate as they do not vary peak pressure but only distance. As a result, the curve fitting and machine learning method are predictably the clear, superior choices for this problem.

Observing the differences between results across timesteps, the overpressure increases with cloud volume and time (as expected), with the exception of the TNO method results, as previously discussed. More interestingly, the machine learning estimation results transition from being quite conservative, and in somewhat of an agreement with the curve fitting method at early timesteps, to being one of the more conservative estimates

and straying far from the results of the only other hydrogen-specific method present.

The machine learning method also shows a consistently lower peak overpressure at small distances, but with a slower decay of pressure over time, resulting in higher pressures at higher distances. This is most noticeable at times of 5 and 10 seconds after release.

Overall, the results vary greatly between estimation methods, with the TNT equivalency method consistently very conservative at small distances, with a sharp decay at higher distances. The curve fitting method is consistently the least conservative (excluding the non-variational TNO results), but interestingly shows much similarity at higher distances to the TNT equivalency results, converging to nearly the same values. The BST method appears to be a middle-of-the-road estimation method, with decreasing conservativeness in the results as time increases. It does however, show a consistently low rate of decrease of pressure, resulting in relatively high pressures at higher distances.

8.6 Heat Flux Methods Results Analysis

Of the two heat flux methods investigated, the solid flame model is clearly and consistently far more conservative, with predictions over an order of magnitude greater than that of the BLEVE model. However, the two methods display very similar trends in terms of the behaviour and decay of the thermal radiation as distance increases, with the differences in estimated heat flux between time steps also remarkably similar between the two methods. The only difference other than the magnitude of the results, is that the solid flame model also displays a slightly slower rate of decay of heat flux, resulting in higher estimates at greater distances, while the contrary is true for the BLEVE method.

8.7 Limitations

8.7.1 Data Sparsity

In relation to the data driven methods of distance estimation in this research - the traditional curve fitting method and the machine learning methods - the lack of available data for hydrogen explosion overpressures is evident in the accuracy of the methods. With more accurate and a much greater amount of experimental data, any data driven model - and the machine learning approach in particular - could be reformed and improved to a much higher level of accuracy, resulting in significant improvements in safety predictions and decisions made regarding hydrogen storage plants and systems.

As for heat flux prediction, many attempts to acquire an experimental dataset for thermal radiation were made, however none such data could be found anywhere within the public domain, inhibiting any extensive testing of these methods, as well as halting the development of a similar machine learning method for heat flux prediction.

8.7.2 Time Scale

The short time scale over which this project was undertaken, is reflected in the depth of the investigation carried out. As this was a relatively large project, not every initially proposed goal could be achieved, and priority had to be assigned to different aspects in order to achieve a minimum set of deliverables. The result of this is most notably presented with a lack of sensitivity analysis of the heat flux estimation methods, as well as a lack of different leakage scenarios considered. This project focused primarily on overpressure as a governing parameter of safe distance as this was deemed of greater importance, as available literature would suggest. Developing a worst-case scenario and investigating this was also of high priority - both in terms of safety and in terms of project output.

9 Guided example

The following section details how to use Ansys FLUENT CFD software and numerical code to investigate overpressure and heat flux values for a given flammable cloud of hydrogen gas.

This methodology is useful to anyone who wishes to analyse safe distances for hydrogen storage e.g., in an industrial environment with processing equipment, a hydrogen gas refuelling station or - like the scenario presented here - a hydrogen gas storage facility. In order for the numerical code to predict these safety distances, the following are required:

1. CFD geometry relevant to the site under investigation
 2. Suitable mesh with enough elements to accurately capture the physics of the simulation
 3. Appropriate simulation set up including boundary conditions, operating conditions and simulation time/time-steps
 4. A value for the flammable cloud volume (m^3) at a specified time after release - can be calculated from ANSYS CFD-Post
 5. A value for the hydrogen volume fraction at a specified time after release - can also be calculated from ANSYS CFD-Post
-

Referring to point 1, this investigation uses the geometry outlined in section 5.2. This includes further information on: data provided by Elomatic related to the situation, leakage guidelines which were consulted, and other reasoning and assumptions made in order to create the final CFD geometry of a hydrogen leakage scenario. The particular scenario central to this project is described in greater detail in section 4.3. Data and descriptions provided by Elomatic included: the positioning, size and dimensions of the cylindrical hydrogen storage containers, the positioning and size of the leakage orifice, initial storage pressure and corresponding leakage mass flow rate. An orifice (inlet) size of 2cm was dimensioned in the geometry however this could be easily altered to analyse the effects of a larger/smaller leak orifice. This information was to be applied to an outdoor leakage scenario. The leakage time was selected by consulting Tukes and AEGL leakage standards and as a result of computational capabilities (which were limited in the time allocated for this project).

Meshering is naturally a very important aspect of any CFD model and it can be challenging to successfully create a mesh that accurately simulates and resembles a real flow of fluid. Meshing the model for the scenario here had several challenges due to a combination of factors such as; high initial pressures and corresponding mass flow rates of the leaking gas, a small leakage orifice and the potential of producing a large flammable cloud volume. These factors require lots of elements to accurately capture the flow of the gas leakage. In conjunction with requirement 2, the utilised mesh featured approximately 5.6 million elements - with significant refinement in the region of the inlet and flammable cloud. In future investigations the most refined mesh should be used where possible. However, depending on the CFD license available to the user, a coarser mesh may need to be used. For

example, the ANSYS Fluent Student license restricts users to a maximum number of 512,000 cells. A sphere of influence meshing tool was used to help refine the mesh at these critical regions with the refined element sizes, sphere radii and growth rate further described in section 5.3. When using this methodology, a refined mesh is necessary and highly recommended as this will produce more accurate results. Other mesh refinement tools should be employed where necessary, relative to the scenario under consideration by the user.

The 3rd requirement is concerned with Fluent Setup. The CFD governing equations involved in solving the problem are discussed in earlier section 2.10. As described in section 5.4, Species Transport was used to simulate the mixing and transport of the chemical species involved in the model. Species mass fractions for hydrogen and oxygen were specified at certain locations as described in section 5.4 with approximations and assumptions made. In this research, the flammable cloud is produced as a result of a mass flow inlet of 0.43kg/s (corresponding to a pressure of 35 bar) which simulates the hydrogen gas leaking from the vessel to the atmosphere. This mass flow rate was selected on the named selection of ‘inlet’ which is the leakage orifice (see section 5.2). In future investigations similar to this, it is recommended to use a mass flow inlet boundary condition, however a pressure inlet could also be employed.

The 4th and 5th requirements for this method are related to the results of the CFD simulation. An iso-volume was created to obtain the flammable region of the cloud produced at a given time after the leakage starts. A user defined calculation was implemented within CFD post to find the volume fraction of hydrogen and the flammable cloud volume. This equation is shown in section 5.5.

Once these two values have been obtained, a user can input these into the numerical code which produces data of overpressure and radiation at a range of distances.

The code, or script, contains all that is necessary to produce results for both overpressure and heat flux. It contains functions for all traditional heat flux and overpressure methods of calculation, as well as the training and prediction methods for the best performing machine learning model encapsulated within. The desired values of cloud volume, average hydrogen volume fraction, and target distance, can be entered at the start of the script from the CFD results. Various other controls are also available for recreating the overpressure and heat flux plots, as well as conducting a full Monte-Carlo sensitivity analysis for any input parameters. In this guided example the code is presented as a standalone (with dependencies) Python script that handles the following operations, this script is abstracted to the term “code” in this guide for simplicity.

The code also features the ability to save all plot results in the form of an excel spreadsheet for further analysis, and also the ability to evaluate the average R² score and mean square error scores of all the pressure

estimation methods using a 10-fold cross validation scheme. Desired pressure and heat flux limits can also be specified and the safe distances required for these limits can also be requested in the form of standard console printing of results.

Once the code has the required inputs, graphs of Overpressure vs Distance and Heat Flux vs Distance are produced by the various traditional methods and machine learning methods. This is achieved simply by saving the Python code file and executing it with no additional command line arguments.

Literature and guidelines can provide values of overpressure and radiation corresponding to various levels of damage. For example, in section 4.2.1, figure 15 shows that an overpressure value of 1.35kPa is the maximum overpressure which can be tolerated by a person before they may experience any biological harm. Similarly, figure 16 shows that an overpressure value of 4.8kPa is the maximum which a building can withstand before minor damage (e.g., shattered windows etc).

It is up to the user's discretion which regulation or standards they wish to follow for maximum overpressure and maximum heat flux. Once the maximum values have been decided, the corresponding minimum safety distances can be prescribed.

10 Further Work

Given the limited time to complete this research, there are a number of areas which could have been further investigated or given greater consideration.

While a sensitivity analysis was performed to validate the machine learning methods and code which ultimately provide the results of this study, a CFD mesh sensitivity analysis was not considered in this investigation due to project schedule and the high computational demand which would have been required for a domain as large as the one presented in section 5.2. However, this could be revisited in future work and greater consideration given to the final mesh.

A sensitivity analysis of the heat flux estimation methods could also be performed to investigate their response to variation of the input values, although thermal radiation was of less concern it is still a valid and important part of a hydrogen leakage safety analysis.

As mentioned in section 4.3, the scenario presented here only considers a gas leak when there is no wind, so as to limit the dispersion of the hydrogen and investigate a worst-case scenario. It would be interesting to see how great an impact various wind speeds would have on the dispersion and consequently the size of the flammable cloud. In the proposed location of this hydrogen storage facility, wind gusts have been recorded to reach approximately 9mph. Therefore, it would be worthwhile carrying out simulations for the same geometry and mesh for a range of wind speeds from 0mph to 10mph perhaps. The wind speeds could also be adapted to different weather conditions that are relevant to the location of the possible leakage.

Furthermore, the direction of the wind could be altered. A wind condition could be imposed upstream or downstream of the gas jet and similarly observed perpendicular to the jet. The use of a wind profile within the model as opposed to constant wind speed could be incorporated in further development of the presented research, as in reality the wind speed value would be close to zero at ground level, increasing with height. This would require an external input into the ANSYS Fluent model but it is possible. Wind is just one input which may be varied in future investigations.

Likewise, the size of the orifice from which the gas leaks out of the vessel could be investigated. Here, the orifice is modelled and assumed as a perfect circle. In reality this would be an arbitrary shape – something which is also worth considering. A parametric study could be conducted to investigate the effect of altering any number of variables in the simulation.

The level of congestion of the selected geometry is another area that may be investigated in further detail in line with other studies, which analyse the effects of congestion on the formation of a flammable vapour cloud. The two buildings from the scenario in this study could be moved closer or further from the leak orifice, or removed altogether and the resulting effects observed.

Cloud shape is another factor which should be considered and could result in varied safety distances. The methods implemented here approximate the formed cloud in the shape of a perfect sphere. Other cloud shape approximations could be investigated - ellipsoid or ovoid for example.

The safety distance values reported in section 7.6 are approximate and final recommended distances should also include a margin of error if applied in a real-world context where consequences are tangible.

While cloud volumes can vary significantly as a result of vessel pressure, hole size etc. the actual leak orifice location on the surface of the gas cylinder can have a substantial impact on recommended safety distances. When a leak occurs, it is impossible to say beforehand which side of a vessel the gas could leak from. Based on this, it is worth adding a further safety margin to the final recommended value to account for the range of locations where the leak hole may originate.

The addition of a reinforced structure enclosing the pressurised gas vessels could be investigated. The structure would prevent gas from spreading centrifugally from the orifice and drive the gas cloud upwards, to an extent and the resulting effects could be analysed.

There is clearly a significant number of factors which could be reviewed in future studies related to this area. When considering the above-mentioned variables, there are numerous scenarios that could be simulated in the future and would make for useful comparisons with the scenario presented here. The more scenarios that may be analysed, the more safety solutions and standards be put in place and the better prepared society will be, should a similar event occur in reality. This further justifies the need for future studies in the area of hydrogen and hydrogen storage.

11 Conclusion

The recent developments in hydrogen powered technology are an encouraging addition in the wake of our climate conscious world. These technologies - whether it be hydrogen fuel cell vehicles or hydrogen powered ships - will accelerate society in the transition to net zero/carbon neutrality. Like all evolving technology, hydrogen power is not without its challenges and safety considerations are perhaps the greatest challenge of all to overcome. This alludes to the need for safety analyses such as this study which will be of great use in the creation of hydrogen storage locations, production plants or hydrogen fuelling stations which are set to increase in number as hydrogen grows in demand as a fuel.

A potential worst-case hydrogen leakage scenario followed by explosion is described here in detail and modelled using ANSYS Fluent CFD software. The scenario considers the ignition and explosion of a cloud of hydrogen vapour as a result of leakage from a cylindrical storage vessel. The CFD model provided input values which were utilised in both traditional methods and modern machine learning methods for the calculation of safety distances. These safety distances were evaluated in terms of the overpressure and heat flux resulting from the explosion. This systematic methodology was developed into a 'user guide' which may be of great benefit to future hydrogen storage related projects to evaluate safety distances specific to a particular scenario where hydrogen storage is involved. Indeed, safety distances will vary on a case-by-case basis as a result of the number of factors and variables involved.

Given the variety of factors that can be considered in evaluating safety distances for hydrogen explosions, future work is highly anticipated in this area. For example, the leakage scenario explored here could be investigated further with the addition of; wind conditions, a higher storage pressure or alternative leak orifice dimensions. The different combinations of potential scenarios are vast and investigating these would be of great value in understanding the aspects of safety which should be considered for hydrogen storage.

The methodology proposed in this study was a result of significant background research and review of existing literature. The broad scope of this project covers numerous areas such as; hydrogen characteristics and behaviour, governing bodies and safety standards, potential causes of leakage, hydrogen applications, calculation methods and CFD modelling. As well as a guide to the developed methodology for calculating safety distances, this comprehensive investigation intends to aid in the rollout of hydrogen powered innovations which will be of benefit for the world and future generations to come.

12 References

- [1] R. Reider and F. J. Edeskuty, "Hydrogen Safety Problems," *International Journal of Hydrogen Energy*, vol. 4, pp. 41–45, 1979.
- [2] K. Matsuura, H. Kanayama, H. Tsukikawa, and M. Inoue, "Numerical simulation of leaking hydrogen dispersion behavior in a partially open space," *International Journal of Hydrogen Energy*, vol. 33, no. 1, pp. 240–247, 2008, doi: 10.1016/j.ijhydene.2007.08.028.
- [3] "Hydrogen Compared with Other Fuels | Hydrogen Tools." <https://h2tools.org/hydrogen-compared-other-fuels> (accessed Dec. 05, 2021).
- [4] R. W. Schefer, W. G. Houf, and T. C. Williams, "Investigation of small-scale unintended releases of hydrogen: Buoyancy effects," *International Journal of Hydrogen Energy*, vol. 33, no. 17, pp. 4702–4712, 2008, doi: 10.1016/j.ijhydene.2008.05.091.
- [5] K. Verfondern and A. Teodorczyk, "Chapter I : HYDROGEN FUNDAMENTALS," 2007. Accessed: Oct. 29, 2021. [Online]. Available: http://www.hysafe.org/download/1196/BRHS_Chap1_V1p2.pdf
- [6] K. Ramamurthi, K. Bhadraiah, and S. S. Murthy, "Formation of flammable hydrogen-air clouds from hydrogen leakage," *International Journal of Hydrogen Energy*, vol. 34, no. 19, pp. 8428–8437, 2009, doi: 10.1016/j.ijhydene.2009.07.104.
- [7] "Hydrogen Behaviour - Myth Busting." <https://www.osti.gov/servlets/purl/1145695> (accessed Dec. 05, 2021).
- [8] "Stability Class | AIChE." <https://www.aiche.org/ccps/resources/glossary/process-safety-glossary/stability-class> (accessed Dec. 05, 2021).
- [9] "Hydrogen Fuel Cell Engines MODULE 1: HYDROGEN PROPERTIES CONTENTS." https://www1.eere.energy.gov/hydrogenandfuelcells/tech_validation/pdfs/fcm01r0.pdf (accessed Dec. 05, 2021).
- [10] V. Molkov, "Hazards related to hydrogen properties and comparison with other fuels".
- [11] Olaf Jedicke et al., "The State-of-the-Art in Physical and Mathematical Modelling of Safety Phenomena Relevant to Fuel Cells and Hydrogen Technologies."
- [12] Hankwang, "Joule-Thompson curves 2 Image." Wikipedia.

- [13] V. Schroeder and K. Holtappels, "Explosion Characteristics of Hydrogen-Air and Hydrogen-Oxygen Mixtures at Elevated Pressures," *International Conference on Hydrogen Safety*, 2005.
- [14] P. M. Ordin, "Safety standard for hydgoen and hydrogen systems. Guidelines for Hydrogen System Design, Materials Selection, Operations, Storage, and Transportation," *National Aeronautics and Space Administration*, 1997.
- [15] "HYDROGEN | CAMEO Chemicals | NOAA." <https://cameochemicals.noaa.gov/chemical/8729> (accessed Dec. 05, 2021).
- [16] M. Molnarne and V. Schroeder, "Flammability of gases in focus of European and US standards," *Journal of Loss Prevention in the Process Industries*, vol. 48, pp. 297–304, Jul. 2017, doi: 10.1016/J.JLP.2017.05.012.
- [17] R. Wurster and E. Hof, "The German hydrogen regulation, codes and standards roadmap," *International Journal of Energy Research*, vol. 45, no. 4, 2021, doi: 10.1002/er.6249.
- [18] "Database | HyLAW Online Database." <https://www.hylaw.eu/database> (accessed Nov. 23, 2021).
- [19] "COMMITTEE AND THE COMMITTEE OF THE REGIONS A hydrogen strategy for a climate-neutral Europe." [Online]. Available: <https://www.eu2018.at/calendar-events/political-events/BMNT->
- [20] "Nine new hydrogen standards to assist Australia's transition to a more sustainable energy future : NERA National Energy Resources Australia." <https://www.nera.org.au/News/ME-93-nine-new-standards> (accessed Nov. 23, 2021).
- [21] W. Fleeson, "Latin American hydrogen demand could increase by up to two-thirds by 2030: IEA | IHS Markit," Aug. 19, 2021. <https://ihsmarkit.com/research-analysis/latin-american-hydrogen-demand-could-grow-by-up-to-twothirds-b.html> (accessed Nov. 23, 2021).
- [22] "Protecting Scotland's Future: the Government's Programme for Scotland 2019-2020 - gov.scot." <https://www.gov.scot/publications/protecting-scotlands-future-governments-programme-scotland-2019-20/pages/5/> (accessed Nov. 23, 2021).
- [23] "Scottish Hydrogen & Fuel Cell Association SHFCA submission to the UK Parliament Environment Audit Committee", Accessed: Nov. 23, 2021. [Online]. Available: www.shfca.org.uk
- [24] Tukes, "tukes - Tuotantolaitosten sijoittaminen (Production facilities placement)," 2015.

- <https://tukes.fi/documents/5470659/6406815/Tuotantolaitosten+sijoittaminen/ab664564-66f7-49b7-96bb-316dfefe4517/Tuotantolaitosten+sijoittaminen.pdf> (accessed Dec. 10, 2021).
- [25] “Acute Exposure Guideline Levels (AEGLs).” <https://response.restoration.noaa.gov/oil-and-chemical-spills/chemical-spills/resources/acute-exposure-guideline-levels-aegls.html> (accessed Dec. 05, 2021).
- [26] “AEGL - Acute Exposure Guideline Levels: Definition and Methods | Umweltbundesamt.” <https://www.umweltbundesamt.de/en/aegl-acute-exposure-guideline-levels-definition?parent=15018> (accessed Dec. 05, 2021).
- [27] Mechanical Engineering and Metals Industry Standardization in Finland, “Explosive atmospheres. Explosion prevention and protection. Part 1: Basic concepts and methodology,” *Standard - EN 1127-1:2019:en*. Aug. 29, 2019. Accessed: Jan. 04, 2022. [Online]. Available: <https://online.sfs.fi/en/index/tuotteet/SFS/CEN/ID2/1/803209.html.stx>
- [28] Mechanical Engineering and Metals Industry Standardization in Finland, “Potentially explosive atmospheres. Terms and definitions for equipment and protective systems intended for use in potentially explosive atmospheres,” *Standard - SFS-EN 13237*. Mar. 07, 2014. Accessed: Jan. 04, 2022. [Online]. Available: <https://online.sfs.fi/en/index/tuotteet/SFS/CEN/ID2/1/243629.html.stx>
- [29] Mechanical Engineering and Metals Industry Standardization in Finland, “Explosion suppression systems,” *Standard - SFS-EN 14373:2021:en*. Nov. 23, 2021. Accessed: Jan. 04, 2022. [Online]. Available: <https://online.sfs.fi/en/index/tuotteet/SFS/CEN/ID2/1/1043342.html.stx>
- [30] Mechanical Engineering and Metals Industry Standardization in Finland, “Explosion resistant equipment,” *Standard - SFS-EN 14460:2018:en*. Feb. 13, 2018. Accessed: Jan. 04, 2022. [Online]. Available: <https://online.sfs.fi/en/index/tuotteet/SFS/CEN/ID2/1/644303.html.stx>
- [31] Mechanical Engineering and Metals Industry Standardization in Finland, “Explosion isolation systems,” *Standard - SFS-EN 15089:en*. Sep. 04, 2009. Accessed: Jan. 04, 2022. [Online]. Available:

[https://online.sfs.fi/en/index/tuotteet/SFS/CEN/ID2/1/129004.html
.stx](https://online.sfs.fi/en/index/tuotteet/SFS/CEN/ID2/1/129004.html.stx)

- [32] Mechanical Engineering and Metals Industry Standardization in Finland, “Methodology for functional safety assessment of protective systems for potentially explosive atmospheres,” *Standard - SFS-EN 15233:en*. Feb. 08, 2008. Accessed: Jan. 04, 2022. [Online]. Available: [https://online.sfs.fi/en/index/tuotteet/SFS/CEN/ID2/1/46420.html
.stx](https://online.sfs.fi/en/index/tuotteet/SFS/CEN/ID2/1/46420.html.stx)
- [33] Mechanical Engineering and Metals Industry Standardization in Finland, “Determination of maximum explosion pressure and the maximum rate of pressure rise of gases and vapours,” *Standard - SFS-EN 15967:en*. Oct. 28, 2011. Accessed: Jan. 04, 2022. [Online]. Available: [https://online.sfs.fi/en/index/tuotteet/SFS/CEN/ID2/1/172205.html
.stx](https://online.sfs.fi/en/index/tuotteet/SFS/CEN/ID2/1/172205.html.stx)
- [34] Mechanical Engineering and Metals Industry Standardization in Finland, “Determination of the explosion limits and the limiting oxygen concentration(LOC) for flammable gases and vapours,” *Standard - SFS-EN 1839:2017:en*. Jan. 31, 2017. Accessed: Jan. 04, 2022. [Online]. Available: [https://online.sfs.fi/en/index/tuotteet/SFS/CEN/ID2/1/464207.html
.stx](https://online.sfs.fi/en/index/tuotteet/SFS/CEN/ID2/1/464207.html.stx)
- [35] “ISO - ISO/TR 15916:2015 - Basic considerations for the safety of hydrogen systems.” <https://www.iso.org/standard/56546.html> (accessed Jan. 04, 2022).
- [36] E. D. Mukhim, T. Abbasi, S. M. Tauseef, and S. A. Abbasi, “A method for the estimation of overpressure generated by open air hydrogen explosions,” *Journal of Loss Prevention in the Process Industries*, vol. 52, pp. 99–107, Mar. 2018, doi: 10.1016/j.jlp.2018.01.009.
- [37] “Hydrogen Flames | Hydrogen Tools.” <https://h2tools.org/bestpractices/hydrogen-flames> (accessed Dec. 05, 2021).
- [38] “Explosive Lessons in Hydrogen Safety | APPEL Knowledge Services.” <https://appel.nasa.gov/2011/02/02/explosive-lessons-in-hydrogen-safety/> (accessed Dec. 05, 2021).
- [39] “Ignition Hazard Assessment.” <https://www.gexcon.com/products-services/ignition-hazard-assessment-for-mechanical-equipment-and-protective-systems/> (accessed Jan. 05, 2022).

- [40] “Explosion Mitigation Systems Testing.” <https://www.gexcon.com/products-services/fire-and-explosion-mitigation-system-testing/> (accessed Jan. 05, 2022).
- [41] H. Barthélémy, “Hydrogen storage – Industrial prospectives,” *International Journal of Hydrogen Energy*, vol. 37, no. 22, pp. 17364–17372, Nov. 2012, doi: 10.1016/J.IJHYDENE.2012.04.121.
- [42] “Secure and profitable storage and transportation solutions,” 2018. [Online]. Available: www.uac.no
- [43] J. Sakamoto, R. Sato, J. Nakayama, N. Kasai, T. Shibutani, and A. Miyake, “Leakage-type-based analysis of accidents involving hydrogen fueling stations in Japan and USA,” *International Journal of Hydrogen Energy*, vol. 41, no. 46, 2016, doi: 10.1016/j.ijhydene.2016.08.060.
- [44] D. Hao, X. Wang, Y. Zhang, R. Wang, G. Chen, and J. Li, “Experimental Study on Hydrogen Leakage and Emission of Fuel Cell Vehicles in Confined Spaces,” *Automotive Innovation*, vol. 3, no. 2, 2020, doi: 10.1007/s42154-020-00096-z.
- [45] A. A. Malakhov, A. v. Avdeenkov, M. H. du Toit, and D. G. Bessarabov, “CFD simulation and experimental study of a hydrogen leak in a semi-closed space with the purpose of risk mitigation,” *International Journal of Hydrogen Energy*, vol. 45, no. 15, 2020, doi: 10.1016/j.ijhydene.2020.01.035.
- [46] E. M. Edelia, R. Winkler, D. Sengupta, M. M. El-Halwagi, and M. S. Mannan, “A computational fluid dynamics evaluation of unconfined hydrogen explosions in high pressure applications,” *International Journal of Hydrogen Energy*, vol. 43, no. 33, pp. 16411–16420, Aug. 2018, doi: 10.1016/J.IJHYDENE.2018.06.108.
- [47] F. Li, Y. Yuan, X. Yan, R. Malekian, and Z. Li, “A study on a numerical simulation of the leakage and diffusion of hydrogen in a fuel cell ship,” *Renewable and Sustainable Energy Reviews*, vol. 97, pp. 177–185, Dec. 2018, doi: 10.1016/J.RSER.2018.08.034.
- [48] X. Mao, R. Ying, Y. Yuan, F. Li, and B. Shen, “Simulation and analysis of hydrogen leakage and explosion behaviors in various compartments on a hydrogen fuel cell ship,” *International Journal of Hydrogen Energy*, vol. 46, no. 9, pp. 6857–6872, Feb. 2021, doi: 10.1016/J.IJHYDENE.2020.11.158.
- [49] D. Gielen, E. Taibi, and R. Miranda, “HYDROGEN: A RENEWABLE ENERGY PERSPECTIVE,” 2019, Accessed: Nov. 24, 2021. [Online]. Available: www.irena.org

- [50] “Autofrettage - Fundamentals, Industrial Applications and Benefits.” <https://www.azom.com/article.aspx?ArticleID=7893> (accessed Nov. 24, 2021).
- [51] C. Repplinger, S. Sellen, S. Kedziora, A. Zürbes, T. B. Cao, and S. Maas, “Numerical determination and experimental verification of the optimum autofrettage pressure for a complex aluminium high-pressure valve to foster crack closure,” *Fatigue & Fracture of Engineering Materials & Structures*, vol. 43, no. 10, pp. 2183–2199, Oct. 2020, doi: <https://doi.org/10.1111/ffe.13227>.
- [52] I. Sochet, *Blast Effects: Physical Properties of Shock Waves*. 2018.
- [53] S. B. Doroфеев, “Evaluation of safety distances related to unconfined hydrogen explosions,” *International Journal of Hydrogen Energy*, vol. 32, no. 13, pp. 2118–2124, 2007, doi: 10.1016/j.ijhydene.2007.04.003.
- [54] C. J. H. van den Bosch and R. A. P. M. Weterings, “Methods for the Calculation of Physical Effects Due to releases of hazardous materials (liquids and gases) ‘Yellow Book,’” *Tno Cpr 14E*, 2005.
- [55] S. B. Doroфеев, “Evaluation of safety distances related to unconfined hydrogen explosions,” *International Journal of Hydrogen Energy*, vol. 32, no. 13, pp. 2118–2124, Sep. 2007, doi: 10.1016/J.IJHYDENE.2007.04.003.
- [56] Q. A. Baker, M. J. Tang, E. A. Scheier, and G. J. Silva, “Vapor cloud explosion analysis,” *Process Safety Progress*, vol. 15, no. 2, pp. 106–109, Jun. 1996, doi: <https://doi.org/10.1002/prs.680150211>.
- [57] Mélani, Rocourt, and Jallais, “REVIEW OF METHODS FOR ESTIMATING THE OVERPRESSURE AND IMPULSE RESULTING FROM A HYDROGEN EXPLOSION IN A CONFINED/OBSTRUCTED VOLUME,” 2009.
- [58] A. Pierorazio, J. Kelly, Q. Baker, and D. Ketchum, “An update to the Baker–Strehlow–Tang vapor cloud explosion prediction methodology flame speed table,” *Process Safety Progress*, vol. 24, pp. 59–65, Mar. 2005, doi: 10.1002/prs.10048.
- [59] Z. abdul rashid, A. Alias, K. Hamid, M. Bani, and M. El-Harbawi, “Analysis the Effect of Explosion Efficiency in the TNT Equivalent Blast Explosion Model,” 2015, pp. 381–390. doi: 10.1007/978-981-287-505-1_45.
- [60] E. López, R. Rengel, G. Mair, and F. Isorna, *Analysis of high-pressure hydrogen and natural gas cylinders explosions through TNT equivalent method*. 2015. doi: 10.13140/RG.2.1.2336.8401.
- [61] K. J. Cranz, *Lehrbuch der ballistik*, vol. 1. Рипол Классик, 1925.

- [62] B. Hopkinson, "British ordnance board minutes 13565," *The National Archives, Kew, UK*, vol. 11, 1915.
- [63] S. W. Science, *Experimental Methods of Shock Wave*. 2016.
- [64] R. G. Sachs, "The dependence of blast on ambient pressure and temperature, BRL Rep. 466, Army Ballistics Res," *Lab., Aberdeen Proving Grounds, Md*, 1944.
- [65] J. M. Dewey, "The air velocity in blast waves from TNT explosions," *Proceedings of the Royal Society of London. Series A. Mathematical and Physical Sciences*, vol. 279, no. 1378, pp. 366–385, 1964.
- [66] "Mach effect EM1."
- [67] F. Isorna, G. Mair, E. Lopez, and R. Rengel, "Analysis of high-pressure hydrogen and natural gas cylinders explosions through TNT equivalent method," no. July, 2015, doi: 10.13140/RG.2.1.2336.8401.
- [68] E. D. Mukhim, T. Abbasi, S. M. Tauseef, and S. A. Abbasi, "A method for the estimation of overpressure generated by open air hydrogen explosions," *Journal of Loss Prevention in the Process Industries*, vol. 52, pp. 99–107, Mar. 2018, doi: 10.1016/j.jlp.2018.01.009.
- [69] "HySafe." hysafe.net
- [70] F. D. Alonso, E. G. Ferradás, J. F. S. Pérez, A. M. Aznar, J. R. Gimeno, and J. M. Alonso, "Characteristic overpressure-impulse-distance curves for vapour cloud explosions using the TNO Multi-Energy model," *Journal of Hazardous Materials*, vol. 137, no. 2, pp. 734–741, Oct. 2006, doi: 10.1016/j.jhazmat.2006.04.005.
- [71] F. D. Alonso, E. G. Ferradás, J. F. S. Pérez, A. M. Aznar, J. R. Gimeno, and J. M. Alonso, "Characteristic overpressure-impulse-distance curves for vapour cloud explosions using the TNO Multi-Energy model," *Journal of Hazardous Materials*, vol. 137, no. 2, pp. 734–741, Sep. 2006, doi: 10.1016/j.jhazmat.2006.04.005.
- [72] L. Mélani, I. Sochet, X. Rocourt, and Jallais, "REVIEW OF METHODS FOR ESTIMATING THE OVERPRESSURE AND IMPULSE RESULTING FROM A HYDROGEN EXPLOSION IN A CONFINED/OBSTRUCTED VOLUME."
- [73] *Guidelines for consequence analysis of chemical releases*. New York: New York : American Institute of Chemical Engineers, 1999.
- [74] R. Gupta and A. Przekwas, "Mathematical Models of Blast-Induced TBI: Current Status, Challenges, and Prospects," *Frontiers in neurology*, vol. 4, p. 59, 2013, doi: 10.3389/fneur.2013.00059.

- [75] D. E. Edmunds, L. E. Fraenkel, and M. Pemberton, "Obituary-Frederick Gerard Friedlander. 25 December 1917 — 20 May 2001," 2017.
- [76] J. M. Dewey, "The shape of the blast wave: studies of the friedlander equation." Dewey McMillin & Associates, Victoria, BC Canada, 2010.
- [77] F. Ustolin, N. Paltrinieri, and G. Landucci, "An innovative and comprehensive approach for the consequence analysis of liquid hydrogen vessel explosions," *Journal of Loss Prevention in the Process Industries*, vol. 68, p. 104323, Nov. 2020, doi: 10.1016/J.JLP.2020.104323.
- [78] F. Ustolin and N. Paltrinieri, "Hydrogen Fireball Consequence Analysis," *Chemical Engineering Transactions*, vol. 82, pp. 211–216, Jul. 2020, doi: 10.3303/CET2082036.
- [79] L. J. Marchetti, "Fire Dynamics Series: Estimating Fire Flame Height and Radiant Heat Flux From Fire," 2012. Accessed: Nov. 25, 2021. [Online]. Available: <https://pdhonline.com/courses/m312/Radiant%20Flux.pdf>
- [80] H. Nguyen and X. N. Bui, "Predicting Blast-Induced Air Overpressure: A Robust Artificial Intelligence System Based on Artificial Neural Networks and Random Forest," *Natural Resources Research*, vol. 28, no. 3, pp. 893–907, 2019, doi: 10.1007/s11053-018-9424-1.
- [81] M. Khandelwal and T. N. Singh, "Prediction of blast induced air overpressure in opencast mine," *Noise and Vibration Worldwide*, vol. 36, no. 2, pp. 7–16, 2005, doi: 10.1260/0957456053499095.
- [82] D. J. Armaghani *et al.*, "Neuro-fuzzy technique to predict air-overpressure induced by blasting," *Arabian Journal of Geosciences*, vol. 8, no. 12, pp. 10937–10950, 2015, doi: 10.1007/s12517-015-1984-3.
- [83] H. Nguyen, X. N. Bui, H. B. Bui, and N. L. Mai, "A comparative study of artificial neural networks in predicting blast-induced air-blast overpressure at Deo Nai open-pit coal mine, Vietnam," *Neural Computing and Applications*, vol. 32, no. 8, pp. 3939–3955, 2020, doi: 10.1007/s00521-018-3717-5.
- [84] D. Jahed Armaghani, M. Hasanipanah, and E. Tonnizam Mohamad, "A combination of the ICA-ANN model to predict air-overpressure resulting from blasting," *Engineering with Computers*, vol. 32, no. 1, pp. 155–171, 2016, doi: 10.1007/s00366-015-0408-z.
- [85] A. J. Myles, R. N. Feudale, Y. Liu, N. A. Woody, and S. D. Brown, "An introduction to decision tree modeling," *Journal of*

Chemometrics, vol. 18, no. 6. pp. 275–285, Jun. 2004. doi: 10.1002/cem.873.

- [86] Scikit Learn, “Scikit Learn, Ensemble Methods, Extremely Randomised Trees,” *Scikit Learn Documentation*.
- [87] L. Breiman, “Random Forests,” 2001.
- [88] H. Nguyen and X. N. Bui, “Predicting Blast-Induced Air Overpressure: A Robust Artificial Intelligence System Based on Artificial Neural Networks and Random Forest,” *Natural Resources Research*, vol. 28, no. 3, pp. 893–907, Jul. 2019, doi: 10.1007/s11053-018-9424-1.
- [89] K. Ho, “The Random Subspace Method for Constructing Decision Forests,” 1998.
- [90] L. Breiman, “Arcing Classifiers,” *Annals of Statistics*, 1998.
- [91] T. Chen and C. Guestrin, “XGBoost: A scalable tree boosting system,” in *Proceedings of the ACM SIGKDD International Conference on Knowledge Discovery and Data Mining*, Aug. 2016, vol. 13-17-August-2016, pp. 785–794. doi: 10.1145/2939672.2939785.
- [92] J. H. Friedman, “Stochastic gradient boosting,” *Computational Statistics and Data Analysis*, vol. 38, no. 4, pp. 367–378, Feb. 2002, doi: 10.1016/S0167-9473(01)00065-2.
- [93] Y. Freund and R. E. Schapire, “Journal of Computer and System Sciences s SS1504 journal of computer and system sciences,” 1997.
- [94] SIGACT, “2003 Gödel Prize,” 2003.
<https://www.sigact.org/prizes/gödel/2003.html>
- [95] Scikit Learn, “Scikit Learn, Neighbors Methods,” *Scikit Learn Documentation*.
- [96] Fix Evelyn and J. L. Hodges, “Discriminatory Analysis. Nonparametric Discrimination: Consistency Properties,” Feb. 1951.
- [97] M. Amiri, H. Bakhshandeh Amniah, M. Hasanipanah, and L. Mohammad Khanli, “A new combination of artificial neural network and K-nearest neighbors models to predict blast-induced ground vibration and air-overpressure,” *Engineering with Computers*, vol. 32, no. 4, pp. 631–644, Oct. 2016, doi: 10.1007/s00366-016-0442-5.
- [98] B. Sch, R. C. Williamson, and P. L. Bartlett, “New support vector algorithms,” *Neural Computation*, vol. 12, pp. 1207–1245, 2000.

- [99] A. J. Smola and B. Scholkopf, "A tutorial on support vector regression*," *Statistics and Computing*, vol. 14, no. 3, pp. 199–222, 2004.
- [100] Scikit Learn, "Scikit-Learn - Support Vector Machines," *Scikit Learn Documentation*. <https://scikit-learn.org/stable/modules/svm.html> (accessed Jan. 02, 2022).
- [101] L. A. Camuñas-Mesa, B. Linares-Barranco, and T. Serrano-Gotarredona, "Neuromorphic spiking neural networks and their memristor-CMOS hardware implementations," *Materials*, vol. 12, no. 7. MDPI AG, 2019. doi: 10.3390/ma12172745.
- [102] R. Waterman Ph.D, "R-squared and Root Mean Squared Error (RMSE) - Fundamentals of Quantitative Modeling." Wharton, Philadelphia, Pennsylvania, 2014. doi: 10.4135/9781473996991.
- [103] D. Chicco, M. J. Warrens, and G. Jurman, "The coefficient of determination R-squared is more informative than SMAPE, MAE, MAPE, MSE and RMSE in regression analysis evaluation," *PeerJ Computer Science*, vol. 7, pp. 1–24, 2021, doi: 10.7717/PEERJ-CS.623.
- [104] Z.-H. Zhou, *Machine Learning*. Singapore: Springer Singapore, 2021. doi: 10.1007/978-981-15-1967-3.
- [105] "ANSYS Fluent Theory Guide 15." <http://www.pmt.usp.br/academic/martoran/notasmodelosgrad/ANSYS%20Fluent%20Theory%20Guide%2015.pdf> (accessed Dec. 10, 2021).
- [106] "About DNV - DNV." <https://www.dnv.com/about/index.html> (accessed Jan. 05, 2022).
- [107] "Process hazard analysis software - Phast - DNV." <https://www.dnv.com/software/services/phast/phast-our-service.html> (accessed Jan. 05, 2022).
- [108] "Phast 3D Explosions - Explosion modelling software - Vapour cloud explosion tool - DNV." <https://www.dnv.com/software/services/phast/phast-module-3d-explosions.html> (accessed Jan. 05, 2022).
- [109] "Hydrogen Safety." <https://www.gexcon.com/wp-content/uploads/2020/10/Gexcon-Services-Hydrogen-EN-eBrochure.pdf> (accessed Nov. 10, 2021).
- [110] Hydrogen Tools, "Hydrogen applications." <https://h2tools.org/bestpractices/hydrogen-applications>
- [111] Air Liquide, "Uses of Hydrogen," 2021. <https://energies.airliquide.com/resources-planet-hydrogen/uses-hydrogen> (accessed Oct. 08, 2021).

- [112] Ted Bergman, “Elomatic: Is the hydrogen future here already?,” Jan. 02, 2021.
<https://meriteollisuus.teknologiateollisuus.fi/en/ajankohtaista/blog/elomatic-hydrogen-future-here-already> (accessed Oct. 05, 2021).
- [113] “Ferry Industry Facts – Interferry.” <https://interferry.com/ferry-industry-facts/> (accessed Nov. 24, 2021).
- [114] “First step to Europe’s first hydrogen powered ferry taken for Orkney route | The National.”
<https://www.thenational.scot/news/19349049.first-step-europe-s-first-hydrogen-powered-ferry-taken-orkney-route/> (accessed Nov. 24, 2021).
- [115] “Unveiling Europe’s first hydrogen-powered seagoing ferry | News | CORDIS | European Commission.”
<https://cordis.europa.eu/article/id/435312-unveiling-europe-s-first-hydrogen-powered-seagoing-ferry> (accessed Nov. 24, 2021).
- [116] Anna Häger, “Hydrogen ferries might soon traffic the Baltic Sea,” *Flexens*, Nov. 23, 2020. <https://flexens.com/hydrogen-ferries-might-soon-traffic-the-baltic-sea/> (accessed Sep. 06, 2021).
- [117] “World’s 1st hydrogen-powered ferry delivered - Offshore Energy.” <https://www.offshore-energy.biz/worlds-1st-hydrogen-powered-ferry-delivered/> (accessed Nov. 24, 2021).
- [118] “First hydrogen fuel-cell vessel: San Francisco ferry ready to go.” https://www.greencarreports.com/news/1133318_first-hydrogen-fuel-cell-vessel-san-francisco-ferry-ready-to-go (accessed Nov. 24, 2021).
- [119] “World’s first liquid hydrogen fuel cell cruise ship planned for Norway’s fjords | Recharge.”
<https://www.rechargenews.com/transition/world-s-first-liquid-hydrogen-fuel-cell-cruise-ship-planned-for-norway-s-fjords/2-1-749070> (accessed Nov. 24, 2021).
- [120] “Hydrogen Fuel Cell Vehicle Market Size, Outlook, Trends by 2030.” <https://www.alliedmarketresearch.com/hydrogen-fuel-cell-vehicle-market> (accessed Nov. 24, 2021).
- [121] “Volvo Group and Daimler Truck AG fully committed to hydrogen-based fuel-cells – launch of new joint venture cellcentric.”
<https://www.volvogroup.com/en/news-and-media/news/2021/apr/news-3960135.html> (accessed Nov. 24, 2021).
- [122] “Volvo CE opens fuel cell test lab in Sweden - electrive.com.”
<https://www.electrive.com/2021/05/19/volvo-ce-opens-fuel-cell-test-lab-in-sweden/> (accessed Nov. 24, 2021).

- [123] “Interactive map – Truck hydrogen refuelling stations needed in Europe by 2025 and 2030, per country - ACEA - European Automobile Manufacturers’ Association.”
<https://www.acea.auto/figure/interactive-map-truck-hydrogen-refuelling-stations-needed-in-europe-by-2025-and-2030-per-country/> (accessed Nov. 24, 2021).
- [124] F. D. Gregory, “Associate Administrator for Safety and Mission Assurance iii ACKNOWLEDGMENTS,” 1997.
- [125] E. López and F. Isorna, “Analysis of high-pressure hydrogen and natural gas cylinders explosions through TNT equivalent method,” 2015, doi: 10.13140/RG.2.1.2336.8401.
- [126] “Dealing with hydrogen explosions.”
http://www.hyreponse.eu/files/Lectures/Dealing_with_hydrogen_explosions_notes.pdf (accessed Dec. 01, 2021).
- [127] F. Pedregosa *et al.*, “Scikit-learn: Machine Learning in Python,” *Journal of Machine Learning Research*, vol. 12, pp. 2825–2830, 2011.

13 Appendices

13.1 Appendix 1 – Hydrogen VCE Experimental Dataset

Experiment Data	Cloud Total		
H2 Concentration%	Volume (m3)	Distance (m)	Overpressure(kPa)
20	37	4.9	2.07
20	37	9.35	1.9
20	37	13.72	1.4
20	37	17.84	1.12
20	37	25.67	0.86
20	37	36.92	0.69
20	37	48	0.43
20	37	71.9	0.29
20	5.2	2.5	2.58
20	5.2	24.48	0.51
20	5.2	47.66	0.23
20	5.2	92.83	0.13
22.72	1.4	0.98	2.25
22.72	1.4	1.5	1.8
22.72	1.4	2.5	1.32
22.72	1.4	3.45	1.04
22.72	1.4	3.63	0.85
22.72	1.4	4.56	0.7
22.72	1.4	5.58	0.5
27.8	9.4	9.15	3.51
27.8	9.4	10.49	2.97
27.8	9.4	23.18	1.39
27.8	9.4	62.83	0.47
29.58	1.4	0.98	3.37
29.58	1.4	1.48	2.77
29.58	1.4	2.49	1.92
29.58	1.4	3.43	1.56
29.58	1.4	3.6	1.41
29.58	1.4	4.58	1.17
29.58	1.4	5.6	0.84
30	37	4.87	9.56
30	37	9.29	5.66
30	37	13.63	4.96
30	37	17.73	3.82
30	37	24.99	2.69
30	37	37.43	2.07
30	37	47.7	1.59
30	37	71.44	1.07
30	37	92.89	0.98
30	37	96.72	0.72
30	5.2	2.53	5.91
30	5.2	6.95	5.41

30	5.2	11.52	3.07
30	5.2	24.82	1.66
30	5.2	47.36	0.9
30	5.2	94.12	0.41
30	300	9.35	25.45
30	300	13.99	25.45
30	300	18.75	29.41
30	300	26.72	22.03
30	300	35.37	17.74
30	300	49.18	13.77
30	300	70.92	10.32
30	300	95.04	8.01
30	300	119.83	6
30	300	355.02	2.71
30.4	75	19.38	11.96
30.4	75	28.82	7.77
30.4	75	42.83	5.77
30.4	75	63.27	4.14
30.7	200	24.69	8.04
30.7	200	42.57	5.4
30.7	200	71.18	3.75
30.7	200	116.82	2.6
30.7	200	190.56	1.53
43.05	1.4	0.98	10.19
43.05	1.4	1.49	8.25
43.05	1.4	2.49	5.8
43.05	1.4	3.39	4.76
43.05	1.4	4.62	3.75
43.05	1.4	5.59	2.75
45.65	1.4	0.98	6.42
45.65	1.4	1.48	5.81
45.65	1.4	2.5	4.27
45.65	1.4	3.3	3.6
45.65	1.4	3.62	3.4
45.65	1.4	4.6	2.92
45.65	1.4	5.56	2.11
55.75	1.4	0.98	12.27
55.75	1.4	1.48	10.51
55.75	1.4	2.49	6.7
55.75	1.4	3.44	5.35
55.75	1.4	4.59	3.87
55.75	1.4	5.61	2.68
57	5.2	25.55	3.05
57	5.2	48.87	1.57
57	5.2	94.86	0.78

Appendix 2: Group Work and Project Management Reflection



A Systematic Methodology for Estimation of Safe Distances for Hydrogen Storage Containers

Group Work and Project Management Reflection

Angus MacMillan - 201732968

Jacob Currie - 201718558

James Hinshelwood - 201732900

Supervisor: Eero Immonen

eero.immonen@turkuamk.fi

Table of Contents (Group Work and Project Management Reflection)

1.0	Introduction	128
2.0	Initial Project Plan	129
2.1	Initial Task Board	129
2.2	Initial Project Milestones	129
2.3	Gantt Chart	130
2.4	Work Breakdown Structure (WBS)	131
2.5	Aims and Deliverables	132
3.0	Resultant project plan	133
4.0	Logbook	134
5.0	Meetings	135
5.1	Student Meetings & Independent Tasks	135
5.2	Milestone Meetings and Presentations	135
5.3	Other Meetings	136
5.4	Meeting Documentation	137
6.0	Project Issues and Schedule Adjustments	138
6.1	Lack of Method Description	138
6.2	Lack of Data	138
6.3	Inadequate Methods	138
6.4	The Introduction of Machine Learning	138
6.5	Final Submission Date	139
7.0	Risk Management	140
8.0	Group Roles and Resource Management	141
8.1	Jacob's Role	141
8.2	Angus' Role	141
8.3	James' Role	141
9.0	Group Performance	142
10.0	Project Reflection	143
11.0	Closing Statement	144

1.0 Introduction

Over the course of the project, the group have made use of various project management techniques and tools to help keep tasks and deliverables on track. This has allowed the group to ensure successful execution of the project and fulfil the relevant assessment criteria. Moreover, this has allowed the group to have efficient time and workload/resource management and gain a better understanding of what it means to be part of a team, contributing to something more than an individual piece of work as well as developing various other skills throughout the process.

2.0 Initial Project Plan

Following the first meeting between the group, the group's supervisor and stakeholder, Elomatic an initial project plan was constructed – based upon the discussions and recommendations made at the meeting.

The group made use of a project management software, Monday.com which has useful built-in tools that made the process of planning this project efficient and straight forward. In addition, the software has a clean and user-friendly interface which proved to be of great use in meetings and for the purpose of presenting.

2.1 Initial Task Board

The main project tasks were documented on a “board”. Each task was given; an associated status, time period to be completed and a week allocation. Many tasks were broken down into subtasks. Similarly, these subtasks were given; an associated status, time period and week allocation. Monday.com also stored any changes and updates made to a particular task. These changes were timestamped which was useful in later stages when the group may have had to evaluate when they carried out the specific tasks in earlier stages.

The initial project task board which was constructed at the start of the semester (beginning of September) is shown below:

Project Outline	Subitems	Subitems Status	Status	Timeline	Week(s)
Hydrogen Characteristics and Behaviour	▶ 4		Done	✓ Sep 13 - 19	1
Standards	▶ 5		Done	✓ Sep 13 - 24	1-2
Investigate Methods of Analysis/Leakage Calculatio...	▶ 3		Done	✓ Sep 20 - 24	2
Literature + Articles	▶ 5		Done	✓ Sep 13 - Oct 1	1-3
Select 2/3 Methods to find ballpark	▶ 2		Done	✓ Sep 27 - Oct 1	3
Find Ballpark Figures	▶ 4		Done	✓ Oct 4 - 15	4 - 5
CFD Models	▶ 9	█ 1	Working on it	Oct 11 - 29	5-7
Parametric Study/Testing and Changing Variables	▶ 4		Future steps	Nov 1 - 12	8-9
Complete Report	▶ 3			Nov 15 - Dec 3	10-12
Presentation	▶ 6			Dec 6 - 14	13
Closure	▶			Dec 13 - 17	14
Strathclyde Presentation (+ Prep)	▶			Jan 5 - 14	(New Year)

Figure 147: Main Project tasks, Task Status and Time Allocation

2.2 Initial Project Milestones

Project milestones were documented on a separate board. Like the task board, these milestones were given a status and date for which they were due to be completed. Clarifying these milestones before beginning the project was of great use to all involved and allowed the project to be broken into smaller, more manageable areas so as to not be overwhelmed with the enormity of the project as a whole. Meeting a milestone also allowed the group to feel a sense of achievement and find smaller victories within the journey of completing the group project and thesis document. The milestone dates also allowed the group to confer with stakeholders (Elomatic and group

supervisor) and organise meetings at which the group could provide everyone with updates on their work and present their latest findings associated with that particular milestone.

Milestones	Status	Timeline
Document All Standards	Done	◆ ✓ Sep 24
Complete Research + Start Literature Review	Done	◆ ✓ Oct 1
Finalise Math methods + Calculations	Done	◆ ✓ Oct 15
Finalise CFD Models	Done	◆ ✓ Oct 29
Finalise Parametric Study		-
Finalise Report	Done	◆ ✓ Dec 3
Finalise Presentation	Done	◆ ✓ Dec 10

Figure 2: Project Milestones

2.3 Gantt Chart

From the task board (figure 1) and project milestones board (figure 2), Monday.com has the capability to automatically produce an equivalent Gantt chart through extrapolating the dates from the timeline columns. The Gantt chart corresponding to these boards is shown below:

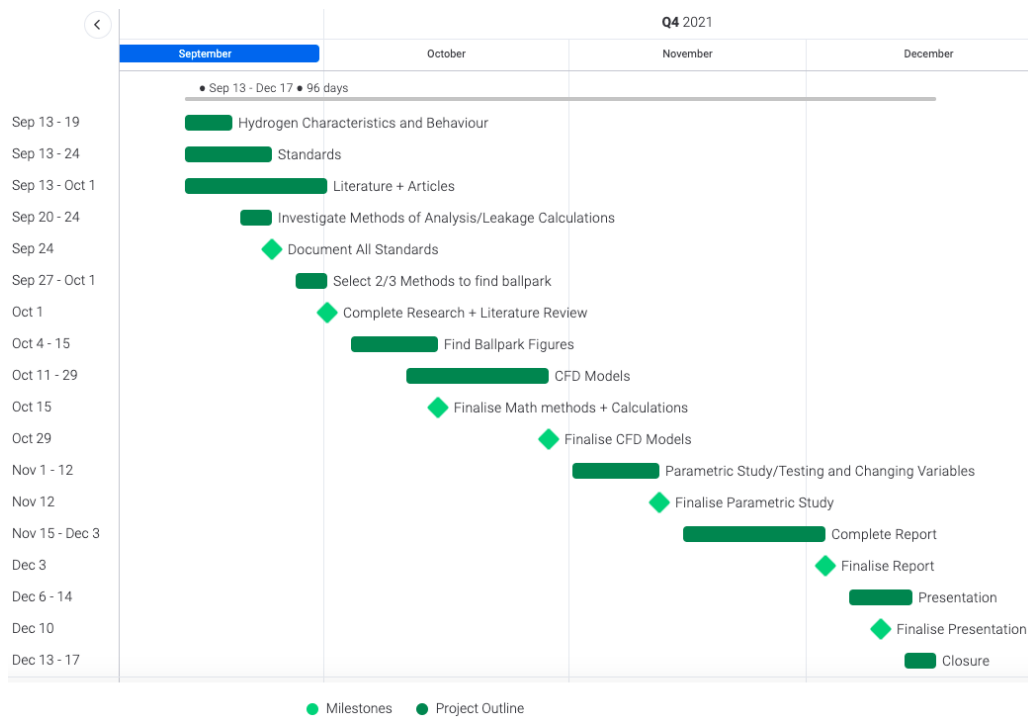


Figure 348: Project Gantt Chart Corresponding to Figure 1 & 2

As with any project, timeline changes and changes to scope are highly likely. Additionally, the group's initial project plan was created *before* assessment criteria was distributed. Therefore, significant parts to the project were not considered at this stage e.g. statement of purpose and interim report.

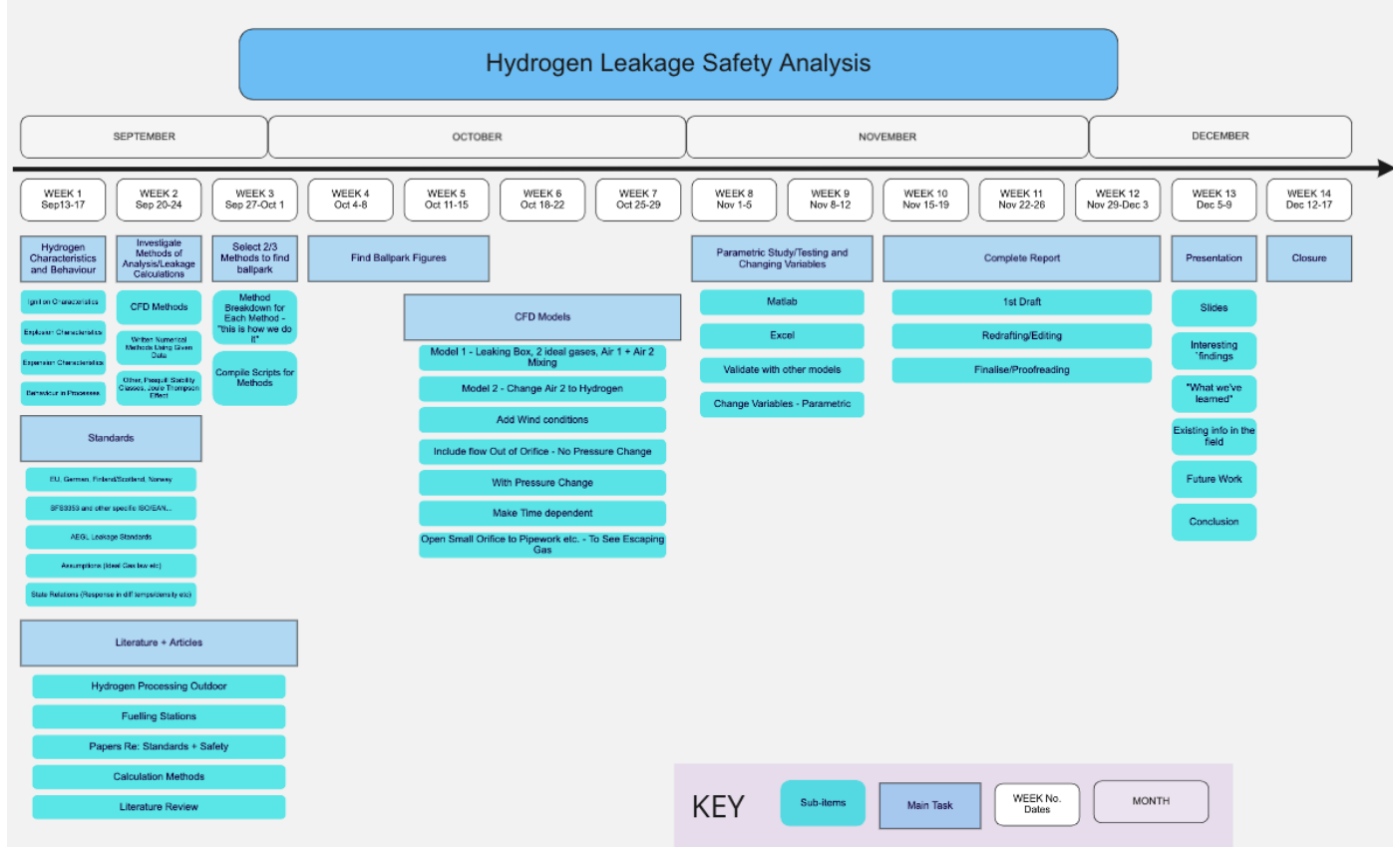


Figure 4: Work Breakdown Structure Plan

Similarly, the final submission date had not been specified at that time and so the date the group had initially planned to complete the thesis was likely to change as more details were made available to the group. These are just some of the changes to the timeline the group experienced during their project. The group included a “closure” week to account for these potential additional tasks. However, other changes were also made to the project scope and schedule. All changes could be classified as potential risks to the project and as such, were documented in the project risk and change control log. More details regarding change to scope and project risks are discussed further in later sections of this reflection.

2.4 Work Breakdown Structure (WBS)

The tasks and sub tasks were also presented in a ‘Work Breakdown Structure’ view which can be observed in Fig. 4 below. Similar to the Gantt chart, this view allowed the group to look at all existing tasks and their current position within the entirety of the project timeline.

2.5 Aims and Deliverables

In the earlier stages of the process, the group declared their aims and deliverables as described below. The group aimed to plan, develop and test a systematic methodology for the estimation of safe distances from hydrogen storage facilities. This would be achieved through the following:

- Research the relevant literature regarding current hydrogen safety standards
- Research the underlying science concerning the behaviour of hydrogen
- Research the various pre-existing methods of safe distance estimation
- Implement and test the selected distance estimation methods
- Clarify the typical distance where the maximum allowable overpressure is achieved
- Clarify the typical distance where the maximum allowable thermal radiation is achieved
- Validate results using CFD modelling
- Carry out a parametric study to investigate how different variables impact a hydrogen leakage scenario, e.g., leak size, pressure, or wind conditions.

3.0 Resultant project plan

Reflecting on the initial plan, it is worthwhile analysing how this compares to the plan in the later stages, once all adjustments were made. The figure below shows the initial plan - including initial tasks and dates - and how these have changed over time as well as tasks which were discarded or introduced at a later stage.

Project Tasks	Initial Timeline	Actual Timeline
Hydrogen Characteristics and Behaviour	Sep 13 - 19	Sep 13 - 19
Standards	Sep 13 - 24	Sep 13 - 24
Investigate Methods of Analysis/Leakage Calculati...	Sep 20 - 27	Sep 20 - 27
Literature + Articles	Sep 13 - Oct 1	Sep 13 - Oct 1
Select 2/3 Methods to find ballpark	Sep 27 - Oct 4	Sep 27 - Oct 8
Find Ballpark Figures	Oct 4 - 15	Oct 4 - 22
CFD Models	Oct 11 - 31	Oct 18 - Nov 5
Machine learning methods	-	Nov 22 - Dec 17
Parametric Study/Testing and Changing Variables	Nov 1 - 12	-
Complete Report	Nov 15 - Dec 3	Nov 15 - Dec 31
Presentation	Dec 6 - 14	Dec 3 - 8
Closure	Dec 13 - 17	-
Strathclyde Presentation (+ Prep)	Jan 5 - 14	Jan 1 - 12

Figure 5: Initial vs Actual Project Timeline

Referring to the 5th row of the board, more time was required in researching and selecting methods to obtain the initial ballpark figures. The group originally planned to use 2 or 3 methods in this project. In the end, a total of 4 traditional methods for overpressure estimation and 2 methods for heat flux estimations were used – 6 methods in total. Ultimately, the group doubled the number of methods they initially intended to utilise, and this only had a slight adjustment on the project schedule – taking 4 days more than intended. This was the first major change to the project schedule which had a slight knock-on effect and resulted in timeline changes for the tasks that followed ('Find Ballpark Figures' and 'CFD models'). In hindsight, the group believe this delay in the schedule was beneficial to the success of the project as more research regarding methods could be undertaken allowing for more comprehensive results.

The initial timeline column has no dates for 'Machine learning Methods'. When the initial plan was constructed, machine learning was not considered to be a major part of the project. On the contrary, the actual timeline for 'Parametric study....' is blank as this task was removed from the schedule. The reasons for the introduction and removal of these tasks are explored in more detail in section 5.0 – Project Issues and Schedule Adjustments. Section 5.0 highlights all reasons for changes to the schedule.

4.0 Logbook

The group kept a (digital) logbook for their own personal benefit. This was updated often and acted as a diary. The group members found keeping a logbook to be of great use in their 4th year individual research project and believed they could have an equally positive experience in using one for this group project.

The logbook allows the group to keep track of any tasks which the group executed on a particular date and was also used for noting any information associated with the project. This meant all related info could be stored in one location which was useful in relation to project organisation. Monday.com also provided the platform for which this digital logbook was stored. This was also useful as it meant all project management related tools could be found together in the one place, on one software.

5.0 Meetings

5.1 Student Meetings & Independent Tasks

All group members met at least 3 times a week in person at Turku University of Applied Sciences (TUAS). Depending on difficulty of tasks, the group would meet more often. This also meant time was set aside for independent tasks which may have been specifically assigned to a particular individual, in which case there was no need to meet together as a group.

5.2 Milestone Meetings and Presentations

The group reported to Elomatic approximately every 2 weeks through Microsoft Teams meetings but were also in regular contact by email. As previously explained, the meetings corresponded to particular project milestones (as shown in figures 2 and 3) and were for the group and Elomatic to discuss the progress made in reaching that milestone. All milestone meetings are described below:

- Introduction to the Project @ TUAS (31.08.21)
The group were acquainted with one another, their supervisor and the Erasmus exchange coordinator at Turku University of Applied Sciences. This was when the group were also first introduced to their project topic – “A Hydrogen Leakage Safety Analysis”.
- Introductory Meeting with Elomatic (08.09.21)
The group met the team at Elomatic with whom they would be working with on the project. The group also presented their initial Work Breakdown Structure (WBS) plan, project board and Gantt chart to the stakeholders. In this meeting, academic areas of strength of group members were discussed as were the specialities of the team at Elomatic. This was a great chance to get acquainted with everyone who would be involved in the project over the semester.
- Project Plan Presentation & Initial Research (29.09.21)
After taking some time to familiarise themselves with the concepts involved in this project and various pieces of literature/studies, the group discussed the calculation methods they would investigate over the following weeks which would provide them with initial ballpark figures.
- Initial “Ballpark” Figures (18.10.21)
The group presented their initial results to Elomatic which were obtained using several methods to calculate overpressure values at various distances as well as heat flux values at various distances.
- CFD Models & Machine Learning Presentation (5.11.21)
The group presented the 2 initial CFD models they created to Elomatic. These models would be used to investigate the dispersion of hydrogen gas from a leaking orifice. The developments made regarding machine learning methods were also presented.

- CFD & Machine Learning Update (25.11.21)
2 variations of a 3D CFD model were presented to Elomatic along with the associated results of hydrogen cloud volume and hydrogen volume fraction. By this meeting, the CFD results were ready to be used as inputs for the machine learning methods.
- Thesis Review (26.11.21)
The group discussed the progress they had made to date in their thesis documentation, with their group supervisor. This was beneficial and gave the group an idea of areas which required greater attention. Furthermore, the group's supervisor provided some encouraging feedback discussing the potential of having this work published at a later date. The group supervisor also introduced the possibility of publishing a modified version of the project in a scientific journal, with the project showing promising signs of truly novel and unique research.
- Final Technical Presentation – Elomatic (08.12.21)
The group presented their final results to Elomatic and the methodology they developed which can be used in future scenarios to establish safety distances from hydrogen gas storage.
- Final General Presentation - TUAS (08.12.21)
TUAS held a presentation afternoon where different groups of students had the opportunity to showcase their projects to their host companies and other TUAS staff. The group gave a general overview of the entirety of their project, what was involved and how they executed this. They also described how they managed their project and how this research is useful to real world applications.

These meetings and presentations provided an opportunity for the team at Elomatic to suggest improvements and recommendations for the team to consider over the weeks that followed. These meetings were scheduled based on personal availability and workload of all involved.

5.3 Other Meetings

As well as the higher priority milestone meetings and presentations outlined above, the group also had some sporadic Microsoft Teams meetings with Elomatic employees to run through some of the more technical or specific queries (such as CFD simulation set up and post processing). These were arranged by communication over email and often planned just before the meeting itself. These were beneficial to the group and also a great opportunity to work with the team at Elomatic and utilise their expertise. These impromptu meetings gave the group a flavour of what it means to work in a fast-paced environment where project changes occur frequently and should be dealt with in timely fashion.

5.4 Meeting Documentation

Meeting notes were recorded at each meeting. These were later summarised and sent out to all involved, as a follow up to the meeting. This also left an electronic paper trail of what was discussed so that everyone was up to date with the latest progress and if there were any queries further down the line, everyone was able to check the notes from any meeting earlier in the process.

6.0 Project Issues and Schedule Adjustments

While there were no major problems with the group's progress or performance, there were minor areas of concern that the group have dealt with and slight adjustments made to the schedule (as shown in Fig. 5) which are discussed in the follow section.

6.1 Lack of Method Description

In the earlier calculation stages, the group experienced issues with some numerical methods. In particular, the group had difficulty in finding numerical methods for calculation of heat flux from a hydrogen vapour cloud explosion. This is indeed a rather specific scenario, and no literature or previous research provided a full step by step methodology related to such. Upon recommendation from Elomatic, the group were able to progress with methods related to fireball explosions which are similar in nature. By approximating the vapour cloud explosion to that of a fireball, the group were able to implement two methods for calculation of heat flux and this issue had no significant impact on the project schedule.

6.2 Lack of Data

As well as having difficulty finding appropriate methods of heat flux calculation, the group were also unable to source existing data related to heat fluxes recorded at various distances to validate the implemented methods. On the contrary, the methods for evaluating overpressure at certain distances were validated which was of higher priority, given that many safety standards and measures define safety distances in terms of overpressure values as opposed to heat flux values.

6.3 Inadequate Methods

A similar problem was encountered when the group attempted to implement a specific calculation method for overpressure values. After most of one particular method had been written as a script in Python, it was discovered that one step in the method required a parameter which the group had no way of calculating. The group had two options: proceed with the method based on a substantial number of assumptions or discard the method. The latter was the final decision of the group as the number of assumptions suggested the method was no longer reliable. Furthermore, several other methods had already been implemented for overpressure calculation and the group felt more confident in the reliability of these.

6.4 The Introduction of Machine Learning

After the presentation of initial "ballpark figures" to the project stakeholders, there was much interest in the proposed machine learning methods. The group had initially planned to only mention the prospects of machine learning as a method of calculation however Elomatic were quite interested in this area. Therefore, following that presentation, machine learning methods were explored in greater detail and resulted in a substantial contribution to the final report. This is an additional part of the project that was not originally accounted for in the planning stage and had an impact on the project schedule. The group closely monitored the affect this has on the schedule but discussed the most efficient way to proceed with the next tasks while

simultaneously introducing this new area to the project scope. The group felt it was necessary to heavily research and implement this area, as initial research and reading made it impossible to ignore that machine learning models have been successfully implemented with considerably high levels of performance in very similar explosion-overpressure prediction scenarios.

6.5 Final Submission Date

When the group began this project, details of the final submission date had yet to be released. Therefore, when the group created their plan, they set a final date well in advance of the actual deadline. Naturally, once the finalised date was announced, the group adjusted the schedule allowing for more time to finalise their thesis.

7.0 Risk Management

All risks etc. were recorded in the group's risk management 'ARiaD' log. This allowed the group to keep track of all the project's associated assumptions, risks, issues and dependencies (ARiaD) which is an important practice in project management as it allows potential problems to be flagged quickly and dealt with appropriately, preventing other issues from arising further into the project timeline.

ARiaD	ARiaD	Creation Date	Status	Closed Date	Description	Mitigating Action	Area affected	Impact	Probability
Referencing	⊕ Assumption	Sep 13	Ongoing		The group s...	Students should i...	Schedule	Medium	low
Incorrect Translation	⊕ Risk	Sep 23	Ongoing		Documents ...	Once translated, s...	Results	Medium	Medium
No Existing Data	⊕ Issue	Sep 24	Closed	Oct 29	Heat Flux: G...	Students should ...	Results	Medium	High
Changes to Timeline	⊕ Assumption	Sep 27	Ongoing		It is assume...	Continually monit...	Schedule	low	Medium
Software Requirements	⊕ Dependency	Sep 27	Ongoing		The group a...	Keep all those inv...	Results	low	low
Covid-19 Infection	⊕ Risk	Sep 28	Ongoing		If a group m...	The infected grou...	Schedule	Medium	low
Dorofeev Method	⊕ Issue	Sep 28	Closed	Oct 1	Method of c...	Disregard this me...	Schedule Results	Medium	Medium
Residence Permit Rejected	⊕ Risk	Oct 1	Closed	Nov 19	Outcome of ...	Appeal rejection ...	Schedule	Medium	low
Virtual Desktop Issues	⊕ Issue	Oct 19	Closed	Nov 12	Two group ...	Seek alternative s...	Schedule	Medium	High
Machine learning - Impact	⊕ Issue	Oct 20	Closed	Nov 3	The positive...	The timeline date...	Schedule Results	low	Medium
Interim Report	⊕ Issue	Oct 25	Closed	Nov 8	The project ...	Move all other tim...	Schedule	Medium	High
ANSYS Student Capabilities	⊕ Issue	Nov 15	Closed	Nov 25	The student ...	Students can crea...	Results Schedule	High	Medium
Elomatic - Software	⊕ Dependency	Nov 17	Closed	Nov 25	As student li...	Remain in frequen...	Results Schedule	Medium	Medium
New Covid Variant	⊕ Risk	Nov 26	Ongoing		New covid v...	Follow official gui...	Schedule	Medium	Medium
Error in Code	⊕ Assumption	Nov 26	Closed	Dec 3	Assuming t...	Results from the ...	Results	low	low
Sensitive Code	⊕ Issue	Nov 25	Closed	Dec 3	Since a mes...	the CFD values ha...	Results	High	Medium

Figure 6: A Snapshot of the Project ARiaD Log

The ARiaD log contains all the necessary information related to all project ARiaDs. Monday.com is especially useful at tracking ARiaDs as they can be filtered or arranged by almost any related piece of information at the click of a button. For example, these can be arranged to show the most recent ARiaDs, the ones which will have a high impact, low probability etc. Figure 6 displays the ARiaDs from oldest to newest created.

8.0 Group Roles and Resource Management

As a smaller group of three members, the more involved tasks were executed together while secondary tasks were carried out individually. The task board on Monday.com software has a built-in feature which allows tasks to be assigned to a specific individual or multiple individuals and therefore was also useful as a resource management tool.

8.1 Jacob's Role

Group member Jacob has extensive knowledge and experience using coding software – in particular, using python and as such was responsible for implementing the various numerical methods into a python script. In addition, Jacob saw potential in using machine learning algorithms as a means of calculating safety distances. As the project has progressed, machine learning has become a principal aspect, contrary to what was initially planned. It has been wonderful to observe how group members' external interests have been utilised within the project and have played such an influential role in the outputs and final results. This has also meant the project has greater personal meaning to the group. Jacob researched ignition characteristics of hydrogen and hydrogen behaviour in processes. He assisted in the creation of the final CFD model to simulate hydrogen gas leakage and also investigated hydrogen characteristics during the initial research stage.

8.2 Angus' Role

Angus was primarily responsible for creating various CFD models and creating the final model which would be used to provide input values for the numerical code. Angus has previous experience in using ANSYS for his 4th year individual project, "Development of a Finite Element Model for Closed die forging in the FutureForge facility" and also enjoyed CFD modules in 3rd and 4th year of university. In the initial research stage, Angus investigated Finnish national (Tukes) safety standards - given this investigation was concerned primarily with a local Finnish hydrogen gas storage facility - and also the applications of the study at hand in a real-world context. Angus also researched hydrogen expansion characteristics and explosion characteristics of hydrogen in air.

8.3 James' Role

James focussed on European safety standards related to the topic, explosion characteristics, behaviour and looked at other scientific investigations into hydrogen leakage and hydrogen explosions. James also investigated recent real-world applications where this project would be of great benefit. He also helped source several of the traditional methods for calculation of overpressure and heat flux. Upon recommendation from the group's supervisor, James took up the role of key liaison between the students, Elomatic and the group's supervisor. Being familiar with some project management concepts, he was responsible for tracking the project using the various tools - task board, ARlaD log and logbook. James also assisted Angus with the creation of the CFD models.

All group members contributed to the writing of the final thesis document and final presentations.

9.0 Group Performance

Given the positive feedback from Elomatic throughout the process, the group feel confident with the extent of research and efforts they have made in their endeavours. While the group have proven they effectively work well together, their individual abilities have contributed to different parts of the project which is an important attribute in any group work setting. Overall, the group believe they have performed well and have enjoyed this learning experience together.

10.0 Project Reflection

With the project now complete, the group have had a chance to reflect on areas they could have executed differently and things they could have done at the start of the project which would have made for a more efficient process.

The group believe they could have been more specific in their original project aims (section 2.0) – particularly related to CFD modelling. The group created 5 different CFD models and yet only one model displayed any real worth in the final research. A more in-depth discussion with Elomatic at an earlier stage would have alleviated any discrepancies in what was expected of the final CFD model and therefore the final results. This would have also reduced the total time the group spent on CFD which could have been better spent on other areas of the thesis.

The group were unsuccessful in meeting 1 of 8 aims described in section 2.0. While a parametric study was intended to make up a substantial section of this project, the introduction of machine learning within the project scope replaced a parametric study. CFD modelling took slightly longer to execute than originally planned and this also suggests a parametric study would have been impossible. Furthermore, given the number of variables involved in a leakage scenario, a fully comprehensive parametric study would have been difficult to perform in the time allocated for this project.

The group met the 7 other project aims to a high extent and are pleased to have delivered the majority of what they set out at the beginning of this process.

11.0 Closing Statement

The group have thoroughly enjoyed carrying out and completing this group project together and wish to thank everyone who was involved in the success of this project.

As hydrogen fuel becomes more available and significant developments regarding hydrogen powered technology are made in the coming years, the group are extremely grateful to have investigated an area within engineering which is so highly topical. In addition, this is an area which many engineers may encounter at some point in their future careers and so this project will have been of great benefit to the group.

Working with a professional company has allowed the group to develop many skills on top of those they have developed through completing their thesis - in particular, teamwork skills, presentation skills, leadership skills, analytical skills and technical skills, management and organisational skills. Developing these skills has prepared the students for life after university, as they enter the world of work. The students also now have a greater appreciation for project management and understand its importance to the success of any project. As professional engineer's post-graduation, the group know that project management is something that will always be central to their work. This experience has given them an understanding of how to utilise project management tools which they will be able to use in future.

Living and working on a project abroad has also been a wonderful experience from both a cultural and social perspective. Working cross-collaboratively with people from another country has been rewarding in that it has given the group insight into the way people work differently in other countries. During their time abroad, the group also built many friendships with other Erasmus students and enjoyed learning about their native customs and cultures.